Forschungszentrum Karlsruhe
Technik und Umwelt

Wissenschaftliche Berichte
FZKA 6178

ITER ECRF Coaxial Gyrotron and Window Development

Part I: Coaxial Gyrotron Development

– Final Report –

M. Thumm, B. Piosczyk, O. Braz, G. Dammertz, M. Kuntze, G. Michel

Institut für Technische Physik

Projekt Kernfusion
Association EURATOM-FZK

Oktober 1998

Forschungszentrum Karlsruhe
Technik und Umwelt
Wissenschaftliche Bericht
FZKA 6178

ITER ECRF COAXIAL GYROTRON AND WINDOW DEVELOPMENT

Part I: Coaxial Gyrotron Development

- Final Report -

M. Thumm[1)], B. Piosczyk, O. Braz[1)] , G. Dammertz, M. Kuntze, G. Michel

Institut für Technische Physik,
Projekt Kernfusion
Association EURATOM-FZK

1) also Universität Karlsruhe, Institut für Höchstfrequenztechnik und Elektronik

Forschungszentrum Karlsruhe GmbH, Karlsruhe
1998

Als Manuskript gedruckt

Forschungszentrum Karlsruhe GmbH
Postfach 3640, 76021 Karlsruhe

Mitglied der Hermann von Helmholtz-Gemeinschaft
Deutscher Forschungszentren (HGF)

ISSN 0947-8620

ITER ECRF COAXIAL GYROTRON AND WINDOW DEVELOPMENT

Part I: Coaxial Gyrotron Development

- Final Report -

Task No.: G 52 TT 10 FE
ID-No.: GB6 – EU - T245/6

Executive Summary:

The status of the development of a coaxial cavity gyrotron with an rf-output power of 1.5 MW is given and experimental and theoretical results are presented. Experiments in two different modes, the $TE_{28,16}$ mode at 140 GHz and the $TE_{31,17}$ mode at 165 GHz have been performed. The selection of the upper frequency is based on limitations imposed by the maximum field of the superconducting magnet at FZK and the use of the electron gun designed originally for the 140 GHz - $TE_{28,16}$ mode. Further, for selection of both modes the possibility of transforming the cavity modes to a degenerate whispering gallery mode appropriate for the dual-beam quasi-optical (q.o.) output coupler and the two output windows has been taken into account. The cavity consists of a cylindrical outer wall and a radially tapered inner rod with longitudinal corrugations. The coaxial insert is supported from the gun side.

First, experimental investigations have been performed in an arrangement with an axial waveguide output. A maximum rf-output power of 1.17 MW has been measured as well at 140 GHz and 165 GHz with an efficiency of almost 28 %. Stable single-mode operation has been found over a wide range of operating parameters. In both cases the experimental values agree well with the results of multimode calculations if for the simulations the experimental parameters are taken. Frequency step tuning has been performed over a wide frequency range by changing the value of the magnetic field with constant magnetic compression. Under that condition single mode operation has been achieved in 20 different modes in the frequency range between 115.6 and 164.2 GHz with the 140 GHz-$TE_{28,16}$-mode cavity. In particular, an output power of 0.9 MW has been measured in the $TE_{25,14}$ mode at 123.0 GHz and 1.16 MW in the $TE_{32,18}$ mode at 158.9 GHz. Similar measurements with the 165 GHz-$TE_{31,17}$ mode cavity resulted in an output power of 1.02 MW at 167.14 GHz in the $TE_{32,17}$ mode, 0.63 MW at 169.46 GHz in the $TE_{33,17}$ mode and 0.35 MW at 171.80 GHz in the $TE_{34,17}$ mode. At frequencies with strong window reflections the parameter range for which stable operation is possible is reduced significantly.

Second, the $TE_{28,16}$ - coaxial cavity gyrotron at 140 GHz has been redesigned for operation with a dual rf-beam output. For the first time the generated rf power has been split in two parts and coupled out through two rf output windows in order to reduce the power loading in the windows. The q.o. output system is based on a two-step mode conversion scheme. First, the cavity mode $TE_{-28,16}$ is converted into its degenerate whispering gallery mode $TE_{+76,2}$

using a rippled-wall mode converter with longitudinal corrugations. Then this mode is transformed into two output wave beams. A maximum rf-output power of 0.95 MW with an output efficiency of 20 % has been measured. According to numerical calculations an rf-power above 1.5 MW is expected to be generated in the cavity. Even if all losses are taken into account a discrepancy between experiment and calculations remains. The power deficit seems to be partly caused due to the influence of the stray radiation captured inside the tube. It was observed that an increased amount of captured stray radiation reduced the stability of operation. However, the two main reasons for the discrepancy in the rf-output power are probably an incomplete mode conversion from $TE_{-28,16}$ to $TE_{+76,2}$ and a large spread of the electron beam energy caused by trapped electrons. A single-stage depressed collector was used successfully, increasing the rf-output efficiency from 20 % to 29 %. In single pulses the pulse length has been extented up to 7 ms limited by the increase of pressure inside the tube. A further extension of the pulse length would require additional time-consuming conditioning of the gyrotron.

KOAXIALGYROTRON- UND FENSTER-ENTWICKLUNG FÜR ITER ECRF

Teil I: Entwicklung eines Koaxialgyrotrons

- Schlußbericht -

Task No.: G 52 TT 10 FE
ID-No.: GB6 – EU - T245/6

Kurzfassung:

Der Stand der Entwicklung von Gyrotrons mit koaxialem Resonator und einer Ausgangsleistung von 1,5 MW wird dargestellt und über experimentelle und theoretische Ergebnisse wird berichtet. Es wurden Experimente mit zwei verschiedenen Arbeitsmoden, der $TE_{28,16}$-Mode bei 140 GHz und der $TE_{31,17}$-Mode bei 165 GHz durchgeführt. Die Auswahl der oberen Frequenz wird durch das maximale Magnetfeld des am FZK vorhandenen supraleitenden Magneten und durch den Gebrauch der ursprünglich für die 140 GHz, $TE_{28,16}$-Mode ausgelegte Elektronenkanone bestimmt. Außerdem hat die Möglichkeit der Transformation der Resonatormode in eine für einen quasi-optischen Ausgangskoppler mit Doppelstrahl und zwei Ausgangsfenstern geeignete, entartete Flüstergaleriemode die Wahl der Arbeitsmoden bestimmt. Der Resonator besitzt eine zylindrische Außenwand und einen Innenleiter mit veränderlichem Radius und longitudinaler Rillung. Der koaxiale Einsatz wird von der Kanonenseite her gehaltert.

Erste experimentelle Untersuchungen wurden in einer Anordnung mit axialer Wellenleiterauskopplung durchgeführt. Bei beiden Frequenzen, 140 GHz und 165 GHz, wurde eine maximale HF-Ausgangsleistung von 1,17 MW bei einem Wirkungsgrad von nahezu 28 % gemessen. Über einen weiten Arbeitsparameterbereich wurde stabiler Einmodenbetrieb beobachtet. In beiden Fällen stimmen die experimentellen Ergebnisse gut mit Multimodensimulationsrechnungen überein, bei denen die im Experiment eingestellten Betriebsparameter verwendet wurden. Stufenweise Frequenzdurchstimmung durch Veränderung des Magnetfeldes bei konstanter magnetischer Kompression konnte über einen weiten Frequenzbereich durchgeführt werden. Unter diesen Bedingungen wurde mit dem 140 GHz-$TE_{28,16}$-Resonator Einmodenbetrieb für 20 verschiedene Resonatormoden im Frequenzbereich von 115,6 bis 164,2 GHz erreicht. Dabei wurde z.B. eine Ausgangsleistung von 0,9 MW in der $TE_{25,14}$-Mode bei 123,0 GHz und 1,16 MW in der $TE_{32,18}$-Mode bei 158,9 GHz gemessen. Ähnliche Experimente mit dem 165 GHz-$TE_{31,17}$-Resonator ergaben Ausgangsleistungen von 1,02 MW bei 167,14 GHz in der $TE_{32,17}$-Mode, 0,63 MW bei 169,46 GHz in der $TE_{33,17}$-Mode und 0,35 MW bei 171,80 GHz in der $TE_{34,17}$-Mode. Für Frequenzen, bei denen das Ausgangsfenster stark reflektiert, war dabei der Parameterbereich für stabile Schwingungen deutlich reduziert.

In einem zweiten Schritt wurde das $TE_{28,16}$-Gyrotron mit koaxialem Resonator für 140 GHz mit einem Doppelstrahl-Ausgang ausgestattet. Damit wurde die Ausgangsleistung zum erstenmal in einem Gyrotron in zwei Hälften aufgeteilt und zur Verminderung der Leistungsbelastung durch zwei Fenster ausgekoppelt. Das quasi-optische Auskoppelsystem beruht auf einem Zweistufen-Modenwandlungsprinzip. Zuerst wird in einem Wellentypwandler mit longitudinaler Wandrillung die $TE_{-28,16}$-Resonatormode in die zu ihr entartete

Flüstergaleriemode $TE_{+76,2}$ transformiert. Dann wird diese in zwei Ausgangsstrahlen umgewandelt. Es wurde eine maximale HF-Ausgangsleistung von 0,95 MW mit einem Wirkungsgrad von 20 % gemessen. Entsprechend numerischen Rechnungen wird allerdings erwartet, daß mehr als 1,5 MW im Resonator erzeugt werden. Selbst wenn alle Verluste berücksichtigt werden verbleibt eine Diskrepanz zwischen Experiment und Rechnungen. Der Leistungsverlust scheint teilweise durch die in der Röhre gefangene Streustrahlung verursacht zu sein. Es wurde beobachtet, daß mehr gefangene Streustrahlung zu reduzierter Stabilität führt. Als die beiden Hauptgründe für die Abweichung werden allerdings eine nicht vollständige $TE_{-28,16}$ – $TE_{+76,2}$-Umwandlung und eine durch gefangene Elektronen verursachte Energiestreuung vermutet. Durch Einsatz eines einstufigen Kollektors mit Gegenpotential konnte der HF-Ausgangswirkungsgrad von 20 % auf 29 % angehoben werden. In Einzelpulsen wurde die Pulslänge bis auf 7 ms verlängert, wobei diese Grenze durch Druckanstieg in der Röhre gegeben war. Eine weitere Vergrößerung der Pulslänge würde eine zusätzliche zeitaufwendige Konditionierung des Gyrotrons erfordern.

Contents

Report

The goal of the development work is to demonstrate the feasibility and to provide the technical basis for an industrial fabrication of a 2 MW, 170 GHz coaxial-cavity gyrotron. The development work has been divided into several steps:

In a first step the basic problems of interaction between the electron beam and the rf field in a coaxial cavity - the stability of single-mode operation, mode competition, efficiency of rf-generation - have been investigated. Theoretical models and the related numerical tools have been verified. In this step a coaxial-cavity gyrotron with an axial waveguide output has been used. The measurements have been restricted to pulse lengths ≤ 0.5 ms due to the limited heat-load capability of the collector. The investigations have been performed with two different cavities designed for operation in the $TE_{28,16}$ mode at 140 GHz and in the $TE_{31,17}$ mode at 165 GHz, respectively. In the experiments single-mode operation has been found over a wide range of parameters. With both cavities a maximum rf-output power of nearly 1.2 MW has been achieved with an output efficiency of almost 28 % corresponding to a transverse efficiency above 60 %. The experimental and numerical results agree well if for the numerical simulations the experimental parameters are taken. The possibility of step frequency tuning was demonstrated over a wide frequency range with both cavities. In collaborative experiments with the IAP, Nizhny Novgorod, Russia an rf-output power of 1.5 MW with an efficiency of 33 % has been achieved in a similar arrangement of a 140 GHz, $TE_{28,16}$-coaxial cavity gyrotron. A summary of the measurements performed at FZK and a discussion of the results are given in two publications in IEEE Transactions on Plasma Science which are included as the Appendices A1 and A2.

In a second step the coaxial gyrotron with the $TE_{28,16}$ mode at 140 GHz was equipped with a radial dual rf-beam output and a single-stage depressed collector. The quasi-optical (q.o.) mode converter system for the dual rf-beam output is based on a two-step mode conversion scheme,

$$TE_{-28,16} \Rightarrow TE_{+76,2} \Rightarrow TEM_{00}$$

which generates two narrowly-directed output wave beams. A direct conversion of the operating cavity mode into the TEM_{00} mode would require dimensions of the mirror system which are excessively large for a dual rf-beam output since the azimuthal angle of divergence φ of the radiation is as large as $\varphi = 142.6^0$ for the $TE_{28,16}$ mode. For the degenerate $TE_{76,2}$ mode the angle has the value $\varphi = 59.1^0$. The double cut q.o. converter uses a dimple-wall double-beam launcher and generates two diametrically opposed narrowly-directed output wave beams. The two step mode conversion scheme, however, works properly only for the design mode and cannot be used if the possibility of frequency step tuning is considered. The details of the q.o. mode converter are published in the Conference Digests of the 21st and 22nd Int. Conf. on IR&MMWaves and are included as Appendix A3.

In the performed measurements the following results have been achieved:

- the range of single-mode oscillation is in good agreement with results of numerical simulations.

- within the experimental error (± 5 %) the rf output power was distributed symmetrically through the two output windows.
- a maximum rf output power of 950 kW corresponding to an output efficiency of 20 % has been achieved.
- a single-stage depressed collector has been used successfully increasing the efficiency at maximum power to 29 %.
- a relatively high amount of the generated rf power (between about 14 and 20 % in the different experimental runs) has been captured as stray radiation inside the vacuum chamber influencing the operation of the gyrotron.

Also if all rf losses inside the gyrotron are taken into account a power deficit of about 30 % remains in comparison to the results expected from numerical calculations. The reasons for that are not completely clear. Some influence on operation has been observed from the stray radiation captured inside the tube. The relatively low efficiency of the rf output system which is the reason for the high amount of captured stray radiation is thought to be related to the two-step mode conversion scheme, in particular to the conversion from the cavity into the whispering gallery mode, which has been confirmed by cold rf measurements. It has been observed that instabilities of the electron beam are enhanced due to the amount of stray radiation inside the gyrotron tube. In addition there are indications that the reduced efficiency could have been due to an energy spread of the electron beam caused by trapped electrons as a consequence of a poor beam quality. In common experiments with the IAP, Nizhny Novgorod, Russia performed on a similar 140 GHz, $TE_{28,16}$-coaxial cavity gyrotron with a dual rf-beam output an rf-output power of 1.1 MW with an efficiency of 30 % has been achieved (U_{cath} = 90 kV, I_b = 40 A, pulse length = 50 µs). The results of the measurements performed at FZK with the double rf beam output have been summarized and discussed in a paper submitted for publication in the IEEE Transactions on Plasma Science. A copy of the manuscript is included as Appendix A4.

At present an operation of the coaxial gyrotron in the $TE_{31,17}$ mode at 165 GHz is under preparation. Since the development of CVD-diamond rf-output windows is progressing very fast and there is a well-founded expectation that a transmission of even 2 MW rf power at 170 GHz will be possible through one window, it has been decided to built an rf output system in which the cavity mode is directly converted into a Gaussian mode and transmitted through one rf output window only. All needed components have been designed and manufactured already. The rf output system consists of a non-linear uptaper, a conventional Vlasov launcher with a smooth waveguide surface and two mirrors. The distribution of the rf output beam is shaped into an approximately Gaussian beam by the second mirror which has a phase correcting surface. The design of this q.o. converter is published in the Conference Digest of the 22nd Int. Conf. on IR&MMWaves and is included as Appendix A5. The rf beam is transmitted through one window made out of fused silica with a diameter of 100 mm. Since the occurrence of beam instabilities observed in the last experiments may have been related with the poor quality of the electron beam enhanced due to azimuthal inhomogenity of electron emission, the emitter of the gun has been replaced. The properties of the used old emitter are thought to be degraded due to exposion to air for many times. The gyrotron is

under assembling and the rf measurements will start soon. The main goals of the next experiments are:

- to investigate the rf output system with the phase correcting mirror
- to enlighten the influence of stray radiation on the gyrotron operation
- to prove the quality of the electron beam of the gun with the replaced emitter.

As a further step towards the demonstration of the feasibility for industrial fabrication of a coaxial gyrotron a noval 90 kV, 50 A electron gun has been designed. A technical advantage of the gun design are the smaller radial dimensions compared with the present inverse magnetron injection gun. Further, the alignment of the inner rod will be improved and the inner rod will be cooled as required for long pulse operation. In order to reduce the required operating temperature and to improve the emission properties an emitter of dispencer type instead of the presently used LaB_6 type is foreseen. The mechanical design of the gun is underway.

Appendices:

A1: A 1.5 - MW, 140 GHz, $TE_{28,16}$ - Coaxial Cavity Gyrotron

A2: Design and Experimental Operation of a 165 - GHz, 1.5 - MW, Coaxial-Cavity Gyrotron with Axial RF Output

A3: Built-In Mode Converters for Coaxial Gyrotrons

Low Power Excitation and Mode Purity Mesurements on Gyrotron Type Modes of High Order

Low Power Performance Tests on Highly Oversized Waveguide Components of High Power Gyrotrons

A4: Coaxial Cavity Gyrotron with Dual RF - Beam Output

A5: Design of a Quasi-Optical Mode Converter for a Coaxial 165 GHz $TE_{31,17}$ Gyrotron

Acknowledgments

This report is an account of work assigned as an ITER TASK to the European Home Team under the Agreement among the European Atomic Energy Community, the Government of Japan, the Government of the Russian Federation and the Government of the United States of America on Cooperation in the Engineering Design Activities for the International Thermonuclear Experimental Reactor ("ITER EDA Agreement") under the auspices of the International Thermonuclear Energy Agency (IAEA). The work was supported by the European Fusion Technology Program under the Projekt Kernfusion of the Forschungszentrum Karlsruhe. We gratefully acknowledge stimulating and useful discussions with colleagues from IAP, Nizhny Novgorod, in particular Drs. V. Flyagin, V. Khishnyak, A. Pavelyev and V. Zapevalov. The contributions of H. Baumgärtner, H. Budig, P. Grundel, H. Kunkel, W. Leonhardt, J. Sczcesny and R. Vincon of the gyrotron team technical staff for the mechanical design, the precise machining and the careful assembly of the coaxial gyrotron as well as for their assistance during the experiments were essential for the success of the work. The authors thank Prof. E. Borie for proofreading of the manuscript.

APPENDIX A1

A 1.5-MW, 140-GHz, $TE_{28,16}$-Coaxial Cavity Gyrotron

Bernhard Piosczyk, Oliver Braz, Günter Dammertz, Christos T. Iatrou, Stefan Kern, Michael Kuntze, A. Möbius, Manfred Thumm, *Senior Member, IEEE* V. A. Flyagin, V. I. Khishnyak, V. I. Malygin, A. B. Pavelyev, and V. E. Zapevalov

***Abstract*—The design of a 1.5-MW, 140-GHz, $TE_{28,16}$-coaxial cavity gyrotron is presented and results of experimental operation are given. A cavity with a cylindrical outer wall and a radially tapered inner rod with longitudinal corrugations was used. A maximum output power of 1.17 MW has been measured in the design mode with an efficiency of 27.2%. Single-mode operation has been found over a wide range of operating parameters. The experimental values agree well with the results of multimode calculations. Frequency-step tuning has been performed between 115.6 and 164.2 GHz. In particular, an output power of 0.9 MW has been measured in the $TE_{25,14}$ mode at 123.0 GHz and 1.16 MW in the $TE_{32,18}$ mode at 158.9 GHz. At frequencies with strong window reflections the parameter range for which stable operation is possible is reduced significantly. In order to obtain results relevant for a technical realization of a continuously operated gyrotron, a tube with a radial radio frequency (rf)-beam output through two output windows and a single-stage depressed collector has been designed and is under fabrication. A two-step mode conversion scheme—$TE_{-28,16}$ to $TE_{+76,2}$ to TEM_{00}—which generates two narrowly directed (60° at the launcher) output wavebeams has been chosen for the a quasioptical (q.o.) mode converter system. A conversion efficiency of 94% is expected.**

***Index Terms*— Coaxial cavity gyrotron, frequency tunability, magnetron injection gun.**

I. Introduction

CONVENTIONAL hollow waveguide-cavity gyrotrons are limited in output power (≈1 MW at frequencies above ≈140 GHz) due to ohmic wall loading, mode competition, and limiting beam current. Conventional gyrotrons with an output power of 1 MW at 170 GHz operated in continuous wave (CW) are presently under development for ITER [1]–[4]. The problem of ohmic wall loading can be reduced by increasing the cavity diameter and using volume modes. This requires operation in high-order modes, where the mode spectrum is dense and mode competition could prevent the gyrotron from stable operation. The use of volume modes, which have relatively low cavity wall loading, leads to a lower limiting current. In coaxial cavities, however, the presence of the inner conductor practically eliminates the restrictions of voltage depression and limiting current. In addition, the use of coaxial cavities offers the possibility of selective influence of the diffractive quality factor of different modes, allowing operation in high-order volume modes with reduced mode competition problems [5], [6]. Gyrotrons with coaxial cavities have the potential to generate, in CW operation, RF output powers in excess of 1 MW at frequencies above 140 GHz. In general, two methods can be applied in a coaxial cavity for an effective control of the diffractive Q-factor of different modes: 1) the use of a longitudinally corrugated tapered inner rod [7], and 2) the use of a resistive inner rod [8]. The first seems preferable for high-power operation and it has been followed in the development of coaxial gyrotrons presented here.

A gyrotron designed for operation at a frequency of 140 GHz with an RF output power of 1.5 MW is under development in a collaboration between the Forschungszentrum Karlsruhe, Association EURATOM-FZK, and the Institute of Applied Physics (IAP) Nizhny Novgorod [9], [10]. The development has been planned to be performed in two steps. The first step, in which the gyrotron has an axial waveguide output with 100-mm diameter, has already been realized and experiments have been performed. The measurements have been done with pulselength ≤0.5 ms due to the limited heat-load capability of the collector, which is part of the output waveguide. Operating problems have been examined and the cavity design has been verified. In particular, a maximum output power of 1.17 MW has been measured in the design mode with an efficiency of 27.2%. Single-mode operation has been found over a wide range of operating parameters. The experimental values agree very well with results of multimode calculations. The operating point with the design output power (1.5 MW) and efficiency (35%) is not accessible in the axial version, probably because of enhanced mode competition due to window reflections and overshooting of the high voltage at the beginning of the pulse. Frequency step tuning has been performed successfully. With a constant magnetic compression 20 modes have been excited in single-mode operation in the frequency range between 115.6 GHz and 164.2 GHz. In particular, an output power of 0.9 MW has been measured in the $TE_{25,14}$ mode at 123.0 GHz and 1.16 MW in the

Manuscript received October 7, 1996; revised April 1, 1997. This work was supported by the Project Kernfusion of the Forschungszentrum Karlsruhe under the European Fusion Technology Program.

B. Piosczyk, G. Dammertz, C. T. Iatrou, and M. Kuntze are with Forschungszentrum Karlsruhe, Association EURATOM-FZK, Institut für Technische Physik, Postfach 3640, Karlsruhe D-76021 Germany.

O. Braz, S. Kern, and M. Thumm are with Forschungszentrum Karlsruhe, Association EURATOM-FZK, Institut für Technische Physik, Postfach 3640, D-76021 Karlsruhe, Germany; they are also with the Universität Karlsruhe, Institut für Höchstfrequenztechnik und Elektronik, Kaiserstrasse 12, Karlsruhe D-76128 Germany.

A. Möbius is with IMT GmbH, Luisenstr. 23, Eggenstein D-76344 Germany.

V. A. Flyagin, V. I. Khishnyak, V. I. Malygin, A. B. Pavelyev, and V. E. Zapevalov are with the Institute of Applied Physics, Russian Academy of Sciences, Nizhny Novgorod 603600 Russia.

Publisher Item Identifier S 0093-3813(97)04864-9.

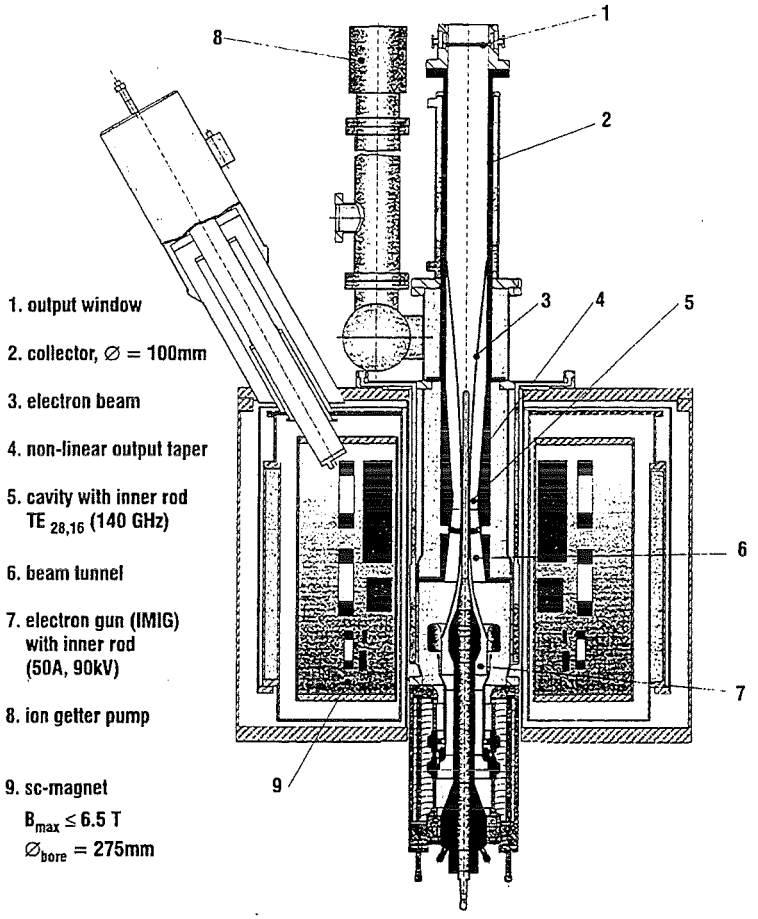

Fig. 1. Schematic layout of the coaxial cavity gyrotron with axial RF output.

$TE_{32,18}$ mode at 158.9 GHz. At frequencies with strong window reflections the parameter range with stable operation is reduced significantly.

In a second step, a tube design relevant for CW operation with a radial RF output will be investigated. Especially because of the present power limit of RF output windows the mm-wave power will be split into two beams and coupled out radially through two windows. In addition, a single-stage depressed collector will be used in order to enhance the total efficiency and to reduce the power loading at the collector surface.

In the following, the design consideration and the components of the 1.5 MW, 140 GHz, $TE_{28,16}$-coaxial cavity gyrotron including the quasioptical (q.o.) output system for the tube with radial dual RF-beam output, are described. Operating experience and results of RF measurements obtained with the axial tube are presented and compared with the results of numerical simulations.

II. Design Parameters and Layout of the Gyrotron

A schematic layout of the gyrotron with the axial waveguide output is shown in Fig. 1. The main design parameters are summarized in Table I. The realistic low wall loading which is about twice the ideal value, $p_\Omega(\text{real}) \approx 2p_\Omega(\text{ideal})$ is very attractive for a technical realization. The peak ohmic losses at the inner rod are calculated to be less than 10% of the peak cavity wall losses and are not considered to be a technical problem. The low value of the ohmic losses at the inner rod is attributed to the radius which is much smaller than the corresponding radius of the caustic. It is not due to the impedance corrugation of the inner rod. The main features of the gyrotron components are described in the following.

TABLE I
Design Parameters of the $TE_{28,16}$ Coaxial Gyrotron at 140 GHz

frequency f / GHz	140
rf output power P_{out} / MW	1.5
cathode voltage U_c / kV	90
beam current I_b / A	50
velocity ratio α	1.35
cavity radius R_{cav} / mm	29.81
beam radius R_b / mm	10.0
voltage depression ΔU_b / kV	1.6
limiting current I_{lim} / A	≈ 400
peak wall loading (ideal copper) p_Ω / kWcm^{-2}	0.63

A. The Superconducting Magnet and the Electron Gun

For the operation of the gyrotron tube, an existing superconducting (sc) magnet—with a maximum magnetic field of

6.5 T and a warm bore hole having a diameter of 275 mm—is used. In addition to the solenoidal coils, the magnet has a set of dipole coils which permits a radial shift of the electron beam in the region of the cavity. With the help of these coils the alignment of the beam with respect to the inner rod can be verified and redone if necessary in the installed tube.

The 4.5-MW electron gun is of a diode type having a central rod close to the ground potential surrounded by the cathode ring [inverse magnetron injection gun (IMIG)] [11]. The inner rod is electrically isolated, but is held close to the ground potential. It is fixed and cooled from the gun side. The part of the rod within the cavity can be radially adjusted under fully assembled conditions between two shots. At the design beam current $I_b = 50$ A the emitter current density is $j_e = 2.8$ A cm^2. The design operating voltage is $U_c = 90$ kV. The emitter consists of LaB_6 and has an average radius of 56 mm. The properties of the electron beam, such as the transverse to axial velocity ratio α and the relative transverse velocity spread $\delta\beta_{\perp\mathrm{rms}}$, have been measured with the method of retarding fields. The average value of α was found to be in reasonable agreement with numerical results. The measured velocity spread $\delta\beta_{\perp\mathrm{rms}} \cong 9\%$ is relatively high, but sufficient for reliable operation at the design parameters. For generation of the magnetic field in the gun region, two coils (ES1 and ES2) are available, which allow a variation of the direction of the magnetic field lines relative to the emitter surface. Depending on the ratio of the coil currents the velocity ratio, α changes at the design conditions from 1.15 ($I_{\mathrm{ES1}} = 0$) up to about 1.4 ($I_{\mathrm{ES2}} = 0$).

B. Cavity and Output Taper

The corotating $\mathrm{TE}_{-28,16}$ mode with an eigenvalue $\chi = 87.35$ was chosen as the working mode for operation at 140 GHz. When selecting the operating mode it was considered that for the dual-beam quasioptical output a two-step mode conversion scheme, $\mathrm{TE}_{-28,16}$ to $\mathrm{TE}_{+76,2}$ to TEM_{00}, which generates two narrowly directed (60° at the launcher) output wavebeams is foreseen. In order to allow a simple transformation of the cavity mode into the $\mathrm{TE}_{76,2}$ whispering gallery mode (WGM), the two modes have to be degenerate. The two-step scheme is chosen because a direct transformation of the $\mathrm{TE}_{28,16}$ operating-volume mode to a linearly polarized beam would require an excessively large mirror system for a dual-beam output. This is due to the large (142.6°) azimuthal angle of the radiation at the launcher.

For the resonator (Fig. 2) a cavity with a cylindrical outer wall and a radially tapered and corrugated inner rod is used. The cavity has a length of 20 mm and the inner rod has a negative taper (radius decreases toward the collector, $dR_{\mathrm{rod}}/dz < 0$) of 1°. For a negatively tapered inner rod, a positive/negative slope in the eigenvalue curve $\chi(C)$ of any mode will increase/decrease its diffractive quality factor [7], [12]. $C = R_{\mathrm{cav}}/R_{\mathrm{rod}}$ is the ratio of the outer cavity radius R_{cav} to the radius of the inner rod R_{rod}. The longitudinal impedance corrugation on the inner rod is introduced in order to avoid an increase of the quality factor of some competing modes. The corrugation consists of small longitudinal slots

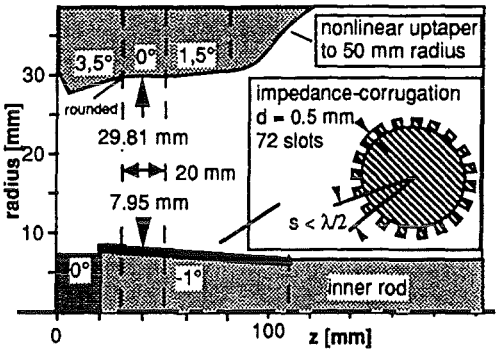

Fig. 2. Geometry of the $\mathrm{TE}_{28,16}$–coaxial cavity with tapered and longitudinally corrugated inner rod.

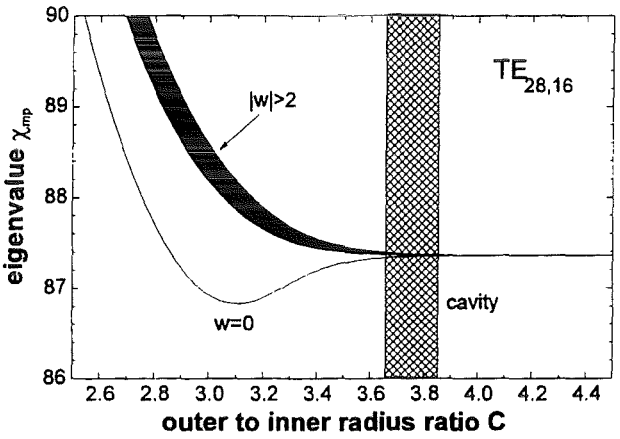

Fig. 3. Influence of longitudinal corrugations of the inner rod on the mode eigenvalue. The C-range within the cavity is indicated.

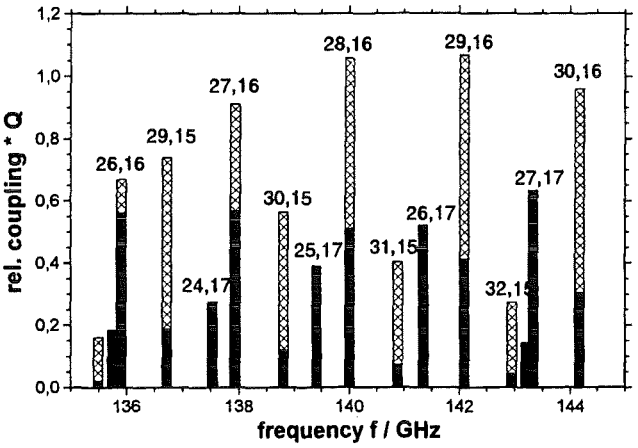

Fig. 4. Mode spectrum of the product (quality factor Q * relative coupling coefficient) for the coaxial cavity. Corotating and counter-rotating modes are given with filled and hatched columns, respectively.

which imply no mode conversion because the period of the corrugation is small compared to $\lambda/2$, the free space half-wavelength. In particular, 72 slots with a depth $d = 0.5$ mm and a width $l = 0.4$ mm of the grooves are taken. The influence of the corrugation on the eigenvalue is shown in Fig. 3. The normalized surface impedance w of the corrugated wall given

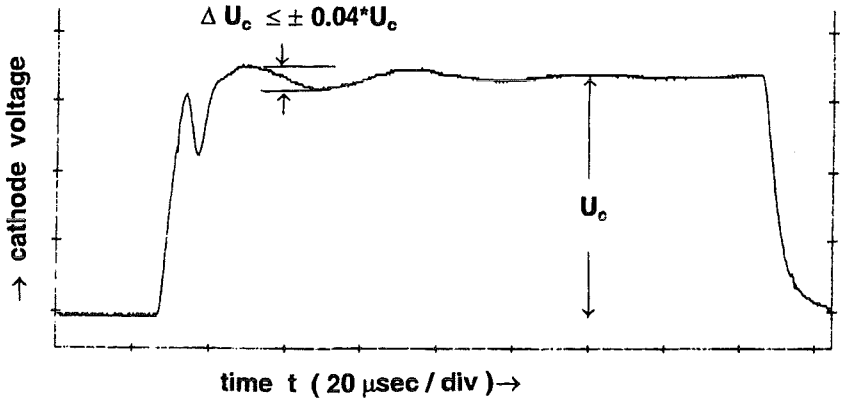

Fig. 5. A typical shape of the high-voltage pulse.

by [7]: $w = (l/s)\,.\tan(2\pi d/\lambda)$ has a value >2 within the resonator. Here, $s < \lambda/2$ is the period of the corrugation.

Appropriate tapering of the rod, together with the impedance corrugation, results in a significantly decreased diffractive quality factor of any mode which is influenced by the rod. The range of C in the cavity is: $3.66 < C < 3.82$. It is chosen such that the working mode is only slightly influenced by the inner rod. Then its Q-factor remains high, while the diffractive quality factors of all other modes with higher radial index are reduced and, consequently, the starting currents are increased. Modes with lower radial index couple significantly less to the electron beam and, therefore, also have a high starting current. The mode spectrum of the product quality factor $Q\cdot$ (relative coupling coefficient) is given in Fig. 4. Only the azimuthal neighbors $TE_{27,16}$ and $TE_{29,16}$, which have almost the same caustic radius as the operating mode and, therefore, are only slightly influenced by the inner conductor, remain as serious competitors. Their Q-factor is almost the same with that of the operating mode and, thus, competition through the phase-amplitude mode interaction can still occur.

To suppress this kind of competition, the azimuthal neighbors may be converted inside the cavity to modes which have a reduced Q-factor and couple out from the resonator. For the conversion, the azimuthal neighbors must be degenerate with two other modes in the C-range of the cavity ($3.66 < C < 3.82$). In the presented case, the azimuthal neighbors $TE_{-27,16}$ and $TE_{-29,16}$ are degenerate within the C-range of cavity with the $TE_{+17,19}$ and $TE_{+15,20}$ modes, respectively. The conversion of the right-hand rotating $TE_{-27,16}$ and $TE_{-29,16}$ modes to the left-hand rotating $TE_{+17,19}$ and $TE_{+15,20}$ modes (difference of the azimuthal indices ($\Delta m = 44$) can be achieved by introduction of a mode-converting longitudinal corrugation on the outer cavity wall (rippled wall converter) according to the formula

$$R_c = R_{c,0} + \rho\cos(\Delta m\phi).$$

where $R_{c,0} = 29.81$ mm is the mean radius of the outer wall, $\rho = 0.066$ mm is the amplitude of corrugations, and $\Delta m = 44$. The corrugation amplitude ρ is optimized in order to keep the unwanted conversion of the operating cavity mode to the modes $TE_{+16,q}$ lower than 2% and to reduce the Q-values of the competing neighbors by a factor of about three. The length of the converter is 20 mm, equal to the length of the cavity midsection. In this way, the mode competition with the azimuthal neighbors can be suppressed [13] and stable single-mode operation can be improved, as has already been verified at IAP. The longitudinal corrugations cause only a marginal (<4%) increase of the ohmic losses at the cavity wall. This is not considered to be of importance for the limitations in CW operation. In addition, the corrugations cause a small (≤2%) unwanted conversion of the design mode. In the experiment described here, a sufficient range of stable single-mode operation has been observed. Therefore, there was no need of an additional reduction of mode competition.

Self-consistent codes, which compute the electron beam-RF wave interaction, predicted an output power of 1.5 MW at 139.97 GHz in the $TE_{28,16}$ mode at a beam current of 42 A with an overall efficiency of 40%. The peak ohmic losses (ideal copper at room temperature) are calculated to be 0.63 kW/cm^2 on the outer wall of the resonator and 0.07kW/cm^2 on the inner conductor wall.

A nonlinear output taper (Fig. 2), having low mode conversion, adapts the diameter of the cavity to the diameter of the collector. Mainly because of voltage depression the inner rod ends above the nonlinear part of the output taper about 25 cm above the cavity.

C. Collector and Output Window

The investigated coaxial gyrotron has an axial waveguide output with a fused silica window of 100-mm diameter and a thickness of 4.61 mm, corresponding to $9\lambda_e/2$ of the $TE_{28,16}$ mode at 140 GHz. The window is transparent at the design mode. However, there is power reflection of about 15% at the frequencies of the nearest competitors, the $TE_{27,16}$ and $TE_{29,16}$ modes. The electron-beam collector is part of the output waveguide with a diameter of 100 mm. At the design parameters the estimated electron-beam power density at the collector surface is as high as 50 kW/cm^2, thus, limiting the maximum allowable pulselength to about 0.5 ms.

The gyrotron version with lateral dual-beam output will have a single-stage depressed collector with an inner diameter of 300 mm, allowing a maximum pulselength of several 10 ms. Two output windows out of fused silica transparent for the

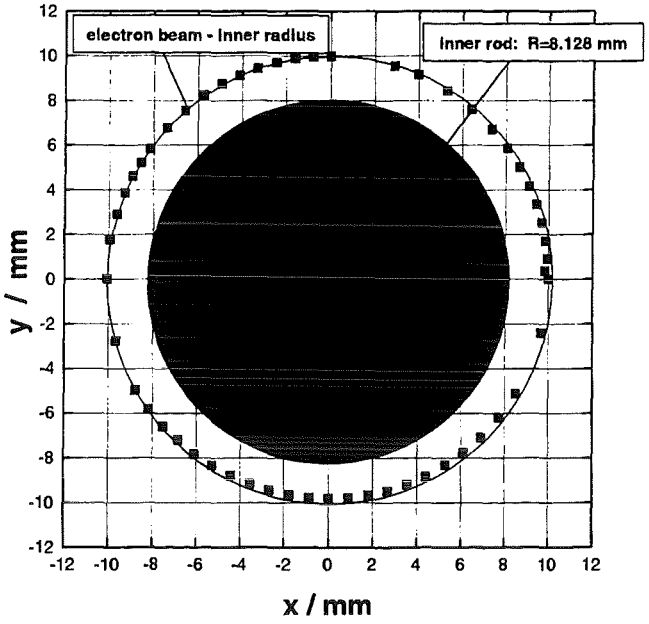

Fig. 6. Position of the electron beam relative to the inner rod at the entrance of the cavity.

Gaussian mode at 140 GHz will be used.

III. Experimental Operation and Results

A. Performance of the Measurements

The measurements have been performed in short-pulse operation. The most data have been taken with a pulselength of 0.15 ms. The repetition rate was 1–2 Hz. However, with low repetition, single pulses have been performed up to 0.5 ms. The available high-voltage power supply delivered a maximum voltage of about $U_c \approx 86$ kV at a beam current $I_b = 50$ A. The shape of the high-voltage pulse was characterized by an overshooting of about 4% as shown in Fig. 5. This overshooting is related to the fast rise time required for operation at the short pulses. The RF power has been measured as an average over typically 30 pulses with a ballistic calorimeter. With a contiguous filter bank consisting of ten 2-GHz channels, a signal of the generated RF power has been observed simultaneously in the different frequency channels, giving information as to whether there was single-mode or multimode oscillation in the cavity. The time dependence of the frequency during a pulse was measured with a time-frequency analyzer. For investigation of the waveguide-mode purity a measurement of the near-field and far-field pattern of the RF power radiated out of the open waveguide has been performed using a thermocamera. The far-field conditions are achieved at the focal plane of a parabolic-shaped teflon lens placed at the end of the open output waveguide [14].

B. Alignment of the Electron Beam

Before assembling the gyrotron tube, all parts were aligned mechanically. However, it turned out that a realignment of the inner rod, with respect to the hollow electron beam became necessary under operating conditions, in the fully installed tube. The realignment of the inner rod, relative to the electron beam, has been performed by using a set of dipole coils in the sc magnet, which enables shift of the electron beam radially in the cavity region until it touches the rod. This is measured by an increase of the current to the inner rod. To perform the alignment, the inner rod is shifted until it becomes concentric to the electron beam. The result of the alignment of the inner rod, relative to the beam, is shown in Fig. 6. The deviation from concentricity is less than 0.1 mm. In the used setup, an alignment of the beam relative to the outer cavity wall was not performed since it was not possible to measure the coaxiality of both of these under operating conditions. From previous measurements, it has been estimated that a misalignment of the beam and the cavity may be as high as about 0.5 mm.

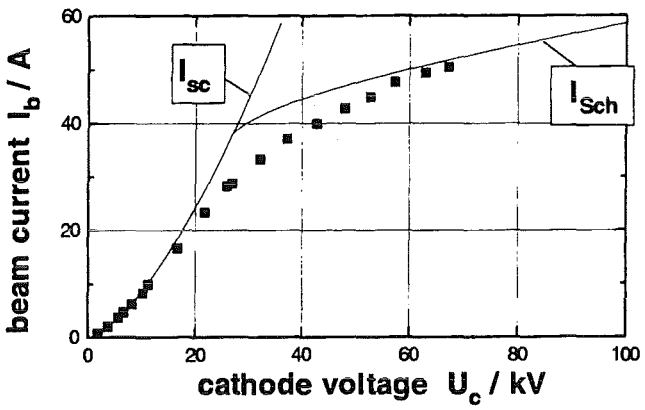

Fig. 7. Measured beam current I_b versus cathode voltage U_c at constant cathode heating. Comparison with space charge limited current I_{sc} and I_{Sch} due to Schottky effect.

C. Electron Emission and the Beam Current

The dependence of the beam current versus cathode voltage is shown in Fig. 7 for a constant cathode heating power and a constant magnetic field. At low voltages the current follows the space charge limited value

$$I_{sc}/\mathrm{A} = 0.272 \cdot (U_c/\mathrm{kV})^{1.5}.$$

At higher voltages the dependence of I_b approaches the value according to the Schottky effect [15]

$$I_{\mathrm{Sch}}/\mathrm{A} \cong 37 \cdot \exp[0.0566\{(U_b/\mathrm{kV})^{0.5} - (U_{sc}/\mathrm{kV})^{0.5}\}]$$
$$\text{with } U_{\mathrm{sc}} \cong 26.5 \text{ kV}.$$

The transition between the two regions is relatively wide and is thought to be a result of nonuniform emission, which may be one reason for an enhanced velocity spread.

An unstable behavior of the electron beam has been observed at a velocity ratio above $\alpha \approx 1.2$. When the gyrotron was operated in modes with frequencies having high window reflections, the stability limit was shifted even toward lower α values. The occurrence of the instability is thought to be related to electrons reflected at the magnetic mirror. The mechanism of the reduction of the stability due to reflected RF power flowing toward the gun is not yet clear.

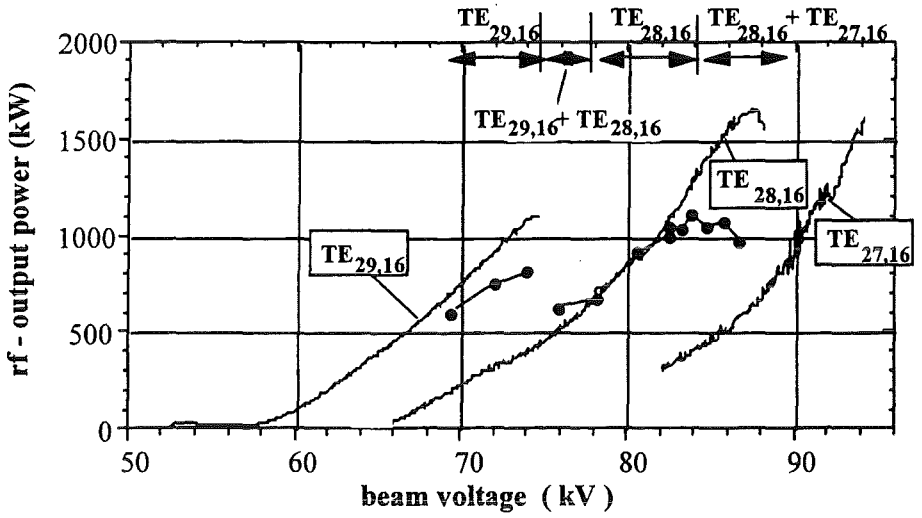

Fig. 8. RF output power versus beam voltage. $I_{cav} = 50 - 52$ A, $B_{cav} = 5.62$ T. Experimental results are given as points, with oscillating modes indicated at top. Solid lines are stable single-mode operation points from multimode calculations performed with experimental parameters and $\delta\beta_{\perp rms} = 6\%$.

D. RF Operation in the Design Mode

The RF operation delivered encouraging results. The design working mode $TE_{28,16}$ was found to oscillate stably over a wide parameter range. This proves the suppression of possible competing modes by the tapered and impedance corrugated rod. A maximum RF output power of 1.17 MW with an output efficiency $\eta_{out} = 27.2\%$ has been measured in the $TE_{28,16}$ mode in single-mode operation at $U_c = 86$ kV, $I_b = 50$ A and $B_{cav} = 5.63$ T. According to numerical calculations, the corresponding transverse efficiency $\eta_\perp$ is around 57% since the velocity ratio is only 1.0 having a numerically calculated spread $\delta\beta_{\perp rms} = 6\%$. The measured frequency of 139.96 GHz is close to the calculated value. The internal losses in the cavity, the output taper and the window are estimated to be about 5.5%.

Fig. 8 shows as an example the measured and the numerically calculated RF output power versus the beam voltage for a magnetic field of $B_{cav} = 5.62$ T and a beam current between 50 A and 52 A. The calculations have been performed with a multimode code [16] using the geometry of the cavity and the operating parameters without any fitting. For the velocity spread $\delta\beta_{\perp rms} = 6\%$ has been taken. As expected from the numerical calculations the azimuthal neighbors $TE_{29,16}$ at 142.02 GHz and $TE_{27,16}$ at 137.86 GHz, which are the remaining competitors, are limiting the stability region of the working mode in the $U_c - B_{cav}$ parameter space. The experimentally observed regions with single and multimode oscillation are indicated at the top of Fig. 8. At a given magnetic field the $TE_{29,16}$ mode oscillates at a voltage below, and the $TE_{27,16}$ above, the oscillating range of the $TE_{28,16}$ mode. Single mode oscillation of the $TE_{28,16}$ mode is found within several kV of U_c. The regions of oscillations of the three measured modes agree well with the numerical predictions. Only the experimental transition region is wider than expected. According to calculations the RF power should rise up to $U_c = 87$ kV while the measured values reach a maximum around 84 kV and above $\approx$86 kV the $TE_{27,16}$ mode is oscillating. In the region between $U_c = 84$–86 kV there is a small amount of the $TE_{27,16}$ mode present simultaneously with the $TE_{28,16}$ mode. This gives an explanation for the reduced efficiency and output power in that region. However, this multimoding is not predicted by the numerical calculations. One reason for the discrepancy is thought to be caused by window reflections, which support the competing $TE_{27,16}$ mode, since the RF window is optimized for 140 GHz and has a reflectivity of about 15% at the frequency of the competitor. Another reason for the loss of single-mode stability at higher voltages is the overshooting of the accelerating voltage (Fig. 5). At the peak of the voltage the competing mode starts oscillations, and after the voltage dropped again these oscillations may remain. Due to the reduction of the single-mode oscillating region the design operating parameters are not accessible. The influence of the window reflections on the gyrotron operation is mainly a problem of tubes with an axial RF output. This effect is expected to be of no importance in the tube with radial output, as has already been proven experimentally with conventional hollow waveguide-cavity gyrotrons.

To estimate the influence of a misaligned inner rod on the mode purity a series of measurements was performed with defined misalignments up to ± 0.6 mm. The distribution of RF power at the output was displayed by observing the thermal image on a target. Single mode operation of the gyrotron was possible with the misaligned rod but at changed operating parameters, however. The influence on efficiency was not investigated. No significant mode conversion due to the radial shift of the inner rod has been observed.

E. Frequency Step Tuning

The possibility of frequency step tuning has been proven over a range from 115.6 GHz to 164.2 GHz. Frequency step tuning was performed by changing the magnetic field with constant magnetic compression corresponding to a beam radius $R_b = 10.0$ mm. The beam radius was not optimized for maximum output power at the different modes except for the

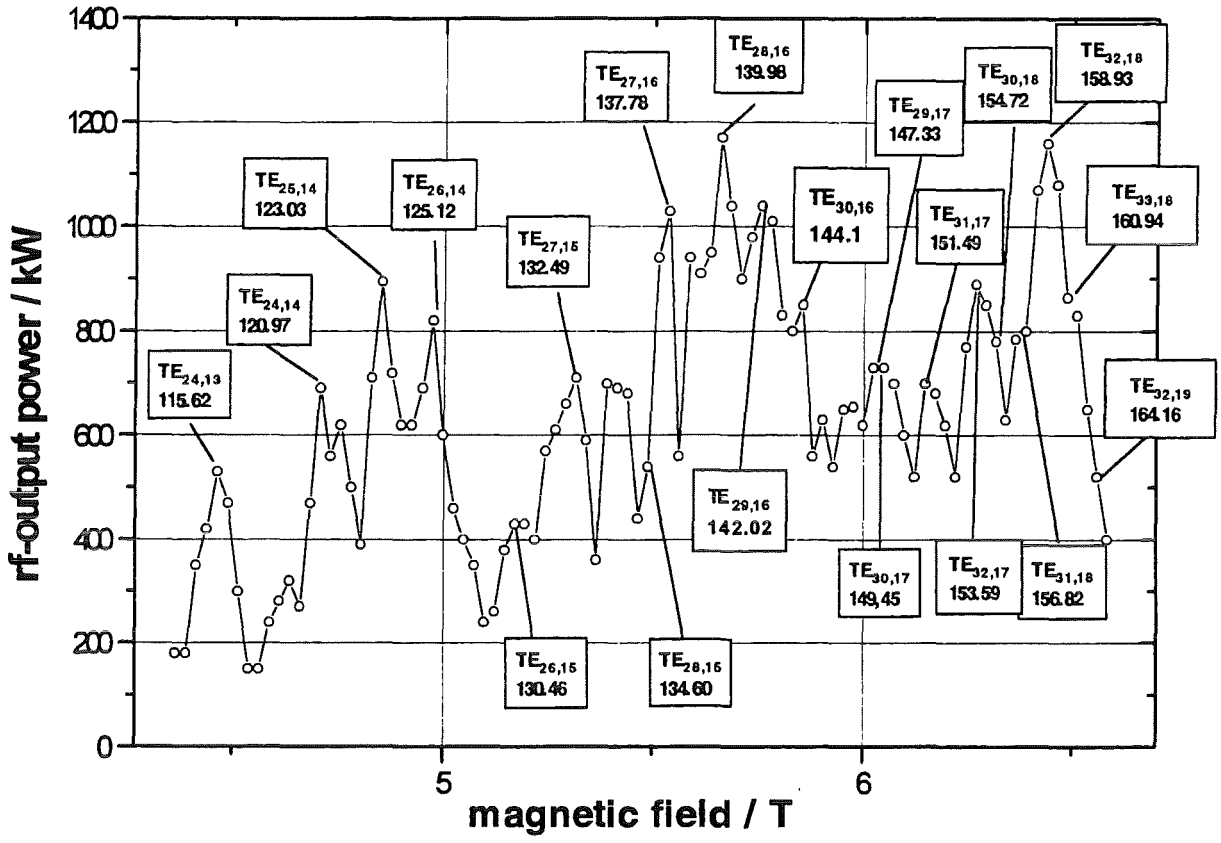

Fig. 9. RF output power versus magnetic field. I_b = 50–52 A. Constant magnetic compression with R_b = 10.0 mm except for the $TE_{28,16}$-mode. Each marked point represents stable single-mode operation with maximum power in the indicated mode.

$TE_{28,16}$ mode. Under that condition, single-mode operation has been achieved in 20 different modes as indicated in Fig. 9. Output powers around 1 MW and output efficiencies above 25% have been achieved near frequencies where the window reflection is minimal (122, 140, and 158 GHz).

Fig. 10 shows the maximum output power P_{out} measured in the different modes together with the output and transverse efficiencies, η_{out} and $\eta_\perp$, the RF-power reflection coefficient R of the window, the caustic radius R_{caust}, and the velocity ratio α. In modes with high reflection coefficient R, the output power P_{out}, and the corresponding efficiencies η_{out} and $\eta_\perp$ have a minimum. At this modes the gun could not be operated at the desired acceleration voltage because of beam instabilities, probably due to leakage of reflected and converted RF power toward the gun. This resulted also in reduced α values. Some influence on P_{out} is also due to the constant beam radius which has not been adjusted for optimum beam-RF interaction in the different modes. It is, therefore, expected that in a radial version with an appropriate broadband q.o. output coupling system any of the possible oscillating modes shown in Fig. 9 will have an output power and efficiency similar to modes at frequencies without window reflections. In some modes the transverse efficiency is as high as about 60%. Using a single stage depressed collector a total efficiency around 50% is expected even with the relatively low α. At frequencies above the design value the maximum achievable velocity ratio is reduced below the design value due to the need of higher magnetic field and the fact that the gun is of diode type.

IV. Gyrotron with a Radial Dual-Beam RF Output

A. Gyrotron with Radial Dual-Beam Output and a Single-Stage Depressed Collector

A gyrotron relevant for cw-operation with a radial dual RF beam output and a depressed collector (Fig. 11) is under construction. Components as output windows and the depressed collector are already available. The double-beam launcher and the mirrors are under fabrication.

For operation with two RF output windows a q.o. mode converter system based on a two-step mode conversion scheme, $TE_{-28,16}$ to $TE_{+76,2}$ to TEM_{00}, which generates two narrowly directed (60° at the launcher) output wavebeams has been designed [17] as shown in Table II and Fig. 12. High conversion efficiencies are expected. If one employs, as in conventional hollow waveguide cavity gyrotrons, a q.o. mode converter for the operating volume mode of the cavity, the dimensions of the mirror system are excessively large for a dual-beam output since the azimuthal angle of divergence φ of the radiation in geometric optical approximation is quite large, e.g., $\varphi = 2\arccos(m/\chi_{mp}) = 142.6°$ for the $TE_{28,16}$ mode (Fig. 12). For a high-order WGM of the type $TE_{m,2}$ the azimuthal angle of divergence φ of the radiation is sufficient

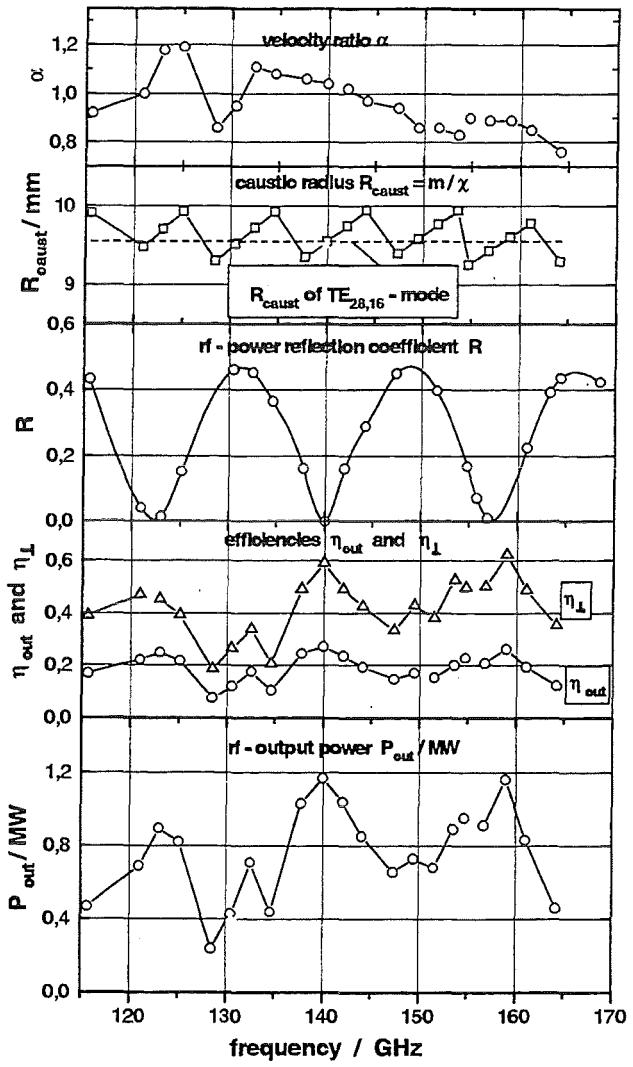

Fig. 10. RF output power P_{out}, output and transverse efficiency η_{out} and $\eta_\perp$, reflection coefficient R, caustic radius R_{caust}, and velocity ratio α versus frequency. Each point corresponds to one mode. Experimental conditions as in Fig. 9.

small, e.g., $\varphi = 2\arccos(m/\chi_{mp}) = 59.1°$ for the $TE_{76,2}$ mode, since the representing rays from its caustic are located closer to the waveguide wall. Thus a double-cut q.o. launcher can generate two diametrically opposed narrowly directed output wavebeams. However, it should be pointed out that the two step mode conversion works properly only for the design mode and cannot be used if the possibility of frequency tuning is considered.

The conversion of the cavity mode to the degenerate whispering gallery mode (WGM) is achieved by introduction of longitudinal corrugations in the output taper (1.5°) consisting of $\Delta m = 104$ slots according to the formula

$$R_w = R_{w,0}(z) + \rho \cos(\Delta m \phi)$$

where $R_{w,0}(z)$ is the mean radius of the output waveguide wall, $\rho = 0.05$ mm is the amplitude of corrugations, and $\Delta m = 104$.

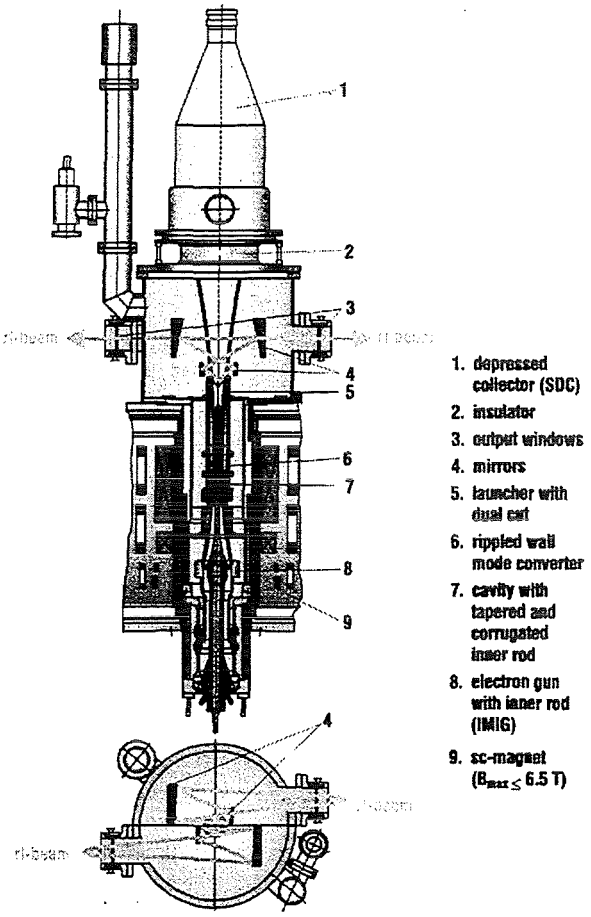

Fig. 11. Schematic layout of the coaxial cavity gyrotron with dual RF beam output.

TABLE II
TWO-STEP MODE CONVERSION SEQUENCE COMPATIBLE WITH THE COAXIAL GYROTRON DUAL-BEAM OUTPUT

$TE_{-28,16}$	$TE_{+76,2}$	TEM_{00}
volume mode	whispering gallery mode	wave beam
degenerate modes longitudinal $\Delta m = 104$, waveguide mode converter		q.o. dual-beam output through two rf output windows

The q.o. converter will use an improved dimple double-beam launcher with $\Delta m_1 = 2$ and $\Delta m_2 = 6$ perturbations for longitudinal and azimuthal bunching of the 2-mm wavebeams [17].

V. SUMMARY

A coaxial-cavity gyrotron with an axial RF output has been tested. A version of the tube with a dual-RF beam output is under fabrication. The power capability of the coaxial gyrotron is higher than of conventional gyrotrons because higher-order volume modes can be used. The tapering and the impedance corrugation of the inner rod reduce mode competition such that only the azimuthal neighbors remain

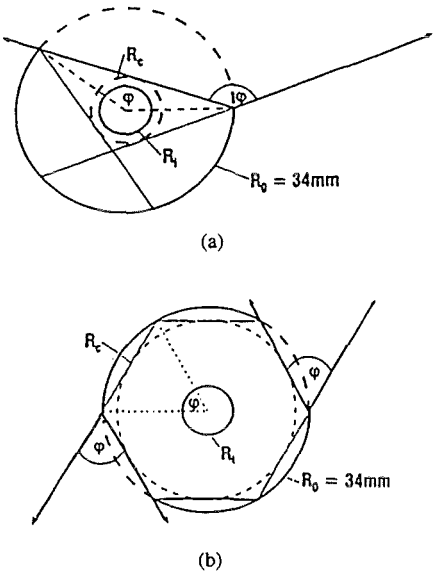

Fig. 12. Azimuthal angle of radiation (a) for the $TE_{76,2}$-mode, foreseen for use in the double-beam q.o. mode converter, and (b) for the $TE_{28,16}$-cavity mode with single-beam q.o. mode converter. The caustic radius $R_c = (m/\chi_{mp}) \cdot R_0 = 29.6$ mm and 10.9 mm for the $TE_{76,2}$ and $TE_{28,16}$ mode, respectively.

as competitors. In the experiment, a single-mode operation has been found over a wide range of parameters. A maximum RF power of 1.17 MW has been achieved with 27.2% output efficiency corresponding to a transverse efficiency of about 60%. The experimental and numerical results agree well if for the simulations the experimental parameters are taken. Stable operation was achieved only at relatively low α values ($\alpha < 1.2$). Above that value beam instability occurred, presumably due to reflected and trapped electrons because of high velocity spread. Step frequency tuning has been performed between 115.6 and 164.2 GHz. Twenty modes have been excited in single-mode operation. As an example an output power of 0.9 MW has been measured in the $TE_{25,14}$ mode at 123.0 GHz and 1.16 MW in the $TE_{32,18}$ mode at 158.9 GHz. At frequencies with high window reflections the occurrence of beam instability was enhanced, presumably due to leakage of reflected and converted RF power toward the gun. In those cases α had to be reduced further down to values below one in order to achieve stable operation. As it is known from conventional gyrotrons, the influence of window reflections on the gyrotron operation is mainly restricted to tubes with axial RF output and it becomes of minor importance in tubes with radial RF output. The investigations will be continued with a gyrotron setup with a dual RF beam output which is now under fabrication.

ACKNOWLEDGMENT

The authors wish to thank H. Baumgärtner, H. Budig, P. Grundel, W. Leonhardt, N. Münch, J. Szczesny, and R. Vincon of the gyrotron team technical staff for the mechanical design, the precise machining and the careful assembly of the tube as well as for their assistance during the experiments. They also thank E. Borie for proofreading the manuscript.

REFERENCES

[1] C. T. Iatrou, D. R. Whaley, S. Kern, M. Thumm, M. Q. Tran, A. Möbius, H.-U. Nickel, P. Norajitra, A. Wien, T. M. Tran, G. Bon-Mardion, M. Pain, and G. Thonon, "Feasibility study of the EU Home Team on a 170-GHz 1-MW CW gyrotron for ECH on ITER," *Int. J. Infrared and Millimeter Waves*, vol. 16, pp. 1129–1158, 1995.

[2] K. Sakamoto, A. Kasugai, M. Tsuneoka, K. Takahashi, T. Imai T. Kariya, Y. Okazaki, K. Hayashi, Y. Mitsunaka, and Y. Hirata, "Development of 170-GHz high-power long-pulse gyrotron for ITER," presented at *21st Int. Conf. Infrared and Millimeter Waves*, Berlin, Germany, 1996, paper AT1, ISBN 3-00-000800-4.

[3] A. L. Goldenberg and A. G. Litvak, "Recent progress of high-power millimeter wavelength gyrodevices," *Phys. Plasmas*, vol. 2, pp. 2562–2572, 1995.

[4] T. Kimura, J. P. Hogge, R. Advani, D. Denison, K. E. Kreischer, R. J. Temkin, and M. E. Read, "Investigation of megawatt power level gyrotrons for ITER," presented at *21st Int. Conf. Infrared and Millimeter Waves*, Berlin, Germany, 1996, paper AM1, ISBN 3-00-000800-4.

[5] S. N. Vlasov, L. I. Zagryadskaya, and I. M. Orlova, "Open coaxial resonators for gyrotrons," *Radio Eng. Electron. Phys.*, vol. 21, pp. 96–102, 1976.

[6] M. E. Read, G. S. Nusinowich, O. Dumbrajs, G. Bird, J. P. Hogge, K. Kreischer, and M. Blank, "Design of a 3-MW 140-GHz gyrotron with a coaxial cavity," *IEEE Trans. Plasma Sci.*, vol. 24, no. 3, pp. 586–595, 1996.

[7] C. T. Iatrou, S. Kern, and A. B. Pavelyev, "Coaxial cavities with corrugated inner conductor for gyrotrons," *IEEE Trans. Microwave Theory Tech.*, vol. 41, pp. 56–64, 1996.

[8] J. J. Barroso and R. A. Correa, "Coaxial resonator for a megawatt, 280-GHz gyrotron", *Int. J. Infrared Millimeter Waves*, vol. 12, pp. 717–728, 1991.

[9] V. A. Flyagin, V. I. Khishnyak, V. N. Manuilov, A. B. Pavelyev, V. G. Pavelyev, B. Piosczyk, G. Dammertz, O. Höchtl, C. T. Iatrou, S. Kern, H.-U. Nickel, M. Thumm, A. Wien, and O. Dumbrajs, "Development of a 1.5-MW coaxial gyrotron at 140 GHz," in *Conf. Dig. 19th Int. Conf. Infrared Millimeter Waves*, 1994, pp. 75–76.

[10] B. Piosczyk, O. Braz, G. Dammertz, C. T. Iatrou, S. Kern, A. Möbius, M. Thumm, A. Wien, S. C. Zhang, V. A. Flyagin, V. I. Khishnyak, A. N. Kuftin, V. N. Manuilov, A. B. Pavelyev, V. G. Pavelyev, A. N. Postnikova, and V. E. Zapevalov, "Development of a 1.5-MW, 140-GHz Coaxial Gyrotron," in *Proc. 20th Int. Co..f. Infrared Millimeter Waves*, 1995, pp. 423–424.

[11] V. K. Lygin, V. N. Manuilov, A. N. Kuftin, A. B. Pavelyev, and B. Piosczyk, "Inverse magnetron injection gun for a 1.5-MW, 140-GHz gyrotron," *Int. J. Electron*, vol. 79, pp. 227–235, 1995.

[12] C. T. Iatrou, "Mode selective properties of coaxial resonators," *IEEE Trans. Plasma Sci.*, vol. 24, no. 3, pp. 596–605, 1996.

[13] S. Kern, C. T. Iatrou, and M. Thumm, "Investigations on mode stability in coaxial gyrotrons," in *Proc. 20th Int. Conf. Infrared and Millimeter Waves*, 1995,, pp. 429–430.

[14] O. Braz, A. Arnold, M. Losert, A. Möbius, M. Pereyaslavets, and M. Thumm, "Low-power excitation and mode-purity measurements on gyrotron-type modes of higher order," presented at *21st Int. Conf. Infrared and Millimeter Waves*, Berlin, 1996, paper ATh6, ISBN 3-00-000800-4.

[15] A. S. Gilmour, Jr., *Principle of Travelling Wave Tubes*. Norwood, MA, Artech House, 1994.

[16] S. Kern, "Numerical codes for interaction calculations in gyrotron cavities at FZK," presented at *21st Int. Conf. Infrared and Millimeter Waves*, Berlin, Germany, paper AF2, Berlin, 1996, ISBN 3-00-000800-4.

[17] M. Thumm, C. T. Iatrou, A. Möbius, and D. Wagner, "Built-in mode converters for coaxial gyrotrons," presented at *21st Int. Conf. Infrared and Millimeter Waves*, BerlinGermany, paperAM6, ISBN3-00-000800-4.

Bernhard Piosczyk was born in Matzkirch/Cosel, Poland, in 1943. He received the Dipl. Ing. degree in physics, in 1969, from the Technical University of Berlin, Germany and the Dr. rer. nat. degree in 1974 from the University of Karlsrhue, Karlsruhe, Germany.

Since 1970 he has been working at the Research Center (Forschungszentrum) Karlsruhe, first in the field of RF superconductivity for accelerator application, then in the development of CW, high-current H^+ and H^- ion sources and since 1987 in the development of high power gyrotrons.

Oliver Braz was born in Simmern, Germany, on November 28, 1965. He received the Dipl. Ing. degree in electrical engineering from the University of Karlsrhue, Karlsruhe, Germany, in 1993.

He has been with the Institute of Microwave and Electronics at the University of Karlsruhe since December 1993. The main emphasis of his work is on various millimeter-wave diagnostics for high-power gyrotrons in the Gyrotron Development and Microwave Division in the Institute for Technical Physics of the Research Center (Forschungszentrum) at Karlsruhe. His research deals with the experimental analysis and optimization for the RF-power out-coupling of gyrotron oscillators.

Günter Dammertz was born in Moers, Germany, on March 3, 1942. He studied physics in Bonn, Germany, at the Rheinische Friedrich Wilhelm University and got the diploma by a work on electron-gamma-angle-correlation. In 1972 he received the Dr. rer. nat. degree in physics with a work on superconducting RF-structures from the University of Karlsruhe, Karlsruhe, Germany.

In 1968 he joined the Research Center (Forschungszentrum) Karlsruhe. He was involved in the development of superconducting RF-accelerators and particle separators, in the development of high-current neutral beam sources and in the investigation of a spallation source. Since 1984 he has been working on the development of high-power gyrotrons, especially in the experimental program and in technical investigations.

Christos T. Iatrou was born in Elefsina, Greece, on April 19, 1962. He received the Dipl. Eng. degree from the Department of Electrical Engineering, University of Patras, Greece, in 1986, and the Ph.D. degree from the Department of Electrical Engineering, National Technical University of Athens, Greece, in 1990.

From October 1990 to December 1992 he held a postdoctoral appointment, at Thomson Tubes Electroniques, Vélizy, France, where he worked on the theory of gyroklystron amplifiers and the development of quasioptical mode converters for gyrotrons. From March 1993 to August 1993 he was Research Fellow at the National Institute of Nuclear Physics (INFN), Legnaro, Italy, where he worked on the development of an electron cyclotron resonance ion source. Since October 1993, he has been with the Research Center (Forschungszentrum) Karlsruhe, Karlsruhe, Germany, working on the development of high-power gyrotron oscillators. His research interests are focused on the physics of electron beam devices, such as gyrotrons, gyroklystrons, harmonic-gyrotrons, and slow-wave electron cyclotron masers.

Stefan Kern was born in Bruchsal, Germany, on December 25, 1965. He received the Dipl. Eng. and the Ph.D. degrees in electrical engineering from the University of Karlsruhe, Karlsruhe, Germany, in 1992 and 1996, respectively.

From 1993 to 1996 he was with the Gyrotron Development and Microwave Technology Division, the Institute for Technical Physics of the Research Center (Forschungszentrum) at Karlsruhe as a Doctoral Fellow of he Gradiuertenkolleg Numerische Felderechnung at the University of Karlsrhue, Karlsruhe, Germany. He is now working as a Research Assistant at the Institut für Höchstfrequenztechnik und Elektronik of the University of Karlsruhe. His research interests concentrate on the numerical simulation of electromagnetic fields in cavities and applicators at microwave frequencies and in the millimeter wave region. He is particularly involved in the development of high-power gyrotrons with advanced cavities.

Michael Kuntze was born in Berlin, Germany, in 1937. He received the Dipl. Phys. and the Dr. rer. nat. degrees from the University of Heidelberg, Germany, in 1962 and 1965, respectively.

Since 1965 he has been with the Institute of Experimental Nuclear Physics at the Research Center (Forschungszentrum) Karlsrhue, Karlsruhe, Germany. He was responsible for the development of a superconducting linear proton accelerator. During this time he has worked on accelerator applications in biology and medicine. Since 1983 he has been with the Institute of Technical Physics at the Research Center Karlsruhe, and he is involved in the gyrotron development group. His research topics include the development of gyrotrons for technical applications outside the field of fusion.

A. Möbius, photograph and biography not available at the time of publication.

Manfred Thumm (SM'94) was born in Magdeburg, Germany, on August 5, 1943. He received the Dipl. Phys. and Dr. rer. nat. degrees in physics from University of Tübingen, Germany, in 1972 and 1976, respectively. At the University of Tübingen he was involved in the investigation of spin-dependent nuclear forces in inelastic neutron scattering. From 1972 to 1975 he was Doctoral Fellow of the Studienstiftung des deutschen Volkes.

In 1976 he joined the Institute for Plasma Research in the Electrical Engineering Department of the University of Stuttgart, Germany, where he worked on RF production and RF heating of toroidal pinch plasmas for thermonuclear-fusion research. From 1982 to May 1990 his research activities were mainly devoted to electromagnetic theory in the areas of component development for the transmission of very high-power millimeter waves through overmoded waveguides and of antenna stuctures for RF plasma heating with microwaves. In June 1990 he became a Full Professor at the Institute for Microwaves and Electronics at the University of Karlsrhue, Karlsruhe, Germany, and Head of the Gyrotron Development and Microwave Technology Division in the Institute for Technical Physics of the Research Center (Forschungszentrum) at Karlsruhe, where the current research projects are the development of high-power gyrotrons, windows, and transmission lines for nuclear fusion plasma heating and material processing.

Dr. Thumm is Chairman of the Chapter 8.6 (Vacuum Electronics and Displays) of the Information Technical Society (ITE) in the German VDE and member of the German Physical Society (DPG).

V. A. Flyagin, photograph and biography not available at the time of publication.

V. I. Khishnyak, photograph and biography not available at the time of publication.

V. I. Malygin, photograph and biography not available at the time of publication.

A. B. Pavelyev, photograph and biography not available at the time of publication.

V. E. Zapevalov, photograph and biography not available at the time of publication.

APPENDIX A2

Design and Experimental Operation of a 165-GHz, 1.5-MW, Coaxial-Cavity Gyrotron with Axial RF Output

C. T. Iatrou, O. Braz, G. Dammertz, S. Kern, M. Kuntze, B. Piosczyk, and M. Thumm, *Senior Member, IEEE*

***Abstract*—The development of a coaxial-cavity gyrotron operating in $TE_{31,17}$ mode at 165 GHz is presented. The selection of the operating frequency and mode are based on the limitations imposed by the maximum field of the superconducting (sc) magnet at Forschungszentrum Karlsruhe, Institut für Technische Physik (FZK), the use of the inverse-magnetron injection gun (IMIG) of the 140-GHz, $TE_{28,16}$ coaxial gyrotron and the possibility of transforming the cavity mode to a whispering gallery mode (WGM) appropriate for the dual-beam quasioptical (q.o.) output coupler and the two output windows, which are foreseen for the next lateral-output version of the tube. The tube with axial output has been tested at FZK to deliver maximum output power of 1.17 MW in the designed $TE_{31,17}$ mode with 26.7% efficiency at 164.98 GHz. Maximum efficiency of 28.2% was achieved at 0.9-MW output power. The design operating point with output power 1.36 MW and 36.7% efficiency was not accessible because of beam instabilities at high electron-velocity ratio α, presumably caused due to high electron-velocity spread. Power at higher frequencies was also detected: 1.02 MW at 167.14 GHz in $TE_{32,17}$ mode with 26.8% efficiency, 0.63 MW at 169.46 GHz in $TE_{33,17}$ mode with 18% efficiency, and 0.35 MW at 171.80 GHz in $TE_{34,17}$ mode with 13.3% efficiency.**

***Index Terms*— Coaxial cavity gyrotron, frequency tunability, magnetron injection gun.**

I. Introduction

CONVENTIONAL cylindrical-cavity gyrotrons are limited in output power and operating frequency (≈1 MW at 170 GHz) due to ohmic wall loading, mode competition, and limiting beam current [1]–[5]. The problem of ohmic wall loading can be reduced by increasing the cavity diameter and using volume modes. The increased cavity diameter and the high operating frequency require operation in high-order modes, where the mode spectrum is dense and mode competition could prevent the gyrotron from stable single-mode operation. Furthermore, the use of volume modes, which do not load significantly the cavity walls, leads to lower limiting currents and reduced total efficiency because of the increased voltage depression. These limiting factors can be considerably reduced by the use of coaxial resonators [6]–[8], which, by tapering the inner conductor, offer the possibility of selective influence of the diffractive quality factor of different modes, allowing operation in high-order volume modes with reduced mode competition problems. In addition, the presence of the inner conductor practically eliminates the restrictions of voltage depression and limiting current. Gyrotrons with coaxial cavities have the potential to generate, in continuous wave (CW) operation, RF-output powers in excess of 1 MW at frequencies above 140 GHz. In general, two methods are available in a coaxial-cavity configuration for an effective control of the total Q factor, and hence of the starting current, of different modes: 1) the use of a longitudinally corrugated tapered inner conductor [7] and 2) the use of a resistive inner conductor [9]. The first method seems preferable for high-power operation and it has been followed in the development of coaxial gyrotrons for fusion applications at Forschungszentrum Karlsruhe, Institut für Technische Physik (FZK).

The goal of the reported development is to achieve an output power of 1.5 MW for an ITER-relevant device, that is a tube able for CW operation with efficiency enhancement due to a depressed collector. The first step of the development is the design, construction, and experimental test of such a tube with axial radio frequency (RF) output. For this, the cavity of the 140-GHz, $TE_{28,16}$ coaxial gyrotron of FZK [10]–[12] has been replaced by a new coaxial cavity with tapered and corrugated inner conductor designed to oscillate at 165 GHz in the $TE_{31,17}$ mode. The RF-output window has also been replaced by an edge-cooled single-disk Boron-Nitride window, transparent at the operating frequency. The rest of the tube [inverse-magnetron injection gun (IMIG), beam tunnel, and collector] remained unchanged. The gyrotron is designed to operate in short pulses (≤0.5 ms) because of the heat-load capability of the collector. In a next step toward CW operation the tube will have a lateral output using a dual-beam quasioptical (q.o.) mode converter and a new single-stage depressed collector.

II. Selection of the Operating Mode and Cavity Design

There are two main limitations in the design of the coaxial gyrotron under description. The first is the use of the sc magnet

Manuscript received October 7, 1996; revised April 1, 1997. This work was supported by the European Fusion Technology Program (ITER Task No: G 52 TT 03 94-08-03 FE, ID No: T 24, Subtask 3) under the Project Kernfusion of the Forschungszentrum Karlsruhe.

C. T. Iatrou, G. Dammertz, M. Kuntze, and B. Piosczyk are with Forschungszentrum Karlsruhe, Institut für Technische Physik, Association EURATOM-FZK, Postfach 3640 Karlsruhe D-76021 Germany.

O. Braz, S. Kern, and M. Thumm are with Forschungszentrum Karlsruhe, Institut für Technische Physik, Association EURATOM-FZK, Postfach 3640 Karlsruhe D-76021 Germany; also with the Universität Karlsruhe, Institut für Höchstfrequenztechnik und Elektronik, Kaiserstrasse 12 Karlsruhe D-76128 Germany.

Publisher Item Identifier S 0093-3813(97)04865-0.

TABLE I
BEAM RADIUS AND ELECTRON-VELOCITY RATIO OF POSSIBLE OPERATING MODE FAMILIES FOR THE 165-GHz COAXIAL GYROTRON

azimuthal index	beam radius /mm	beam α
29	8.2	1.8
30	9.12	1.4
31	9.41	1.1
32	9.71	0.8

existing at FZK, which can reach a maximum field around 6.6 T and the second is the use of the IMIG of the 140-GHz, $TE_{28,16}$ coaxial gyrotron of FZK. This gun is designed to provide an electron beam of 50 A at 90 kV with an electron velocity ratio α of 1.4 at 5.54 T [13]. Due to the first limitation of the sc magnet and the requirement of an operating frequency in the range 165–170 GHz, the acceleration voltage has to be reduced close to 75 kV, in order to increase the cyclotron frequency through a reduced relativistic mass factor γ. The reduction of the accelerating voltage from 90 to 75 kV and the increase of the cavity magnetic field from 5.54 to 6.5 T result in a considerably reduced value of the electron-velocity ratio α. The only available way to increase the value of α is the increase of the magnetic compression through the reduction of the gun magnetic field. This means a smaller electron-beam radius in the cavity, which in turn is limited by the diameter of the nonremovable part of the inner conductor (16 mm), which is fixed to the IMIG and ends up just before the cavity.

Assuming a minimum acceptable beam radius in the resonator of 9 mm, only modes of the azimuthal families $m = 30$ (beam radius $R_b = 9.12$ mm) and $m = 31$ ($R_b = 9.41$ mm) were found to result in reasonable values of α, 1.40 and 1.10, respectively, according to simulations with the electron trajectory code EGUN (Table I). In view of the next version of the tube with a lateral output, the modes with azimuthal index $m = 30$ are excluded because none of them is degenerate with a WGM $TE_{m,2}$, in which the cavity mode should be transformed before the dual-beam output launcher [14]. From the modes of the azimuthal family $m = 31$ only the $TE_{31,17}$ mode (eigenvalue 94.62) is degenerate with a WGM mode, and in particular with the $TE_{83,2}$ mode (eigenvalue 94.69). Therefore, the $TE_{31,17}$ mode was selected as the operating mode of the 165-GHz coaxial gyrotron [14].

A coaxial resonator has been designed, according to the design principles presented in [7] and [16], to oscillate in the $TE_{31,17}$ mode at 165 GHz, and it is shown in Fig. 1. The cutoff section of 22 mm length is tapered by 3.0° and it is connected to the 22 mm long cylindrical midsection with parabolic roundings of 4 mm for reduced mode conversion. Power transmission toward the gun is practically zero and the mode purity of the downtaper is 99.3%. The linear part of the uptaper is 30 mm long with an angle of 1.5°. For the axial-output version of the tube, a nonlinear uptaper was designed and optimized to increase rapidly the diameter to 100 mm in a distance of 330 mm from the middle of the resonator, with negligible mode conversion (output mode purity 99.8%). The radius of the cylindrical part of the resonator is 27.38 mm

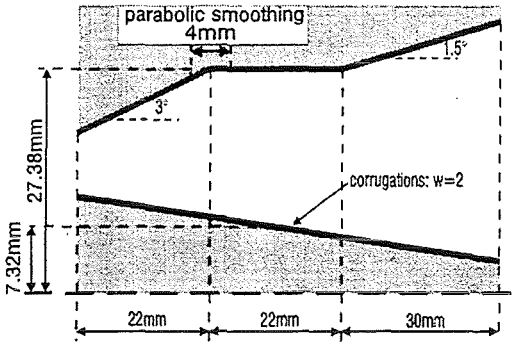

Fig. 1. Simulations model of the 165-GHz, $TE_{31,17}$ coaxial resonator.

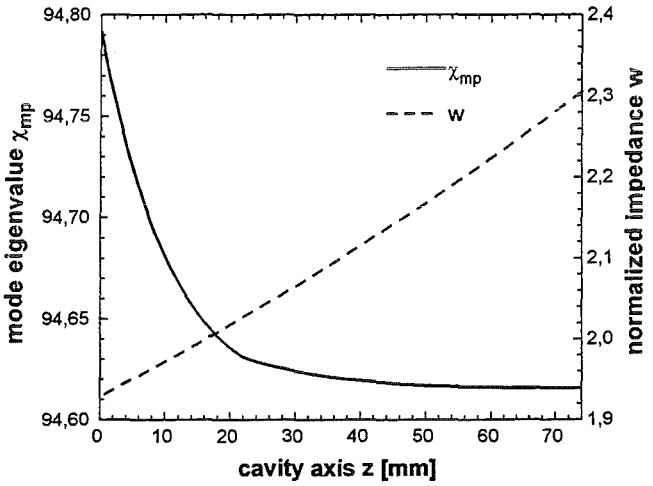

Fig. 2. Eigenvalue and normalized impedance of the $TE_{31,17}$ mode along the cavity axis.

$= 15\lambda_0$, where λ_0 is the free-space wavelength. The inner conductor has a radius of 7.32 mm at the middle of the cylindrical part of the resonator, and it is downtapered by 1° toward the output. The selection of the inner-conductor radius is based on mode discrimination and wall-loading considerations. The wall of this conductor is longitudinally corrugated with 72 rectangular slots of 0.35 mm width and 0.38 mm depth, a value which is close to 0.21 λ_0 ensuring effective mode discrimination and reduced problems from possible mode competition from second cyclotron harmonic interaction [16].

The normalized surface impedance $w = (l/s) \tan(\chi_{mp} d/R_o)$ of the corrugated wall [7] takes the value of 2.1 at the middle of the resonator. Here, s, l, and d are the period, the width, and the depth of the corrugations (see Fig. 1), χ_{mp} is the mode eigenvalue, and R_o is the outer wall radius of the cylindrical part of the resonator. In Fig. 2, the mode eigenvalue χ_{mp} and the normalized impedance w are presented along the cavity axis. The normalized impedance varies in the cylindrical part of the resonator from 2.03 to 2.14, and along the total resonator from 1.93 to 2.31. The negative slope of the mode eigenvalue curve along the cylindrical part results in a slight decrease by 8% of the diffractive Q of the mode from the Q of this mode in an equivalent regular cylindrical resonator with length 22 mm.

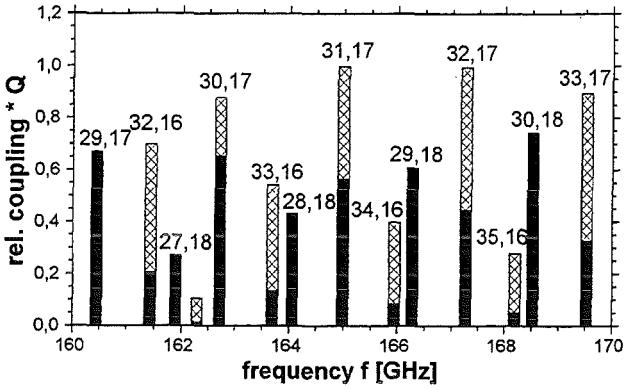

Fig. 3. Mode spectrum of the relative product (quality factor) * (coupling coefficient) for the 165-GHz coaxial gyrotron. Counter-rotating modes are given by filled columns.

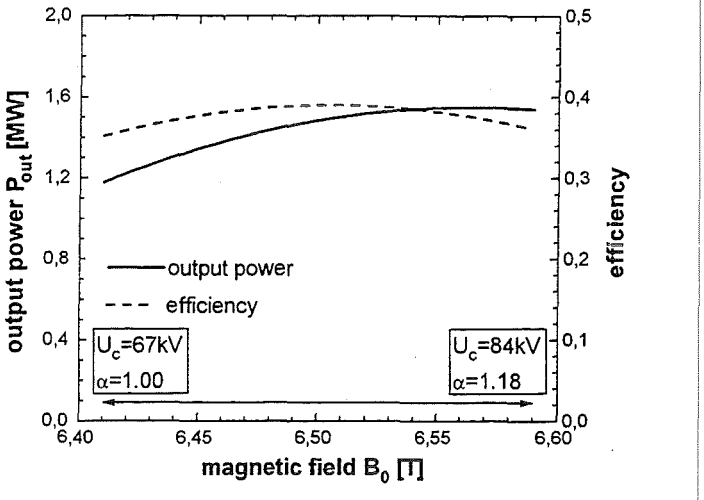

Fig. 4. Output power and efficiency of the $TE_{31,17}$ mode versus magnetic field. The cathode voltage is optimized for maximum power. The beam α follows adiabatically the cathode voltage and magnetic field. The beam current is fixed at 50 A.

The cold-cavity resonant frequency and diffractive Q of the $TE_{31,17}$ mode are 164.976 GHz and 3010. The relatively high diffractive Q is a result of the increased cavity length ($\approx$12 λ_0), which is necessary to compensate the moderate accelerating voltage ($\approx$75 kV) and the low electron-velocity ratio a ($\approx$1.0). The equivalent Gaussian length L_g of the cold-cavity field profile is 24.5 mm, which corresponds to a normalized interaction length $\mu = \pi\alpha\beta_\perp L_g/\lambda$ close to 16. The frequency separation between the operating mode $TE_{31,17}$ and its azimuthal neighbors $TE_{30,17}$ and $TE_{32,17}$ is 2.268 GHz and 2.283 GHz, while their diffractive Q is 2685 and 3254, respectively.

The radius of the inner conductor was selected to be 7.32 mm at the middle of the cavity midsection to provide effective mode selectivity by reducing, as much as possible, the diffractive Q of the more volume modes while keeping the ohmic loading of the inner conductor at low levels. The loading of the inner conductor increases rapidly with decreasing C due to higher magnetic field on the conductor surface [7], [16]. Assuming an RF power of 1.5 MW in the cavity, a diffractive of $Q = 3010$ for the $TE_{31,17}$ mode and a Gaussian field profile along the cavity with equivalent length 24.5 mm, the ideal peak loading of the outer wall is found to be 1.15 kW/cm^2, and at the inner conductor it is limited to 0.17 kW/cm^2.

III. Interaction Calculations

The electron-guiding-center radius that corresponds to maximum coupling of the corotating $TE_{-31,17}$ mode is at $R_b = 9.41$ mm. The mode spectrum of the product (quality factor) * (relative coupling coefficient) is presented in Fig. 3 for this beam radius. This product is inversely proportional to the minimum starting current of the corresponding modes [17]. The only serious remaining competitors are the azimuthal satellites. In a hollow cylindrical cavity the counter-rotating modes $TE_{+28,18}$ and $TE_{+29,18}$ would also be serious competitors, but here they are eliminated thanks to the inner conductor.

The maximum achievable magnetic field of the sc magnet at FZK has been tested to be around 6.5 T. A study was performed for the maximum achievable output power in terms of the magnetic field and the result is presented in Fig. 4. The magnetic field B_0 varies from 6.4 to 6.6 T and the cathode voltage U_c, resulting to maximum RF power, from 67 to 84 kV. The beam α is computed adiabatically to vary from 1.0 to 1.18, the beam radius is at 9.50 mm and the beam current I_b is kept constant at 50 A. The adiabatic computation of the α-value for different cathode voltages has been performed by using the adiabatic equations of a MIG electron gun and fitting to a numerically calculated reference point. A cold beam was assumed in the calculations. The output power, which is computed from the RF power generated in the cavity reduced by 7% due to assumed ohmic losses in the cavity and the output waveguide and window, reaches the value of 1.57 MW at 6.59 T with output efficiency of 36.8%. At 6.48 T, which will be the design value for the magnetic field, the maximum output power is 1.44 MW with an efficiency of 38.9% at a cathode voltage of 74.2 kV. A stationary single-mode code was used for the computations and the results have not been checked in terms of stability. In any case, they give a sense of the benefits expected from a possible increase of the magnetic field.

The output power and efficiency have been also computed varying the beam current from 40 to 60 A at 6.48 T magnetic field and 74 kV cathode voltage and they are presented in Fig. 5. The beam α is kept constant at 1.07 and no velocity spread was assumed. The results are from the stationary single-mode code and no stability of oscillations was considered. At 40 A the output power is 1.08 MW and at 60 A it reaches 1.56 MW. The maximum efficiency is 38.2% at 48 A.

The response of the oscillator in varying the magnetic field at $U_c = 74$ kV and $I_b = 50$ A is presented in Fig. 6, assuming a cold beam. The velocity ratio α follows adiabatically the varying magnetic field. Soft and hard excitation regions are indicated; soft excitation equilibria with a solid line and hard excitation equilibria with a dashed line. Maximum output power of 1.47 MW is achieved in the hard excitation region at 6.47 T. At the border to the hard excitation region ($B_0 = 6.505$ T) the output power is 0.97 MW and the efficiency 26.7%.

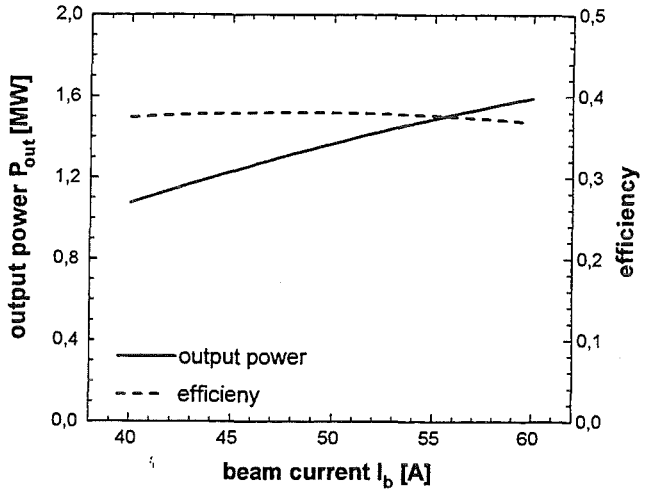

Fig. 5. Output power and efficiency in the $TE_{31,17}$ mode versus beam current at $B_0 = 6.48$ T, $U_c = 74$ kV, and $\alpha = 1.07$.

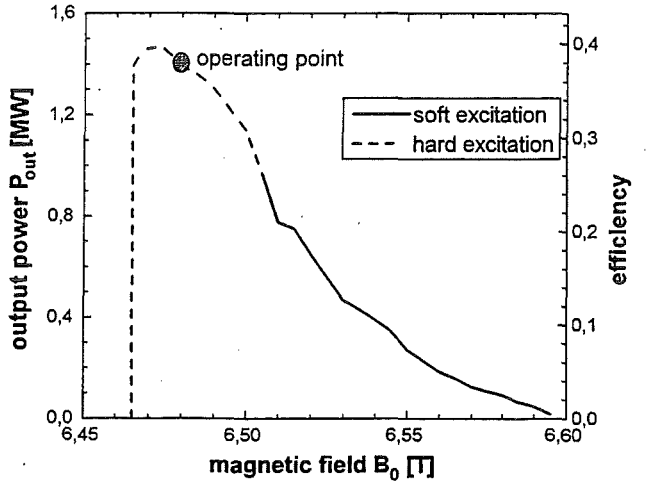

Fig. 6. Output power and efficiency in the $TE_{31,17}$ mode versus magnetic field at $U_c = 74$ kV and $I_b = 50$ A. The beam a follows adiabatically the magnetic field. Solid line shows the soft-exctation region and dashed line the hard-excitation region.

To investigate the startup behavior [18], the starting current curves of the operating mode and its competitors were computed in terms of the beam voltage (beam voltage in the cavity after voltage depression) and are presented in Fig. 7. Here, the magnetic field is constant at 6.48 T and the beam α follows adiabatically the beam voltage. The evolution of the beam current is also shown in Fig. 7. The figure is useful to determine the oscillating-mode sequence during the startup of the tube, where the cathode voltage and beam current rise from zero to their operating values. According to this figure, the first mode to be excited during the startup is the $TE_{33,17}$ at a beam voltage close to 30 kV, which will be replaced by the $TE_{32,17}$ close to 52 kV. The operating mode $TE_{31,17}$ is expected to start oscillations at 62 kV beam voltage ($\approx$64 kV cathode voltage) and to keep oscillating stably up to 72 or 74 kV beam voltage.

The output power and efficiency achieved in each mode during the rise of the cathode voltage have been computed at the designed magnetic field of 6.48 T and is presented in

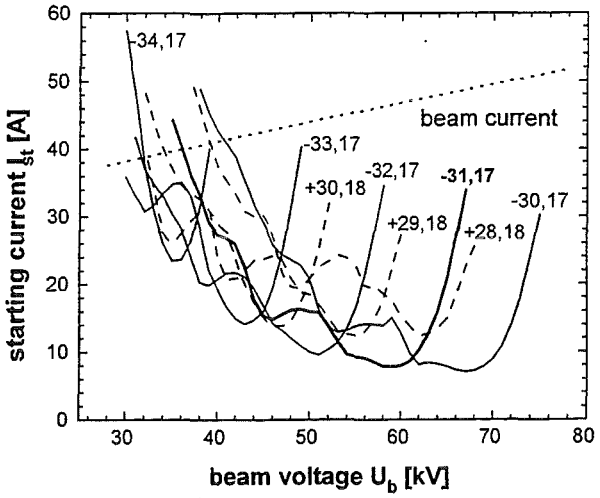

Fig. 7. Starting current of the operating mode and its competitors versus the beam voltage at $B_0 = 6.48$ T. The beam α follows adiabatically the beam voltage.

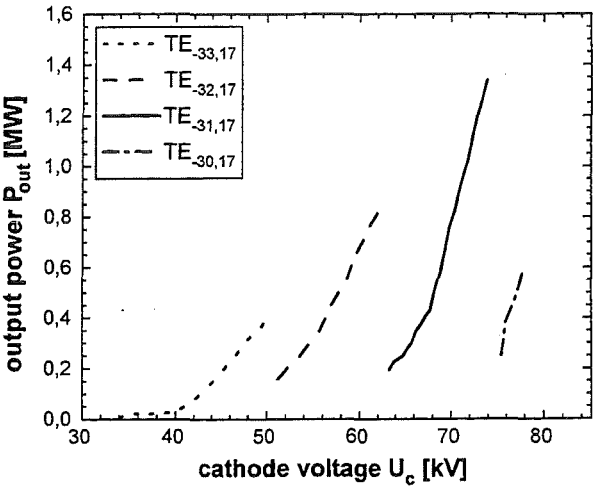

(a)

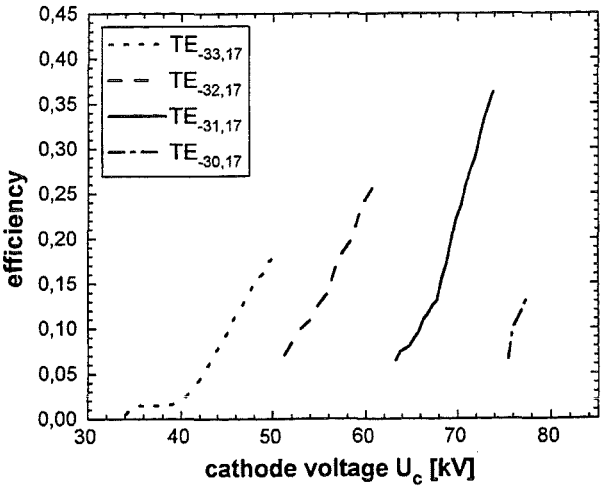

(b)

Fig. 8. (a) Output power and (b) efficiency of different modes excited during the startup versus the cathode voltage at $B_0 = 6.48$ T, $R_b = 9.50$ mm, and $\delta\beta_{\perp rms} = 6\%$.

Fig. 8. The velocity ratio α follows adiabatically the cathode

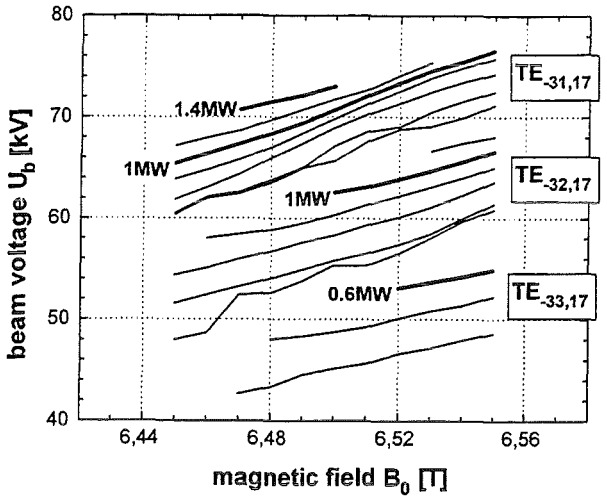

Fig. 9. Stability region of the operating mode and its high-frequency azimuthal neighbors in the $B_0 - U_b$ plane.

voltage and reaches the numerically calculated value of 1.07 at $U_c = 74$ kV and $I_b = 50$ A. A self-consistent time-dependent multimode code [19], [20] has been used, and all the points of the plot have been checked in terms of stability. The $TE_{33,17}$ mode is first excited at 34 kV and reaches, stably, 0.39 MW at 50.7 kV with 17.8% total efficiency. Then the next azimuthal neighbor $TE_{32,17}$ starts oscillations and reaches 0.83 MW at 62.3 kV with 28.5% efficiency. At higher voltages it is suppressed by the operating mode $TE_{31,17}$, which reaches, stably, an output power of 1.34 MW at cathode voltage 74 kV with efficiency 36.2%. At even higher voltages the operating mode loses oscillations suppressed by its neighbor $TE_{30,17}$. The mode stability has been checked using the oscillating TE_{mp} mode and the pairs of azimuthal neighbor modes $TE_{m-1,p}$ and $TE_{m+1,p}$ and leaving the beam voltage constant for a time interval of 200 ns. The oscillating region of the $TE_{31,17}$ mode has been found, using the stationary single-mode code, to extend up to 75.5 kV cathode voltage. For U_c from 74 to 75.5 kV multimode operation was found with power in the modes $TE_{31,17}$ and $TE_{30,17}$. The hard-excitation region of the $TE_{31,17}$ mode starts close to $U_c = 70$ kV with 0.75 MW output power and 22.1% efficiency.

In Fig. 9 the stability region in the $B_0 - U_b$ plane is presented for the operating mode and its high-frequency azimuthal neighbors. For the calculations the time-dependent multimode code was used with the operating mode and the two azimuthal satellites. Here the iso-power curves refer to RF power, that is microwave power generated in the cavity. The output power is assumed to be 7% lower due to overall ohmic losses. An output power in excess of 1 MW seems to be reachable in a wide range of magnetic-field and beam-voltage values.

Table II summarizes the results of the self-consistent calculations at the operating point.

TABLE II
DESIGN PARAMETERS OF THE 165-GHz, $TE_{31,17}$ COAXIAL GYROTRON

operating mode	$TE_{31,17}$
magnetic field/T	6.48
cathode voltage/kV	74
beam voltage/kV	72.1
beam current/A	50
electron velocity ratio	1.07
frequency/GHz	164.98
RF power w/o losses/MW	1.46
electronic efficiency/%	40.6
output power/MW	1.36
total efficiency/%	36.7
cavity wall losses/kW	29
outer wall loading/kW/cm^2	0.95
inner wall loading/kW/cm^2	0.14
diffractive quality factor	2956
Gaussian field length/mm	24.2
normalized field length	15.7

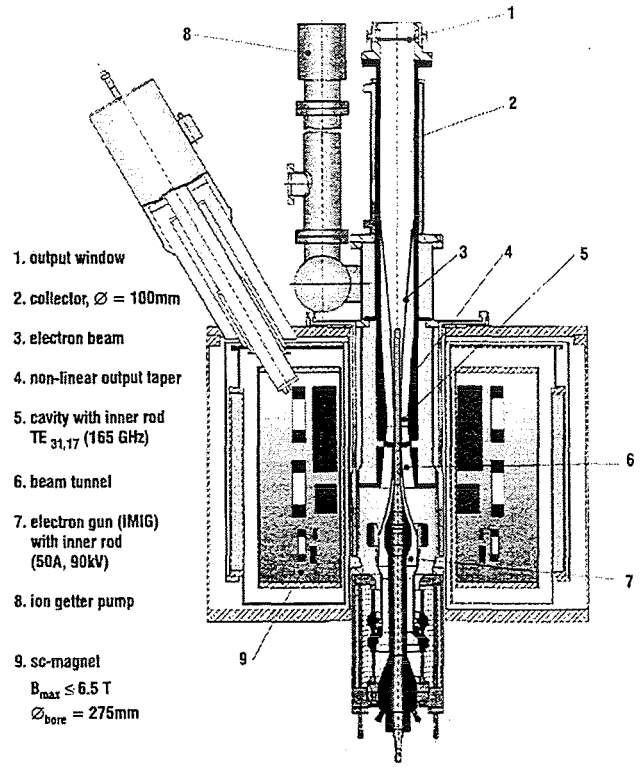

Fig. 10. Schematic of the 165-GHz, $TE_{31,17}$ coaxial gyrotron. The diameter $\phi_{\text{bore}} = 275$ mm can be used as a scale.

IV. Experimental Results and Comparison with Numerical Simulations

The 165-GHz–$TE_{31,17}$-mode coaxial gyrotron (Fig. 10) has been tested in pulsed operation with pulse length 0.15 ms and repetition rate 1 Hz. However, in single pulses the gyrotron has been operated up to 0.5 ms. The presence of two gun coils that can be energized separately allow some limited control on the beam-velocity ratio, although the inverse MIG used in the experiment is a diode-type gun. The first gun coil (ES1), the one below the cathode, corresponds in a relatively high beam α, but in a high velocity spread as well. By energizing the second gun coil (ES2), above the cathode, the electron-emitting angle from the cathode—relative to the magnetic field lines, is changed—resulting in lower beam α and lower velocity spread.

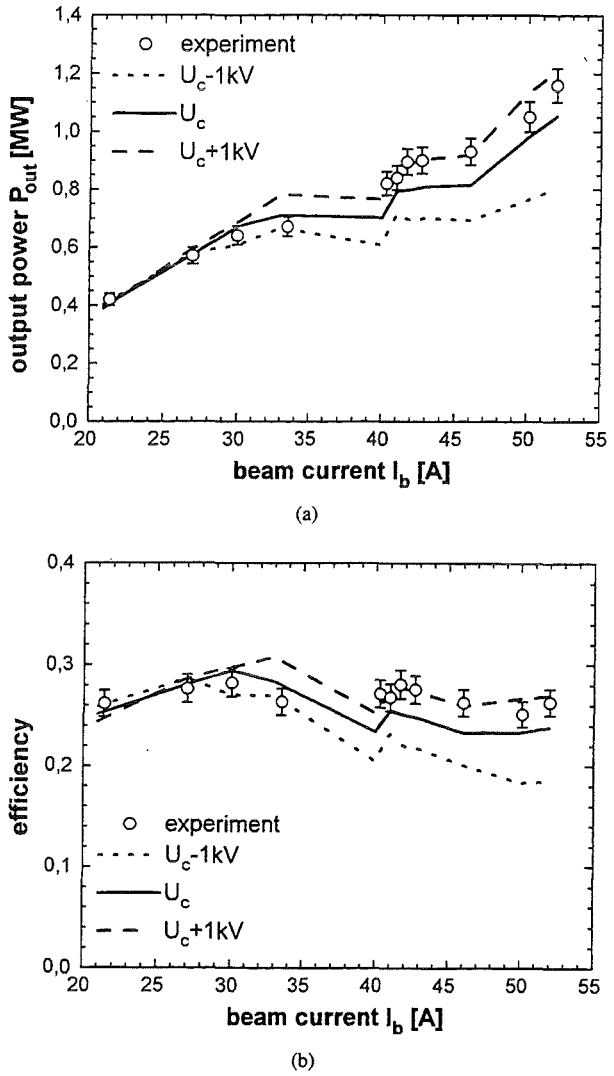

Fig. 11. (a) Maximum measured output power and numerically computed output power in $TE_{31,17}$ mode versus the beam current and (b) corresponding efficiency.

Before starting with RF measurements, the inner rod has been aligned relative to the electron beam with an accuracy of about 0.1 mm as described in [21]. At the beginning of the experiment stable single-mode operation of the device was almost impossible or limited in power (≈0.5 MW) and restricted to a narrow range of parameters, due to unusually high ripples of the cathode voltage and the beam-current pulse. To stabilize the voltage pulse, the voltage regulator tube was removed from the circuit and the gyrotron was directly open to the high voltage. A reasonably stable cathode voltage and beam-current pulse was then obtained and the tube operation in terms of stability and monomode operation was considerably improved.

The experimentally achieved maximum output power in the $TE_{31,17}$ mode and the corresponding total efficiency are presented in Fig. 11 in terms of the beam current. Here, the first gun coil (ES1) was energized. All the experimental data, except the last two at high beam current, correspond to $B_0 = 6.55$ T and $R_b = 9.62$ mm. The cathode voltage corresponds to maximum output power and is in the range from 75 kV to 76.5 kV. Further increase of the cathode voltage resulted in unstable operation and reduction of power. For the last two experimental points, at 50.1 and 52 A, the gun coil (ES2) was energized in order to reduce the α value and to enable an operation at higher cathode voltages. For these points with a magnetic field of 6.61 T, a beam radius of 9.57 mm and an α value of about 0.85 the cathode voltage was 83.4 kV and 84.8 kV, respectively. The reference point for computing adiabatically the beam α (for operation with the gun coil ES1) was the following: at $B_0 = 6.55$ T, $R_b = 9.62$ mm, $U_c = 77$ kV and $I_b = 40$ A beam current, the EGUN code computed a beam α equal to 1.0. The unstable operation, due to beam instabilities, appeared above $\alpha \approx 1$. This is thought to be caused by reflected and trapped electrons because of high velocity spread. A reason for the high spread is seen in the operation of the cathode at about 1400 °C because of the use of a LaB_6 emitter. In Fig. 11 the results of the self-consistent single-mode code are also presented at three different cathode voltages: the experimentally measured cathode voltage, and at plus/minus 1 kV from this value. The rms transverse velocity spread used in the simulations is the one predicted from EGUN, equal to 7%. The output power was computed in the simulations from the RF power generated in the cavity (without ohmic losses) reduced by 7% due to ohmic losses in the cavity, the output waveguide, and the window. The experimental results are well within the three theoretical curves. The range of ±1 kV is not more than the measuring uncertainty of the cathode voltage.

Although there is a very good agreement between the experimental and numerical results presented in Fig. 11, it must be mentioned here that the experimentally obtained output power is the maximum possible, while the computed output power is not the maximum, but simply the output power computed at the experimental parameters. At a given beam current, it is possible in the simulations to increase further the cathode voltage and to obtain even higher power. This was impossible in the experiment because of beam instabilities. In Fig. 12 the maximum output power (both experimental and numerical) is presented. The experimental data are the same as in Fig. 11(a). The theoretical curves were computed using both the stationary and the time-dependent code. At a given beam current the cathode voltage used in the simulations is the maximum voltage, which results in stable operation with maximum computed power (see Fig. 13). The curve computed from the time-dependent code shows the maximum output power found in stable operation. The code was operated with three modes: the operating mode $TE_{31,17}$ and the two azimuthal satellites $TE_{32,17}$ and $TE_{30,17}$. Stability was checked with the cathode voltage constant up to 200 ns. For low beam current (<33 A) the numerical results follow closely the experimental data and the difference in power is not more than 15%. For higher current (40–45 A) the difference grows to 25%, and finally, for a beam current of 50 A it reaches 30% for the stationary code. For beam current up to 46 A no mode competition was found and the two codes predicted the same maximum output power at the same cathode voltage. At higher current 50 A or 52 A the time-dependent code predicted

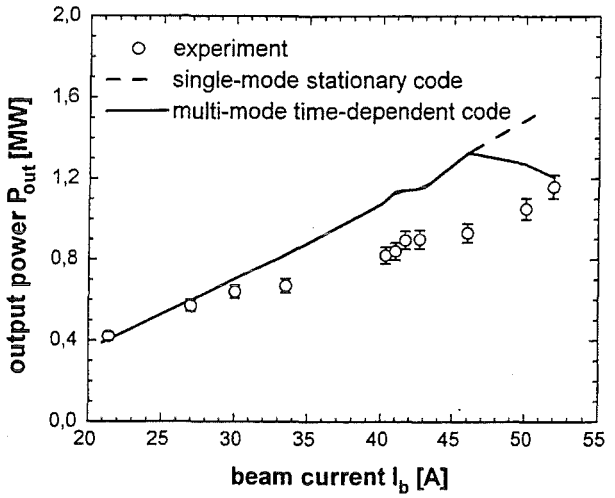

Fig. 12. Maximum output power in the $TE_{31,17}$ mode versus the beam current; theory and experiment.

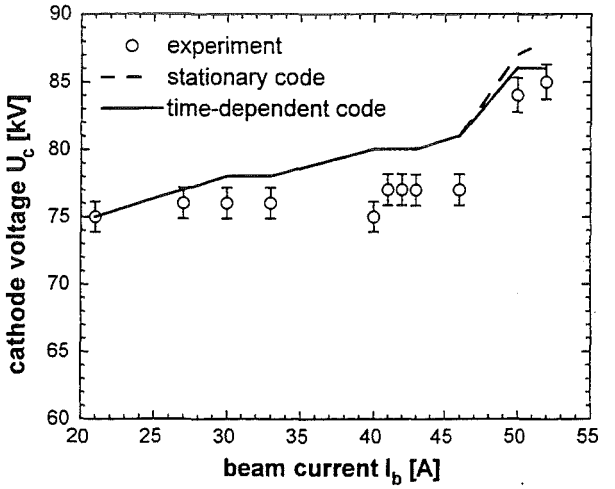

Fig. 13. Stability region of the $TE_{31,17}$ mode; theory and experiment.

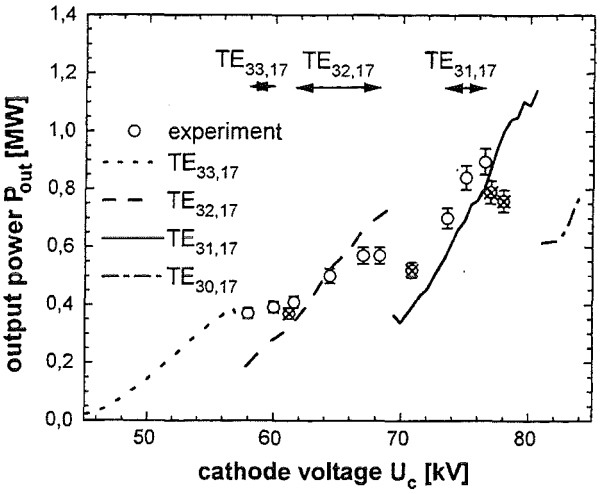

(a)

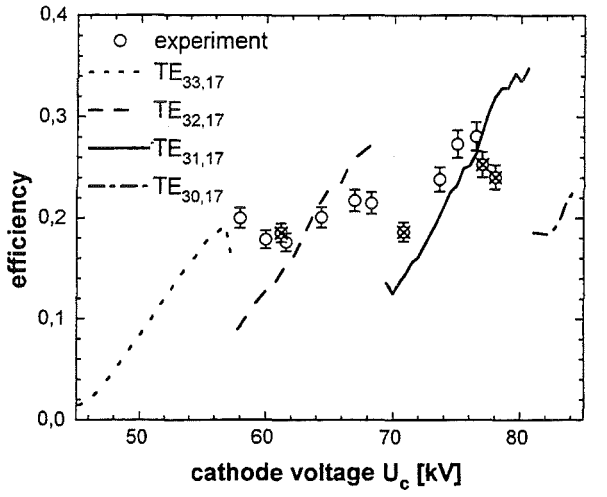

(b)

Fig. 14. (a) Output power and (b) efficiency of different modes versus the cathode voltage. High beam α operation; $B_0 = 6.55$ T, $R_b = 9.62$ mm, $\delta\beta_{\perp rms} = 7\%$ and $\alpha = 1.0$ at $U_c = 77$ kV and $I_b = 40$ A. Open/crossed circles show single/multi mode operation.

less output power in stable operation than the stationary code, due to competition from the azimuthal neighbors. When mode competition is predicted from the multimode code the difference from the experimental result is not significant; 219 and 46 kW in absolute values, respectively. Although at beam current less than 46 A the time-dependent code predicted no mode competition, the difference from the experimental results is considerable (1.33 MW computed and 0.93 MW measured). The reason is probably enhanced mode competition due to window reflections and the increased diffractive quality factor of the competing modes. The experimental and numerically computed stability region of the $TE_{31,17}$ mode in the $I_b - U_c$ plane is presented in Fig. 13.

The output power and the corresponding efficiency in different modes versus the cathode voltage are presented in Fig. 14. The first gun coil ES1 was energized. The cavity magnetic field is 6.55 T, and the beam radius at 9.62 mm. The velocity ratio α follows adiabatically the cathode voltage starting from 0.6 at 45 kV and reaching 1.13 at 84 kV. The beam current also depends on the cathode voltage; at 45 kV it is at 33 A and at 84 kV it comes up to 41 A. At $U_c = 77$ kV and $I_b = 40$ A the beam α is equal to 1.0 and the rms value of the transverse electron velocity spread 7%, according to EGUN computations. Three frequencies were observed in the experiment at different ranges of cathode voltage. Below 60 kV, the tube was oscillating at 169.52 GHz in the $TE_{33,17}$ mode with a maximum output power of 0.39 MW (η = 17.9%). In the voltage range from 62 kV to 68 kV monomode oscillations were observed at 167.27 GHz in the $TE_{32,17}$ mode with maximum output power 0.57 MW (η = 21.5%). The operating mode $TE_{31,17}$ was observed at 164.98 GHz in the cathode voltage range from 71 kV to 76.5 kV. The maximum power delivered in this mode was 0.90 MW at $U_c = 76.5$ kV and $I_b = 41.7$ A with an efficiency of 28.1%. Between the different monomode stages multimode operation was observed. In Fig. 14 open circles present monomode oscillations, and crossed circles show multimoding. The curves represent the numerical results of the time-dependent mul-

timode code. The maximum experimentally obtained output power in the $TE_{33,17}$ mode agrees well with the computed result, but the operating region of this mode is extended experimentally to higher cathode voltages. This can be explained by the significantly increased diffractive-quality factor of this mode due to window reflections. The change from the $TE_{32,17}$ to the $TE_{31,17}$ agrees well with the theory and takes place close to 70 kV cathode voltage. The operating region of the $TE_{31,17}$ is considerably compressed in the experiment. The reasons could be window reflections and the observed beam instabilities at high cathode voltage, possibly because of reflected electrons at high velocity spread. Another reason could be voltage overshooting (±2%) at the beginning of the pulse. At the peak of the voltage the competing mode may start oscillations which may remain after the voltage drop to the operating value. In the experiment the operating mode lost oscillations at cathode voltage 76.5 kV with power of 0.90 MW ($\eta = 28.1\%$), while the simulations predicted stable oscillations even at 80.5 kV with 1.14 MW power ($\eta = 34.8\%$).

The main reason that prevented the tube from stable operation in the designed $TE_{31,17}$ mode at higher cathode voltage is probably the appearance of beam instabilities due to high velocity spread. The same effects were observed trying to increase the beam current above 45 A. The beam was often observed unstable and the operation of the tube was difficult toward the high-power region. With the increase of the cavity beam radius (lower compression-lower beam α), the beam was more stable and vice versa. This is an additional indication for development of beam instabilities due to reflected electrons at high beam α in the magnetic mirror before the cavity. In order to operate stably the tube at higher voltage and current the second gun coil ES2 was energized instead of the ES1, resulting in lower beam α and velocity spread. In Fig. 15 the output power and total efficiency are presented versus the cathode voltage. The cavity magnetic field is 6.63 T and the beam radius at 9.63 mm. The beam α is 0.5 at $U_c = 45$ kV cathode voltage and increases to 0.92 at $U_c = 92$ kV, according to the adiabatic dependence. The beam current starts at 41 A at 45 kV and reaches 52 A at 92 kV. At $U_c = 84$ kV cathode voltage and $I_b = 50$ A current the beam α is equal to 0.84 and the rms electron velocity spread 3.5%, according to EGUN computations. The beam was stable up to 52 A. Experimentally, only two frequencies were measured in single-mode operation: 168.52 GHz ($TE_{33,17}$ mode) and 164.99 GHz ($TE_{31,17}$ mode). In an extended cathode voltage range (70–77 kV) multimoding of these two frequencies and the $TE_{32,17}$ mode at 167.27 GHz was observed. The agreement between the numerical and experimental results of the operating $TE_{31,17}$ mode is excellent. Experimentally, the mode was found to oscillate up to 86-kV cathode voltage and 51 A current with 1.17 MW output power and 26.7% efficiency. Assuming 7% ohmic losses and 1.7 kV voltage depression, an electronic efficiency of 29.2% is computed. The beam α is 0.86 and the transverse electronic efficiency at 68.6%. This operating point is 2.5 kV inside the hard-excitation region, which starts close to 83.5 kV cathode voltage. Numerically, the $TE_{31,17}$ mode was found to oscillate

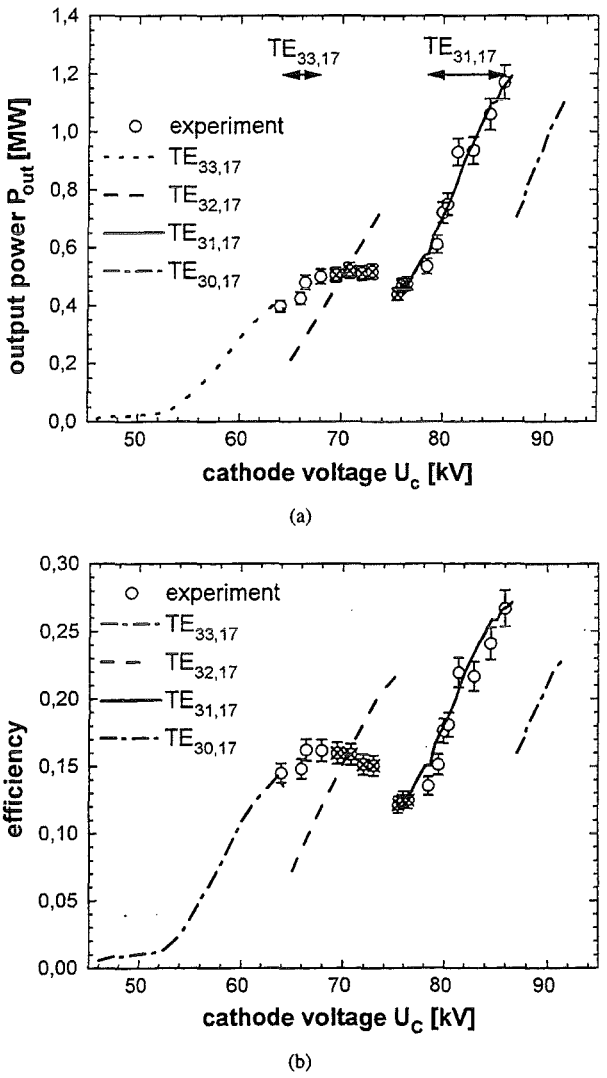

Fig. 15. (a) Output power and (b) efficiency of different modes versus the cathode voltage. Low beam a operation; $B_0 = 6.63$ T, $R_b = 9.63$ mm, $\delta\beta_{\perp rms} = 3.5\%$ and $\alpha = 0.84$ at $U_c = 77$ kV and $I_b = 40$ A. Open/crossed circles show single/multi-mode operation.

stably up to 86.7 kV with output power 1.19 MW and 27.1% total efficiency. It was not possible in the experiment to increase the cathode voltage more than 86 kV because of high-voltage power supply limitations. In general, the operation of the tube with the ES2 gun coil energized was very smooth and easy, because of the low beam α and the absence of any beam instabilities.

The tube was also operated at higher frequencies by controlling the magnetic field and the cathode voltage. The maximum power achieved is given in Table III. Megawatt level output power (1.02 MW) was measured at a frequency of 167.14 GHz with 26.8% efficiency in the $TE_{32,17}$ mode.

The far-field pattern of the $TE_{31,17}$ mode generated in the gyrotron cavity has been measured using the following setup. A nonlinear uptaper was connected behind the RF-output window of the tube to increase the diameter from 100 mm to 140 mm in order to reduce the Brillouin angle of the mode. A quartz glass plate was used to produce a standing wave

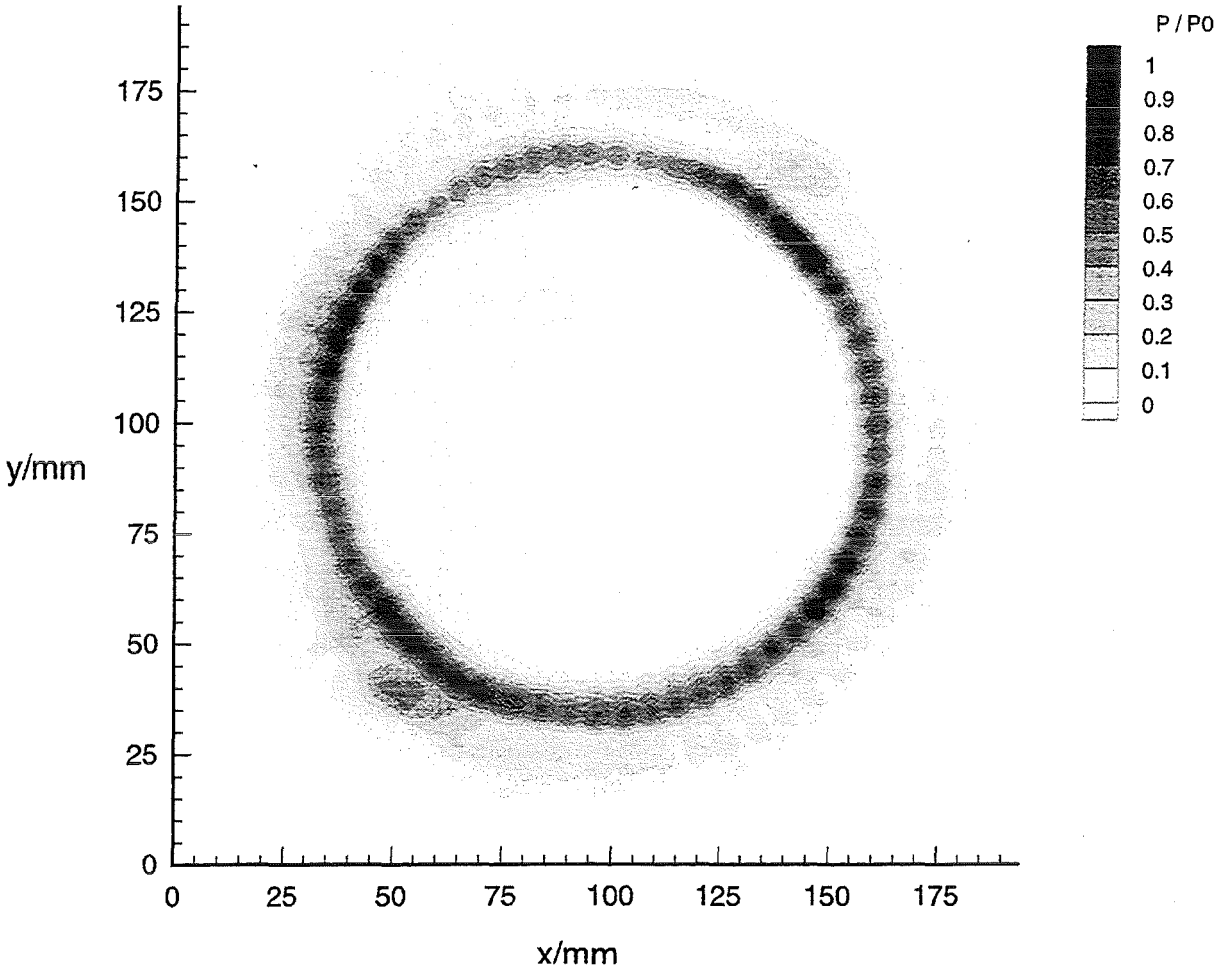

Fig. 16. Far-field pattern of the 165-GHz, $TE_{31,17}$ coaxial gyrotron output.

TABLE III
FREQUENCY TUNABILITY OF THE 165-GHz COAXIAL GYROTRON

mode TE_{mp}	$TE_{31,17}$	$TE_{32,17}$	$TE_{33,17}$	$TE_{34,17}$
frequency/GHz	164.98	167.14	169.46	171.80
magnetic field/T	6.63	6.62	6.62	6.62
beam radius/mm	9.63	9.70	9.75	9.82
cathode voltage/kV	86	76	70	57
beam current/A	51	50	50	46
output power/MW	1.17	1.02	0.63	0.35
total efficiency/%	26.7	26.8	18.0	13.3

pattern from the rotating $TE_{31,17}$ mode and a teflon lens with 165 mm focal length focused the radiation at a dielectric target plate, which was observed by an infrared camera. The far-field pattern of the 165-GHz, $TE_{31,17}$ coaxial gyrotron output is shown in Fig. 16 where 62 minima and maxima are easily recognized.

V. CONCLUSIONS

A coaxial-cavity gyrotron oscillator with axial RF output has been designed at FZK to deliver output power in excess of 1 MW at 165 GHz. The coaxial resonator has been designed with a downtapered and longitudinally corrugated inner conductor to oscillate at 165 GHz in the corotating $TE_{31,17}$ mode. The design calculations predicted stable operation at 1.36 MW output power and 36.7% efficiency with ideal peak wall loading of less than 1 kW/cm^2, relevant to CW operation. In the experiment the pulse length was limited to 0.5 ms because of the heat load capability of the collector. Maximum output power in the designed $TE_{31,17}$ mode at 164.98 GHz was measured in the hard-excitation region at 1.17 MW with 26.7% efficiency, which corresponds to 29.2% electronic efficiency and 68.6% transverse-electronic efficiency. The maximum efficiency was found at 28.2% with an output power of 0.9 MW. Power at higher frequencies was also observed with 1.02 MW at 167.14 GHz in the $TE_{32,17}$ mode. The experimental results have been checked numerically with very good accuracy. The main reason that limited the maximum output power by 200 kW from the design value is probably the observed beam instabilities due to reflected electrons at high beam α in the magnetic mirror before the resonator.

The development of the next version of the tube with lateral output, which will allow operation at longer pulses with a depressed collector, is in progress. A single-step depressed collector is already manufactured and the dual-beam q.o. output system is under optimization. First experimental results are expected in early 1997.

ACKNOWLEDGMENT

The authors gratefully acknowledge H. Baumgärtner, H. Budig, P. Grundel, W. Leonhardt, N. Münch, J. Szczesny, and R. Vincon of the FZK gyrotron team technical staff for the mechanical design, the precise machining and the careful assembly of the tube, as well as for their assistance during the experiments.

REFERENCES

[1] S. Kern and C. T. Iatrou, "Potential of coaxial gyrotrons for ECRH," in *Proc. 21st Int. Conf Infrared and Millimeter Waves*, 1996, paper ATh12, ISBN 3-00-000800-4.

[2] C. T. Iatrou, D. R. Whaley, S. Kern, M. Thumm, M. Q. Tran, A. Möbius, H.-U. Nickel, P. Norajitra, A. Wien, T. M. Tran, G. Bon-Mardion, M. Pain, and G. Thonon, "Feasibility study of the EU Home Team on a 170 GHz 1 MW CW gyrotron for ECH on ITER," *Int. J. Infrared Millimeter Waves*, vol. 16, pp. 1129–1158, 1995.

[3] K. Sakamoto, A. Kasugai, M. Tsuneoka, K. Takahashi, T. Imai T. Kariya, Y. Okazaki, K. Hayashi, Y. Mitsunaka, and Y. Hirata, "Development of 170-GHz high power long pulse gyrotron for ITER," in *Proc. 21st Int. Conf. Infrared and Millimeter Waves*, 1996, paper AT1, ISBN 3-00-000800-4.

[4] A. L. Goldenberg and A. G. Litvak, "Recent progress of high-power millimeter wavelength gyrodevices," *Phys. Plasmas*, 2, 2562–2572, 1995.

[5] T. Kimura, J. P. Hogge, R. Advani, D. Denison, K. E. Kreischer, R. J. Temkin, and M. E. Read, "Investigation of Megawatt Power Level Gyrotrons for ITER," in *Proc. 21st Int. Conf. Infrared and Millimeter Waves*, 1996, paper AM1, ISBN 3-00-000800-4.

[6] S. N. Vlasov, L. I. Zagryadskaya, and I. M. Orlova., "Open coaxial resonators for gyrotrons," *Radio Eng. Electron. Phys.*, vol. 21, pp. 96–102, 1976.

[7] C. T. Iatrou, S. Kern, and A. B. Pavelyev, "Coaxial cavities with corrugated inner conductor for gyrotrons," *IEEE Trans. Microwave Theory, Tech.*, vol. 41, no. 1, pp. 56–64, 1996.

[8] M. E. Read, G. S. Nusinowich, O. Dumbrajs, G. Bird, J. P. Hogge, K. Kreisch, and M. Blank, "Design of a 3-MW 140-GHz gyrotron with a coaxial cavity," *IEEE Trans. Plasma Sci.*, vol. 24, no. 3, pp. 586–595, 1996.

[9] J. J. Barroso and R. A. Correa, "Coaxial resonator for a megawatt, 280 GHz gyrotron," *Int. J. Infrared Millimeter Waves*, vol. 12, pp. 717–728, 1991.

[10] V. A. Flyagin, V. I. Khisnyak, V. N. Manuilov, A. B. Pavelyev, V. G. Pavelyev, B. Piosczyk, G. Dammertz, O. Höchtl, C. T. Iatrou, S. Kern, H. U. Nickel, M. Thumm, A. Wien, and O. Dumbrajs, "Development of a 1.5 MW coaxial gyrotron at 140 GHz," in *Conf. Dig., 19th Int. Conf. Infrared and Millimeter Waves*, 1994, JSAP 941228, pp. 75–76.

[11] B. Piosczyk, O. Braz, G. Dammertz, C. T. Iatrou, S. Kern, A. Möbius, M. Thumm, A. Wien, S. C. Zhang, V. A. Flyagin, V. I. Khishnyak, A. N. Kuftin, V. N. Manuilov, A. B. Pavelyev, V. G. Pavelyev, A. N. Postnikova, and V. E. Zapevalov, "Development of a 1.5 MW, 140 GHz coaxial gyrotron," in *Conf. Dig., 20th Int. Conf. Infrared and Millimeter Waves*, 1995, pp. 423–424.

[12] B. Piosczyk, O. Braz, G. Dammertz, C. T. Iatrou, S. Kern, M. Kuntze, A. Möbius, M. Thumm, V. A. Flyagin, V. I. Khishnyak, A. N. Kuftin, V. I. Malygin, A. B. Pavelyev, and V. E. Zapevalov, "A 140 GHz, 1.5 MW, $TE_{28,16}$-coaxial cavity gyrotron," in *Proc. 21st Int. Conf. Infrared and Millimeter Waves*, 1996, paper AM2, ISBN 3-00-000800-4.

[13] V. K. Lygin, V. N. Manuilov, A. N. Kuftin, A. B. Pavelyev, and B. Piosczyk, "Inverse magnetron injection gun for a 1.5 MW, 140 GHz gyrotron," *Int. J. Electron*, vol. 79, pp. 227–235, 1996.

[14] M. Thumm, C. T. Iatrou, A. Möbius, and D. Wagner, "Built-in mode converters for coaxial gyrotrons" in *Proc. 21st Int. Conf. Infrared and Millimeter Waves*, 1996, paper AM6, ISBN 3-00-000800-4.

[15] C. T. Iatrou, O. Braz, G. Dammertz, S. Kern, B. Piosczyk, M. Thumm, A. Wien, and S. C. Zhang, "Development of a 1.5 MW coaxial gyrotron at 165 GHz," in *Conf. Dig., 20th Int. Conf. Infrared and Millimeter Waves*, 1995, pp. 415–416, 1995.

[16] C. T. Iatrou, "Mode selective properties of coaxial gyrotron resonators," *IEEE Trans. Plasma Sci.*, vol. 24, no. 3, pp. 596–605, 1996.

[17] K. E. Kreischer and R. J. Temkin, "Linear theory of an electron cyclotron maser operating at the fundamental," *Int. J. Electron.*, vol. 1, 195–233, 1980.

[18] D. R. Whaley, M. Q. Tran, T. M. Tran, and T. M. Antonsen, Jr., "Mode competition and startup in cylindrical cavity gyrotrons using high order operating modes," *IEEE Trans. Plasma Sci.*, vol. 22, no. 5, pp. 850–860, 1994.

[19] S. Kern, C. T. Iatrou, and M. Thumm, "Investigations of mode stability in coaxial gyrotrons," in *Conf. Dig., 20th Int. Conf, Infrared and Millimeter Waves*, 1995, pp. 429–430.

[20] S. Kern, "Numerical codes for interaction calculations in gyrotron cavities at FZK," in *Proc. 21st Int. Conf. Infrared and Millimeter Waves*, 1996, paper AF2, ISBN 3-00-000800-4, 1996.

[21] B. Piosczyk, O. Braz, G. Dammertz, C. T. Iatrou, S. Kern, M. Möbius, and M. Thumm, "A 1.5-MW–140-GHz $TE_{28,16}$ coaxial-cavity gyrotron," this issue, pp. 460–469.

Christos T. Iatrou, for a photograph and biography, see this issue p. 469.

Oliver Braz, for a photograph and biography, see this issue p. 469.

Günter Dammertz, for a photograph and biography, see this issue p. 469.

Stefan Kern, for a biography, see this issue p. 469.

Michael Kuntze, for a photograph and biography, see this issue p. 469.

Bernhard Piosczyk, for a photograph and biography, see this issue p. 468.

Manfred Thumm (SM'94), for a photograph and biography, see this issue p. 469.

Built-In Mode Converters for Coaxial Gyrotrons

M. Thumm[1) 2)], C. T. Iatrou[1)], A. Möbius[1)], and D. Wagner[3)]

[1)]Forschungszentrum Karlsruhe, Institut für Technische Physik, Association EURATOM-FZK, P.O. Box 3640, D-76021 Karlsruhe, Germany

[2)]Universität Karlsruhe, Institut für Höchstfrequenztechnik und Elektronik, Kaiserstrasse 12, D-76128 Karlsruhe, Germany

[3)]Universität Stuttgart, Institut für Plasmaforschung, Pfaffenwaldring 31, D-70569 Stuttgart, Germany

Abstract

The optimization and design of improved quasi-optical (q.o.) mode converter systems compatible with the constraints of a coaxial dual-beam output concept for operation with two output windows are presented. The two-step mode conversion schemes $TE_{-28,16}$ -to- $TE_{+76,2}$ -to- TEM_{00} at 140 GHz and $TE_{-31,17}$ -to- $TE_{+83,2}$ -to- TEM_{00} at 165 GHz have been investigated. In both cases two narrowly-directed output wave beams (60° at the launcher) are generated. High conversion efficiencies are expected (94% and 92%, respectively).

Introduction

Owing to the power limit of gyrotron rf windows, the mm-wave output power of a 2 MW coaxial cavity gyrotron must be split into two linearly polarized wave beams and coupled out radially through two 1 MW windows. Beam splitting can be performed either by a quasi-optical 3 dB splitter (e.g. special non-quadratic phase correcting mirror or a diffraction grating), or by a dual-beam launcher of a q.o. mode converter [1].

The advantage of the second solution is that an improved dimple-type launcher generating two output beams is much shorter than an advanced single-beam launcher. If one employs, as in conventional cylindrical cavity gyrotrons, a q.o. mode converter for the operating volume mode of the cavity, the dimensions of the mirror system are excessively large for a dual beam output since the azimuthal angle of divergence φ of the radiation is quite large, e.g. $\varphi = 2\arccos(m/\chi_{mp}) = 142.62°$ for the $TE_{28,16}$ mode.

This is not the case for a high-order whispering gallery mode (WGM) of the type $TE_{m,2}$ since here the representing rays form a caustic located closer at the waveguide wall, e.g. $\varphi \approx 2\arccos(m/\chi_{mp}) = 59.14°$ for the $TE_{76,2}$ mode, so that a double-cut q.o. launcher can generate two diametrically opposed narrowly-directed output wave beams.

The actual design of an improved q.o. mode converter system compatible with the constraints of a coaxial gyrotron dual beam output concept for operation with two output employs the two-step mode conversion schemes:

$$TE_{-28,16}\ (\chi_{mp} = 87.36) \rightarrow TE_{+76,2}\ (\chi_{mp} = 87.38) \rightarrow TEM_{00} \text{ at } 140 \text{ GHz} \quad (1)$$
$$TE_{-31,17}\ (\chi_{mp} = 94.62) \rightarrow TE_{+83,2}\ (\chi_{mp} = 94.69) \rightarrow TEM_{00} \text{ at } 165 \text{ GHz} \quad (2)$$

In-Waveguide Mode Conversion: Cavity Volume Mode to WGM

The conversion of the co-rotating cavity mode to its degenerate counter-rotating WGM is achieved by the introduction of longitudinal corrugations in the output taper (1.5°) of the gyrotron cavity according to the formula

$$R_c(z) = R_{c,0}(z) + \rho\cos(\Delta m\phi)$$

where $R_{c,0}(z)$ is the mean radius of the tapered waveguide wall, r is the amplitude of corrugations and Δm = 104 and Δm = 114 for the mode conversion sequence (1) and (2), respectively. The parameters of the two optimized converters are summarized in Table 1.

	140 GHz (1)	165 GHz (2)
converter length (mm)	78	64
input radius (mm)	30.20	27.77
mean output radius (mm)	32.25	29.45
corrugation amplitude (mm)	0.057	0.052
ohmic losses (%)	1.7	1.8
mode purity (%)	99	99

Table 1: Parameters of two optimized waveguide mode converters.

Conversion of the co-rotating cavity mode to the counter-rotating WGM instead to the co-rotating WGM has the advantage that the coupling coefficient is larger and coupling to unwanted modes is considerably reduced, since all the likely generated modes $TE_{-132,1}$ and $TM_{-132,1}$ in converter (1) and $TE_{-145,1}$ and $TM_{-145,1}$ in converter (2) are below cutoff. Only the modes $TE_{+76,1}$, $TE_{+76,2}$ and $TE_{+76,3}$ (cutoff radius at 140 GHz 31.8 mm) and $TE_{+83,1}$, $TE_{+83,2}$ and $TE_{+83,3}$ (cutoff radius at 165 GHz 29.14 mm) can propagate in converter (1) and (2), respectively.

Quasi-Optical Mode Conversion: WGM to TEM_{00}

The q.o. WGM-to-TEM_{00} converters will use improved dual-beam dimple-type launchers with $\Delta m_1 = 2$ and $\Delta m_2 = 6$ perturbations for longitudinal and azimuthal bunching of the two mm-wave beams. The parameters of the two advanced launchers are given in Table 2.

	140 GHz (1)	165 GHz (2)
launcher length (mm)	228	258
average diameter (mm)	68.3	62.8
Brillouin angle (°)	60.7	60.7
ohmic losses (%)	4.6	5.9
efficiency (%)	95	93

Table 2: Parameters of two dimple-type dual-beam launchers.

Figure 1 shows the theoretical intensity contour map of an advanced double beam launcher for the $TE_{76,2}$ mode at 140 GHz.

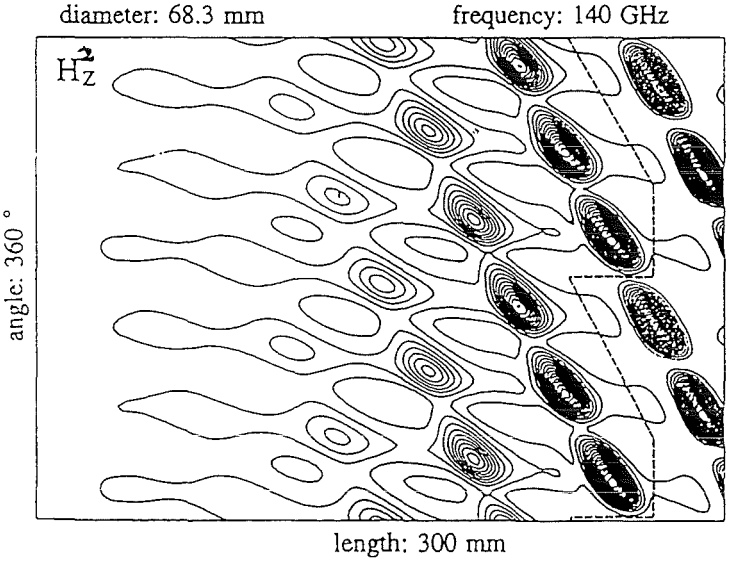

Fig. 1: Theoretical intensity contour map of a dimple-type double-beam launcher for the $TE_{76,2}$ mode at 140 GHz.

References

[1] B. Piosczyk et al., 20th Int. Conf. IR&MM Waves, Orlando (USA), 1995, pp. 423-424.

Low Power Excitation and Mode Purity Measurements on Gyrotron Type Modes of High Order

O. Braz, A. Arnold, M. Losert, A. Möbius, M. Pereyaslavets, M. Thumm
Forschungszentrum Karlsruhe, ITP, Association EURATOM-FZK,
Postfach 3640, D-76021 Karlsruhe, Germany
and Universität Karlsruhe, Institut für Höchstfrequenztechnik und Elektronik,
Kaiserstr. 12, D-76128 Karlsruhe, Germany

V. I. Malygin
Institute of Applied Physics, Russian Academy of Sciences,
46, Uljanov Street, 603600 Nizhny Novgorod, Russia

Abstract

To be able to perform cold tests of waveguide components which have to be integrated into the UHV system of gyrotrons, mode exciters for high order TE modes are required. As the efficiency of the device under test is directly linked to the purity of the input mode special techniques are necessary to analyze the mode content in a highly oversized waveguide system. This paper reports about the efforts undertaken at the Forschungszentrum Karlsruhe to analyze the mode purity of a $TE_{22,6}$-mode exciter. In addition the present status of a $TE_{76,2}$-mode exciter is shown.

Introduction

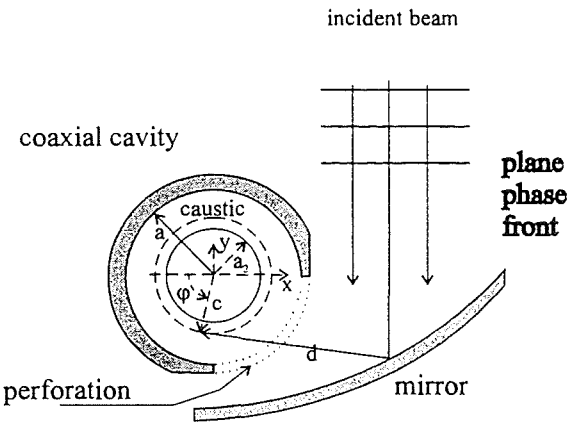

Fig. 1: Schematic of q. o. mode generator

Millimeter wave guiding components in gyrotrons, such as waveguide tapers and quasi-optical mode converters have to be cold tested before they are integrated into the ultra high vacuum (UHV) tube and exposed to high power millimeter waves. To be able to perform the cold tests the gyrotron cavity output must be simulated. This means a high order rotating TE mode must be launched into the devices under test (DUT). Since the behavior of the DUT strongly depends on the quality of the launched mode it needs to be of high purity. As shown in Fig. 1 this can be achieved by means of a mode generator consisting of two q.o. mirrors and a coaxial cavity with a perforated outer wall [1] [2]. Before applying the mode generator its proper behavior must be verified. This is performed by means of field distribution measurements in the near and far field of the mode exciter's output aperture. A second method which also had been applied are k-spectrometer measurements [3].

Mode purity measurements on TE $_{22,6}$ mode generator

The results of a k-spectrometer measurement for the FZK, 140 GHz, $TE_{22,6}$-mode generator are shown in Fig. 2. Since the coupling efficiency through the k-spectrometer's holes is extremely low the dynamic range of the analyzing electronic equipment had to be extended by 40 dB from initially 80 to 120 dB.

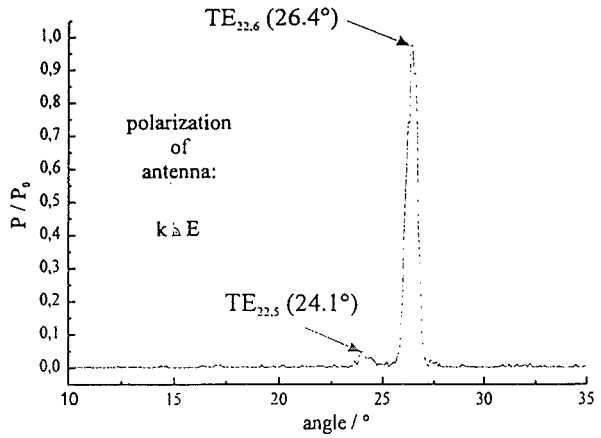

Fig. 2 Measured k-spectrum of $TE_{22,6}$ exciter

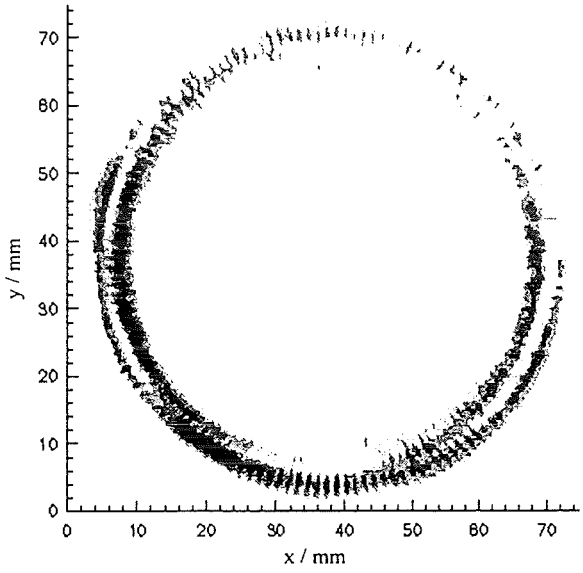

Fig. 3: Near field pattern of $TE_{76,2}$-mode generator

For this reason an existing scalar network analyzer [4] has been modified. This was achieved by integration of a phase locked backward wave oscillator with a linewidth of 10 Hz and an output power of 10 dBm. The mode purity of the $TE_{22,6}$-mode exciter has been determined to be about 91 % in the desired $TE_{22,6}$ mode. Additionally field pattern measurements in the far and near field have been performed which proove this result.

Low power excitation of $TE_{76,2}$ mode

For testing waveguide components of the 140 GHz, 1.5 MW coaxial gyrotron, currently developed at FZK, a mode generator for a rotating $TE_{+76,2}$ mode is required. The operating resonator mode of this tube is the $TE_{-28,16}$. For the foreseen dual beam output coupling of the rf-power this mode will be converted by 104 axial slots in the waveguide wall into a $TE_{+76,2}$ mode. For low power excitation of this whispering gallery mode similar techniques with a different cavity and mirror design have been applied. A near field pattern measured with a horizontally polarized pick-up horn antenna, at the waveguide output of the generator is shown in Fig. 3. The corresponding cavity resonance has been found at a frequency of 139.83 GHz with a quality factor of Q = 2466. A detailed analysis of the mode content is under preparation.

Conclusions

The performed k-spectrometer and field pattern measurements show that the mode purity of gyrotron type modes excited by applying quasi optical techniques is rather high (91 %) for the $TE_{22,6}$. Also the good agreement between low and high power measurements performed on several quasi-optical mode converters have prooven this fact. K-spectrometer measurements made possible by the improved dynamic range of the scalar network analyzer indicate the possibility for further analysis and improvements on such type of mode generators. In addition a mode generator for a rotating $TE_{76,2}$ mode was designed, manufactured and preliminarily tested. Further analysis of its mode purity and content of counter rotating mode will follow.

References

[1] Alexandrov, N. L., Denisov, G. G., Tran, M. Q., Whaley, D. R, 1995, Int. J. Electr., **79**, 215-226.

[2] Braz, O., Kern, S., Losert, M., Möbius, A., Pereyaslavets, M., Thumm, M., 1995, Conf. Digest 20th Int. Conf. on Infrared and Millimeter Waves, Orlando, 471-472.

[3] Kasparek, W., Müller, G. A., 1988, Int. J. Electronics, **64**, 5-20.

[4] Geist, T., Hochschild, G., Wiesbeck, W., 1988, Proc. 18th European Microwave Conf., Stockholm, 339-343.

Low Power Performance Tests on Highly Oversized Waveguide Components of High Power Gyrotrons

O. Braz [1) 2)], A. Arnold [1) 2)], H. - R. Kunkel [1)], M. Thumm [1) 2)]

[1)] Forschungszentrum Karlsruhe (FZK), ITP, Association EURATOM-FZK, Postfach 3640, D-76021 Karlsruhe, Germany

[2)] and Universität Karlsruhe, Institut für Höchstfrequenztechnik und Elektronik, Kaiserstr. 12, D-76128 Karlsruhe, Germany

Abstract

To generate and transport high power micro- and millimeter-waves, highly oversized waveguide components have to be used. For the verification of their performance in cold-test asurements, analyzing systems covering a large dynamic ange (> 100 dB) are needed. This paper describes the realization of a new vector network analyzer (f = 110 GHz to 170 GHz) covering the requirements mentioned above. The analyzing system will be applied to measurements on a low power $TE_{76,2}$ mode generator and a $TE_{28,16}$ - to $-TE_{+76,2}$ mode converter for a 1.5 MW, 140 GHz coaxial cavity gyrotron.

Introduction

High power gyrotrons are nowadays usually equipped with a quasi-optical mode converter system. By converting the operating high order TE cavity mode into a defined free-space distribution the influence of the required vacuum barrier window on the gyrotron's oscillation behavior can be reduced. For low-loss energy transportation either in corrugated HE_{11}-waveguides or in quasi-optical mirror lines a fundamental Gaussian beam is preferred. To decrease the Ohmic loading on the cavity wall and to maximize the achievable millimeter-wave power it is necessary to operate at extremely high-order les. To separate the problem for the most efficient power output coupling from the demand for a high beam quality, currently the use of phase-correcting mirrors outside the gyrotron is under investigation. This results in increasing requirements on the used test facilities. For cold test measurements the gyrotron cavity mode can be excited by mode generators applying quasi-optical techniques [1], [2]. With respect to the achievable mode purity this high-order modes together with the high frequencies (170 GHz planned for ITER plasma heating) lead to extreme requirements on the mechanical precision in fabricating the mode generator. One possibility to overcome these mechanical restrictions is a more complicated design. In our case we prefer a detailed analysis of the excited mode spectrum. By knowing the magnitude and phase of the disturbing competitors their influence on the measured field patterns can be removed by calculation.

A standard method for analyzing the wavenumber spectrum are k-spectrometer measurements [3]. Due to the low coupling characteristics of this device, analyzing systems covering a large dynamic range are needed.

The D-Band vector network analyzer

Figure 1 shows a schematic drawing of the new homemade D-band vector network analyzer. At the desired frequency range from 110 GHz to 170 GHz powerful narrow-band signal sources are of special interest. Therefore a backward-wave oscillator (BWO) has been frequency stabilized by installing a phase locked loop (PLL) circuit. By this way the BWO's output frequency (8 MHz bandwidth unstabilized) could be phase locked to a 10 MHz quartz reference with a line width of less than 10 Hz! In order to achieve a narrow bandwidth and by this way an extremely low noise level (-130 dBm) a multi-stage super-hed receiver was built. To be able to determine the phase shift caused by the device under test (DUT) the required frequencies for down conversion are also derived from the quartz reference. By using the stabilized BWO for the transmitting part of the vector network analyzer its dynamic range is extended to more than 110 dB.

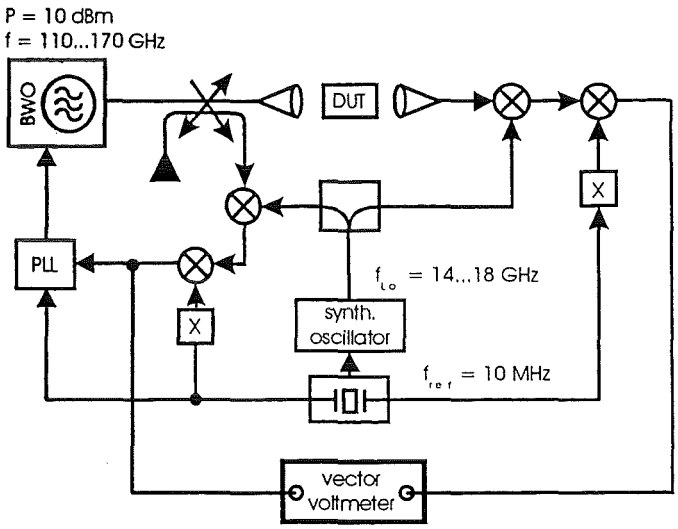

Fig. 1: Schematic drawing of the vector network analyzer.

Figure 2 shows a typical vector k-spectrometer measurement performed on a $TE_{+76,2}$ low power-mode generator. One has to take into account that the coupling attenuation (generator losses and k-spectrometer coupling) has been approximately 85 dB. As it can be seen in the lower part of the figure for each mode also the phase information could be determined.

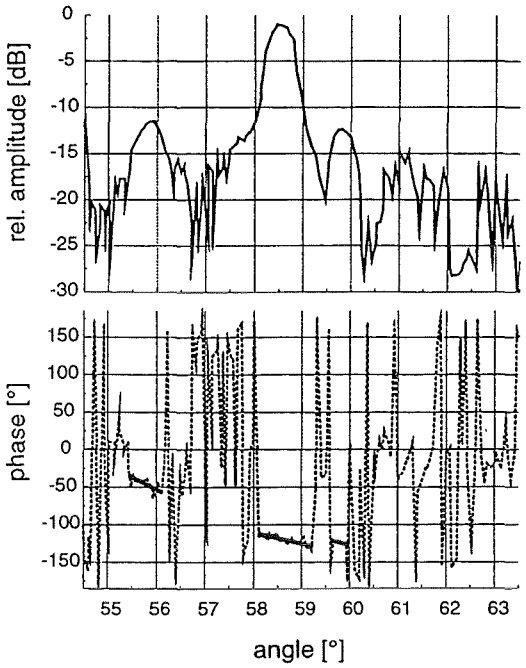

Fig. 2: Vector k-spectrometer measurement of $TE_{76,2}$ generator.

Measurements on the $TE_{76,2}$ mode generator

For testing the dual-beam output coupling system for the RF power of the FZK 140 GHz, 1.5 MW coaxial gyrotron [4] a low-power mode generator for a rotating $TE_{+76,2}$ mode has been built up. The wavenumber spectrum of this generator is shown in Figure 3. In contrast to the measurement shown in Figure 2 a more careful alignment had been performed.

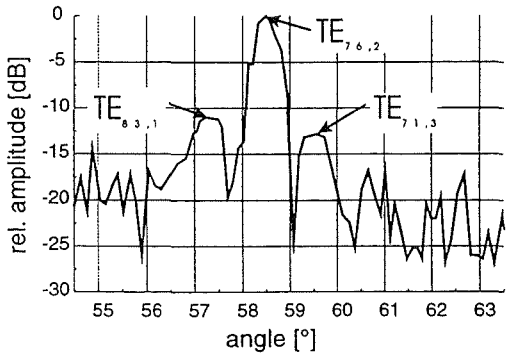

Fig. 3: k-spectrometer measurement of $TE_{+76,2}$ generator.

As it can be seen the main content of RF power is radiated under an angle of 58.3° to the axis of the k-spectrometer waveguide. This angle corresponds to the $TE_{76,2}$ mode propagating at 140 GHz in a 70 mm diameter waveguide. Unfortunately the spectrum shows two undesired competitors at 57.4° and 58.8° which have been identified to be the $TE_{83,1}$ and $TE_{71,3}$ mode respectively. Taking the different k-spectrometer coupling attenuation factors into account the suppressions of the modes $TE_{83,1}$ and $TE_{71,3}$ have been determined to be 16 dB and 11.5 dB. By rotating the k-spectrometer around its waveguide axis the content of the counter rotating $TE_{-76,2}$ mode was determined to be 4 %.

The overall mode purity of the desired $TE_{+76,2}$ mode is approximately 88 %.

The $TE_{-28,16}$ - to -$TE_{+76,2}$ mode converter

In the coaxial gyrotron the needed $TE_{+76,2}$ mode for the dual beam output is achieved by conversion from the $TE_{-28,16}$ gyrotron cavity mode [5]. To check the proper behavior of the required converter (104 axial slots in the waveguide wall) the system was operated in the reverse way. This means that the $TE_{+76,2}$ mode was fed into the converter . The measured field pattern at the converter output (input) is shown in Figure 4. It is obvious that the pattern shows a rather high content of the desired $TE_{28,16}$ mode. This is in agreement with k-spectrometer measurements which also had been performed.

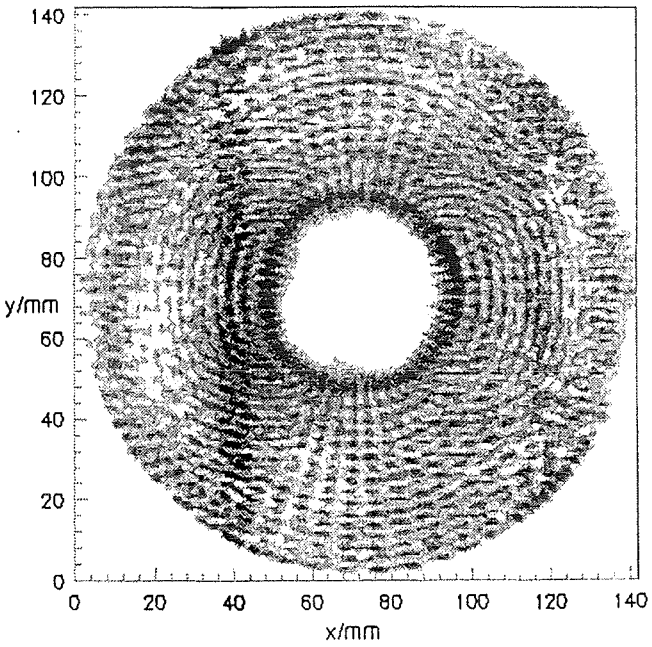

Fig. 4: Measured field pattern of $TE_{28,16}$ mode.

References

[1] Pereyaslavets, M., Braz, O., Kern, S., Losert, M., Möbius, A., Thumm, M., 1997, Int. J. Electronics, **82**, 107-115.

[2] Braz, O., Arnold, A., Losert, M., Möbius, A., Pereyaslavets, M., Thumm, M., 1996, Conf. Proceedings 21th Int. Conf. on Infrared and Millimeter Waves, Berlin, ATh6.

[3] Kasparek, W., Müller, G. A., 1988, Int. J. Electronics, **64**, 5-20.

[4] Piosczyk, B., et al., accepted for IEEE Trans. Plasma Science, June 1997.

[5] Thumm, M., et al., 1996, Conf. Proceedings 21th Int. Conf. on Infrared and Millimeter Waves, Berlin, AM6.

APPENDIX A4

Coaxial Cavity Gyrotron with Dual RF Beam Output

B. Piosczyk, O. Braz, G. Dammertz, C. T. Iatrou, S. Illy, M. Kuntze, G. Michel,
A. Möbius, M. Thumm, V. A. Flyagin, V. I. Khishnyak, A. B. Pavelyev, and V. E. Zapevalov

Abstract— **A 140-GHz, 1.5-MW, $TE_{28,16}$-coaxial cavity gyrotron with a dual rf beam output has been designed, built, and tested. For the first time, the generated rf power has been split into two parts and coupled out through two rf output windows in order to reduce the power loading in the windows. The quasioptical output system is based on a two-step mode conversion scheme. First, the cavity mode $TE_{-28,16}$ is converted into its degenerate whispering gallery mode $TE_{+76,2}$ using a rippled-wall mode converter. Then, this mode is transformed into two TEM_{00} output wave beams. A maximum rf output power of about 950 kW with an output efficiency of 20% has been measured. According to numerical calculations, an rf power above 1.5 MW is expected to be generated in the cavity. Even if all losses are taken into account, a discrepancy between experiment and calculations remains. The power deficit seems to be partly caused by the influence of the stray radiation captured inside the tube. However, the two main reasons are probably an incomplete mode conversion from $TE_{-28,16}$ to $TE_{+76,2}$ and a large energy spread of the electron beam due to trapped electrons. An increased amount of captured stray radiation resulted in a reduced stability of operation. A single-stage depressed collector was used successfully, increasing the rf output efficiency from 20% to 29%.**

Index Terms—**Coaxial gyrotron, dual rf beam.**

I. Introduction

CONVENTIONAL hollow waveguide-cavity gyrotrons at frequencies around 140 GHz are limited in output power to about 1 MW due to ohmic wall loading, mode competition, and limiting beam current. The presence of an inner conductor in coaxial cavities practically eliminates the restrictions of voltage depression and limiting current. In addition, in coaxial cavities, the diffractive quality factor of different modes can be influenced selectively allowing operation in high-order volume modes with reduced-mode competition problems. Thus gyrotrons with coaxial cavities have the potential to generate rf output powers in excess of the above-mentioned limit, even in cw operation [1]–[5].

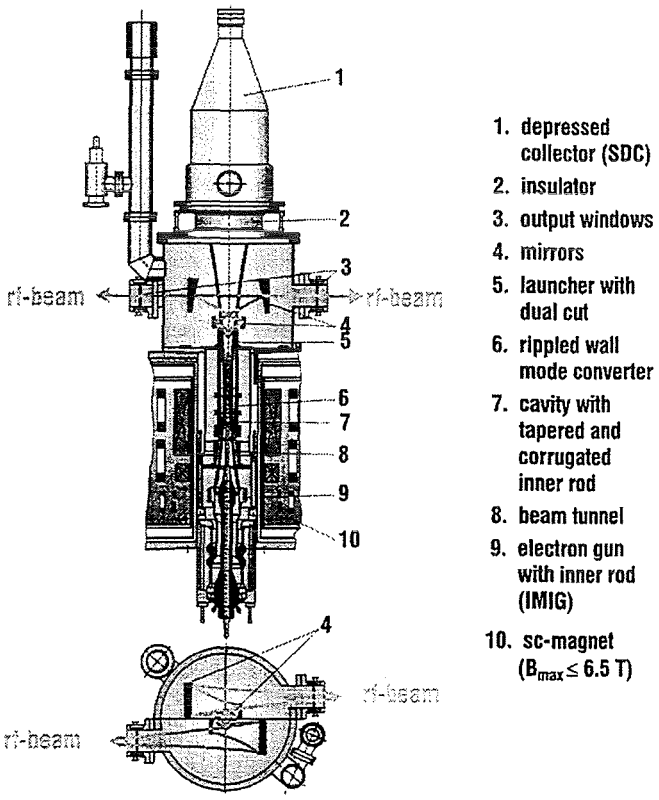

Fig. 1. Schematic layout of the coaxial cavity gyrotron with dual rf beam output.

A gyrotron designed for operation at 140 GHz in the $TE_{-28,16}$ mode and at 165 GHz in the $TE_{-31,17}$ mode with an rf output power of 1.5 MW is under investigation in a collaboration between the FZK and the IAP in Nizhny Novgorod, Russia. The development is planned to be performed in two steps. In a first step, which has already been completed, a coaxial gyrotron equipped with an axial waveguide output was designed, built, and operated. At both frequencies, an rf output power close to 1.2 MW with an efficiency of about 27% was measured [6], [7]. The achieved results have been very encouraging especially because the experimentally measured values of the rf output power were in good agreement with the results of numerical calculations.

The design of a high-power gyrotron relevant for long-pulse and cw operation requires a lateral rf output. The capability for power transmission of rf output windows is still limited at long pulses and cw operation to values below 1 MW at the

Manuscript received September 23, 1997; revised March 26, 1998. This work was supported by the European Fusion Technology Program under the Project Kernfusion of the Forschungszentrum Karlsruhe.

B. Piosczyk, G. Dammertz, S. Illy, M. Kuntze, and G. Michel are with Forschungszentrum Karlsruhe, Association EURATOM-FZK, Institut für Technische Physik, Karlsruhe, Germany (e-mail: bernhard.piosczyk@itp.fzk.de).

O. Braz and M. Thumm are with Forschungszentrum Karlsruhe, Association EURATOM-FZK, Institut für Technische Physik, Karlsruhe, Germany, and with Universität Karlsruhe, Institut für Höchstfrequenztechnik und Elektronik, Karlsruhe, Germany.

C. T. Iatrou is with the National Technical University of Athens, Athens, Greece.

A. Möbius is with IMT GmbH, Eggenstein, Germany.

V. A. Flyagin, V. I. Khishnyak, A. B. Pavelyev, and V. E. Zapevalov are with the Institute of Applied Physics, Russian Academy of Sciences, Nizhny Novgorod, Russia.

Publisher Item Identifier S 0093-3813(98)04276-3.

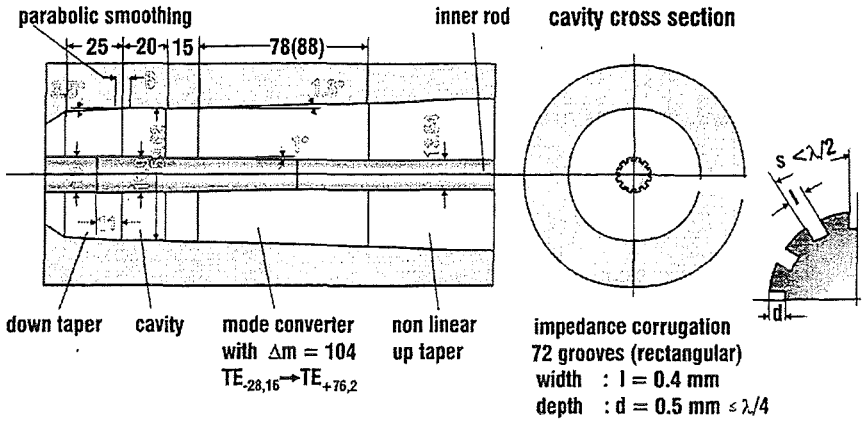

Fig. 2. Geometry of the 140-GHz, $TE_{28,16}$-coaxial cavity and the rippled-wall mode converter.

considered frequencies. Therefore, in the present experiment the rf output power has been split internally into two beams in order to take into account the limitations of the rf output windows. The quasi-optical (q.o.) rf output system is based on a two-step mode conversion scheme $TE_{-28,16} \Rightarrow TE_{+76,2} \Rightarrow TEM_{00}$, which generates two rf output wave beams with an azimuthal divergence of approximately 60° at the launcher.

As a result of rapid progress in the development of new window materials, such as Au-doped silicon [8] and CVD-diamond [9], it may soon become possible to transmit even 2 MW of rf power through a single window at the frequencies considered here. For this reason, the direct conversion of the cavity mode into a single TEM_{00} rf output beam and its transmission through a single window is also of interest for future high-power coaxial gyrotrons.

The gyrotron is equipped with a single-stage depressed collector in order to enhance the total efficiency and to reduce the power loading at the collector surface.

First results on the gyrotron performance have already been reported in [10]. Operating experience and results achieved at IAP Nizhny Novgorod with a very similar experimental setup are summarized in [11].

In the following, the design of the 1.5-MW, 140-GHz, $TE_{28,16}$-coaxial cavity gyrotron with the dual rf beam output is described. The operating experience and results of rf measurements are presented, discussed, and compared with the results of numerical simulations. In particular, the influence of rf radiation captured inside the gyrotron tube on the operation has been investigated and will be discussed.

II. Design Parameters and Experimental Setup

A schematic layout of the gyrotron with the dual rf beam output is shown in Fig. 1. The superconducting (sc) magnet, the electron gun, and the geometry of the cavity are as in the experiment with the axial waveguide output [6]. The 4.5-MW electron gun is of the diode type with a central rod surrounded by the cathode ring [12]. The inner rod is electrically isolated but is held close to the ground potential. It is fixed and cooled from the gun side. More detailed descriptions of the components and some design considerations are given in [6]. The components are arranged in an easily demountable way with no special cooling. This limits the operation to pulse lengths of up to about a few tens of millseconds at low duty factor. For the resonator, a cavity with a smooth cylindrical outer wall and a radially tapered and corrugated inner rod is used, as shown in Fig. 2. The cavity has a length of 20 mm. The inner rod has a negative taper angle of 1°. The impedance corrugation consists of 72 longitudinal grooves with a period s smaller than the half free-space wavelength $s < \lambda/2$. The linear part of the uptaper with an angle of 1.5° is 15 mm long and is followed by the rippled-wall mode converter. Numerical simulations indicate that for the parameter range considered, there should be no parasitic oscillations in this part of the tube, especially if oscillation in the cavity introduces a strong energy dispersion in the electron beam. The main design parameters of the tube are summarized in Table I. Two coils in the gun part permit the generation of different magnetic field configurations in the gun region. Depending on the magnetic field configuration, the velocity ratio $\alpha = \beta_\perp/\beta_\parallel$ varies from 1.1 up to about 1.4 for the design parameters. $\beta_\parallel$ and $\beta_\perp$ are the axial and transverse velocities of the electrons normalized to the speed of light. The realistic peak ohmic losses on the outer wall of the resonator are assumed to be about twice the ideal value $p_\Omega(\text{real}) \approx 2p_\Omega(\text{ideal})$. The voltage depression ΔU_b is calculated for $\alpha = 1.4$. Its low value is due to the presence of the inner rod. The two output windows optimized for maximum transmission of the TEM_{00} wave at 140 GHz have a diameter of 100 mm and consist of fused silica with a thickness $d = 6.04$ mm corresponding to $11 * \lambda/2$ (here, λ is the wavelength inside the window disk). For observation of the stray radiation P_{capt} captured in the gyrotron tube, an additional third window is placed perpendicular to the direction of the rf output beams. This window is a conventional quartz viewglass with a diameter of 60 mm and an approximate

TABLE I
Main Design Parameters of the $TE_{28,16}$ Coaxial Gyrotron at 140 GHz

rf-output power P_{out} / MW	1.5
cathode voltage U_c / kV	90
beam current I_b / A	50
velocity ratio α	1.4 (1.1)
beam radius R_b / mm	10.0
cavity radius R_{cav} / mm	29.81
voltage depression ΔU_b / kV	1.6
peak wall loading (ideal copper) p_Ω / kW/cm^2	0.63

transmission of 50% at 140 GHz. The power radiated through this window has been measured calorimetrically. Its value is taken as a measure for the amount of rf radiation captured inside the gyrotron tube.

The main reason for the selection of the co-rotating $TE_{-28,16}$ mode as the design mode comes from the two-step mode conversion scheme

$$TE_{-28,16} \Rightarrow TE_{+76,2} \Rightarrow TEM_{00}$$

which requires a degeneracy of the $TE_{-28,16}$ cavity mode (eigenvalue $\chi_{mp} = 87.36$) with the $TE_{+76,2}$ whispering gallery mode (WGM) (eigenvalue $\chi_{mp} = 87.38$). This two-step mode converter system for the dual rf beam output generates two narrowly directed output wave beams [13]. A direct conversion of the operating cavity mode into the TEM_{00} mode requires dimensions of the mirror system that are excessively large for a dual rf beam output since the azimuthal angle of divergence φ of the radiation for the $TE_{28,16}$ mode is as large as $\varphi = 2\arccos(m/\chi_{mp}) = 142.6°$. Here, m is the azimuthal number of the mode. For the degenerate $TE_{76,2}$ mode, however, the angle $\varphi = 59.1°$ is sufficiently small since the representing rays from its caustic are located closer to the waveguide wall. The double-cut q.o. converter uses an improved dimpled-wall double-beam launcher with $\Delta m_1 = 2$ and $\Delta m_2 = 6$ perturbations for longitudinal and azimuthal bunching of the 2-mm-wave beams, respectively. From the double-cut q.o. launcher, two diametrically opposed narrowly directed output wave beams are radiated and directed by two pairs of parabolic mirrors toward the rf output windows [13].

The conversion of the $TE_{-28,16}$ mode to the $TE_{+76,2}$ WGM-mode is achieved by introduction of longitudinal corrugations in the linear part of the output taper (1.5°) consisting of 104 slots ($\Delta m = 104$) according to

$$R_w = R_{w,0}(z) + \rho\cos(\Delta m\Phi)$$

where

$R_{w,0}(z)$ mean radius of the output waveguide wall;
ρ amplitude of the corrugations;
Φ azimuthal angle (Fig. 2).

The corrugations have been designed to have a spherical shape with a radius of 1.043 mm and a maximum depth of 0.113 mm corresponding to $\rho = 0.058$ mm. It has been calculated that a deviation of 10% from the ideal corrugation shape leads to conversion losses of about 7%. Fig. 3 shows a view into the rippled wall mode converter. The total length of the longitudinal grooves including the linear input and output tapers (each 12 mm long) was 78 mm long in the first experiment (case 1).

It should be pointed out, however, that in particular, due to the first conversion step $TE_{-28,16} \Rightarrow TE_{+76,2}$, the two-step mode conversion scheme works properly only for the design mode and cannot be used if the option of step-frequency tuning is desired.

A nonlinear uptaper matches the mode converter to the input of the launcher with a diameter of 68.3 mm. A photograph of the launcher with the double cut is shown in Fig. 4. The diffraction losses at the launcher and the mirrors have been

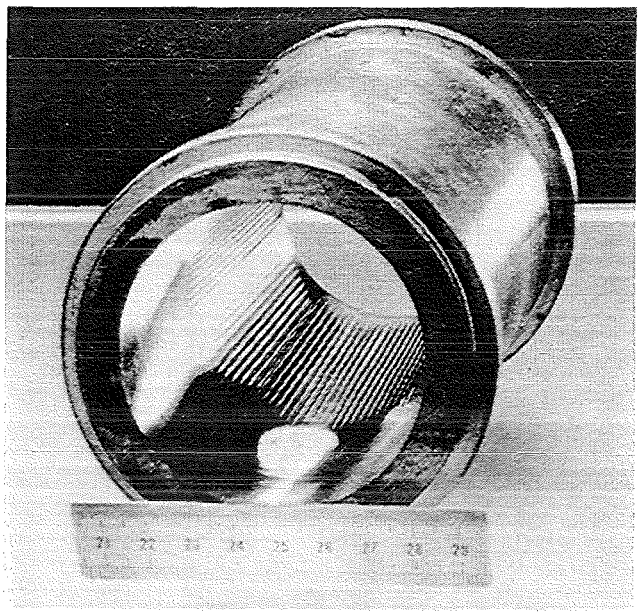

Fig. 3. Rippled-wall mode converter.

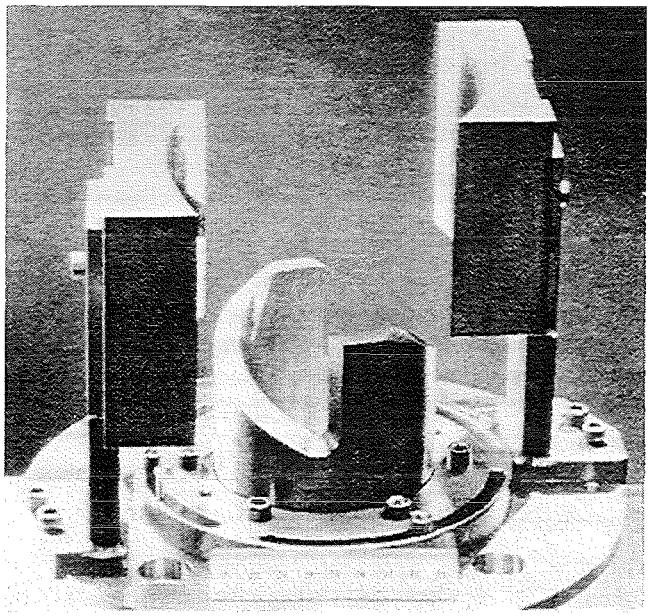

Fig. 4. Launcher with the double cut and the first pair of mirrors.

calculated to be about 6%. The ohmic losses in the cavity, in the rippled wall mode converter, in the launcher, and in the mirrors and the absorption in the windows are estimated to be 13% of the rf output power $P_\Omega = 0.13 * P_{out}$. The relatively high value of the ohmic losses is partly due to the high ohmic losses of the converted WGM mode.

As described in [14], conversion of the $TE_{22,6}$ mode into two rf output wave beams (120° azimuthal separation) using a dimpled-wall double beam launcher with two axially shifted cuts has been successfully demonstrated in cold measurements. In [15], a different method has been used to generate two Gaussian-like beams by splitting a single Gaussian beam with an arrangement of four mirrors.

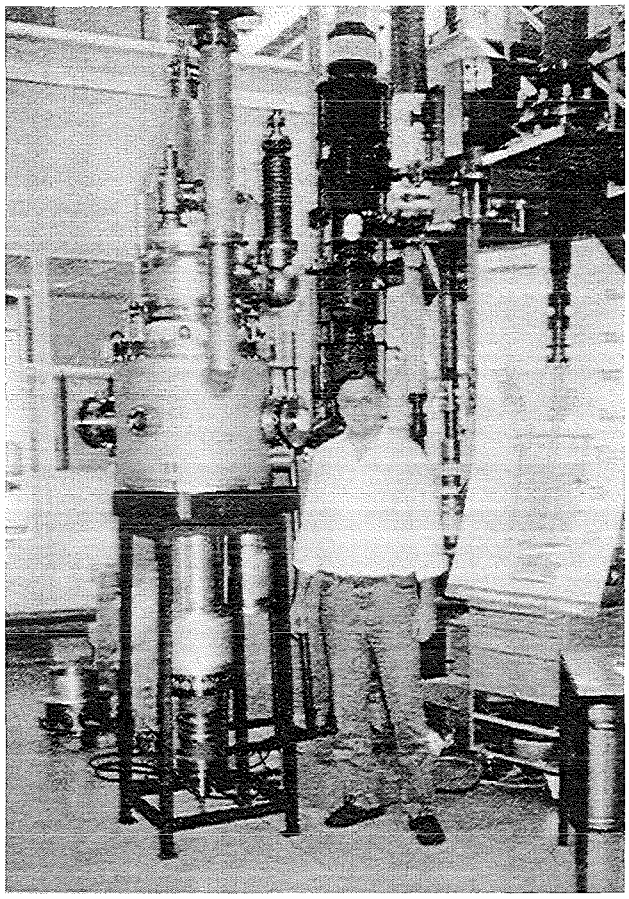

Fig. 5. Fully assembled gyrotron.

The electrically insulated collector with an inner diameter of 300 mm permits a maximum pulse length of several 10 ms without any sweeping of the beam. It can be used as a single-stage depressed collector. A view of the fully assembled tube is given in Fig. 5.

III. Experimental Operation and Results

A. Performance of the Measurements

The measurements have been performed in short-pulse operation. Most data have been taken with an rf pulse length of 0.5 ms and a repetition rate of 1 Hz. In single pulses, the pulse length has been extended up to 7 ms. The high voltage (HV) pulse had a rise time of approximately 0.2 ms without any voltage overshooting. With a contiguous filter bank consisting of ten 2-GHz and three 0.1-GHz channels around the design frequency, a signal of the generated rf power has been observed simultaneously in the different frequency channels giving information as to whether there was single- or multimode oscillation in the cavity. The time dependence of the frequency during a pulse was measured with a time-frequency analyzer. An infrared camera has been used for measuring of the output rf field distribution. The rf output power P_{out} has been measured at both windows simultaneously either with two silicon oil flow calorimeters or with one flow and one ballistic calorimeter. It has been found that within the accuracy of the calorimetric measurements ($\pm 5\%$), the rf power was split equally between both windows. The power of the stray radiation radiated through the third window was measured with a ballistic calorimeter.

The current to the inner rod was less than 20 mA at the design parameters with $I_b = 50$ A. The vacuum pressure during operation was typically around 10^{-6} mbar. The operating temperature of the LaB_6 cathode is about 1400°C. The alignment of the inner rod with respect to the electron beam was performed with the help of dipole coils, as described in [6].

Rf radiation captured inside the tube was suspected to influence the gyrotron operation. Therefore, some modifications have been performed in order to reduce the amount of P_{capt}. Measurements of the depth of some of the grooves of the rippled-wall mode converter indicated that the grooves were not deep enough and that the $\text{TE}_{-28,16} \Rightarrow \text{TE}_{+76,2}$ conversion might be too low. Therefore, the length of the rippled-wall mode converter was increased to 88 mm in order to enhance the conversion efficiency by about 7%. In addition, the full metal copper beam tunnel was replaced by a sandwich-structured tunnel equipped with alternating rings of copper and rf absorbing material. In addition, rf absorbing plates have been placed along the walls of the vacuum chamber in order to reduce the amplitude of the captured stray radiation. Thus, the described experiments have been performed under the following three different conditions:

- case 1: The rippled-wall mode converter machined according to the design (78 mm long) and a conical full metal (copper) beam tunnel was used.
- case 2: The length of the grooves of the rippled-wall mode converter was increased to 88 mm in order to enhance the conversion efficiency by $\approx 7\%$, and the beam tunnel was replaced by a tunnel with rf absorbing material.
- case 3: This is the same as case 2 but with additional rf absorbing plates placed close to the walls of the mirror vacuum chamber in order to reduce the amplitude of the captured stray radiation P_{capt}.

B. Captured Stray Radiation

As a result of diffraction losses about 6% of the rf output power has been estimated to contribute to stray radiation. This stray radiation is distributed within the gyrotron tube, which acts as a highly oversized untuned resonator. According to measurements described later, about one third of the stray radiation is finally radiated through the two output windows. The remaining approximately two thirds of the stray radiation is captured within the gyrotron tube and is finally dissipated in the walls, which consist mainly of stainless steel. The rf power radiated through the third window $P_{3\text{wind}}$ is a measure of the amount of stored energy $W_{\text{capt}} \propto P_{\text{capt}}$ inside the gyrotron tube due to the captured part P_{capt} of the stray radiation. A ballistic calorimeter has been used to measure $P_{3\text{wind}}$. The absolute value of $P_{3\text{wind}}$ is only about 1% of the rf output power P_{out}. Fig. 6 gives the measured value of $P_{3\text{wind}} \propto \Delta T$ versus the output power as achieved in the design mode for

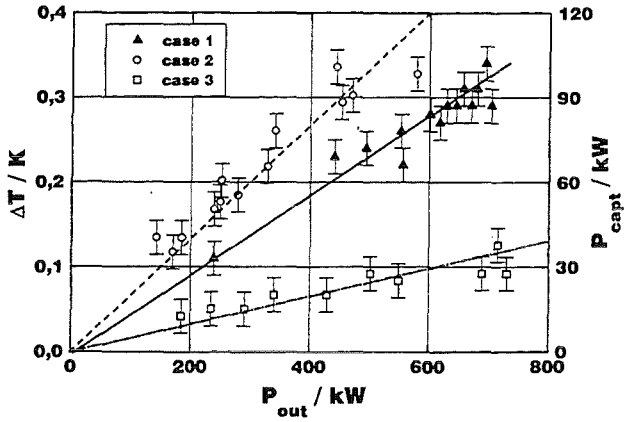

Fig. 6. Captured stray radiation $P_{\text{capt}} \propto \Delta T$ versus the output power P_{out}.

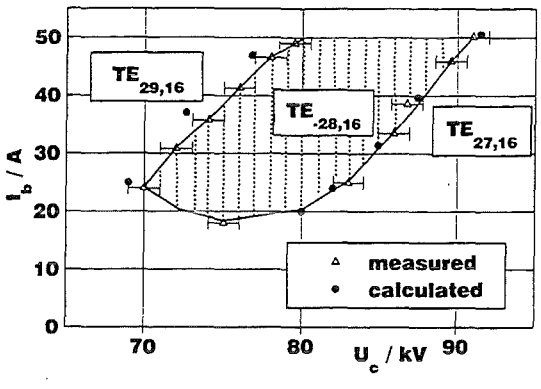

Fig. 7. Single-mode operating range for the $TE_{-28,16}$ mode.

the three operating cases. Here, ΔT is the temperature increase of the ballistic calorimeter. The amount of the captured stray radiation $P_{\text{capt}} \propto P_{3\text{wind}}$ is found to be proportional to the rf output power in all three cases $P_{\text{capt}} \propto P_{\text{out}}$.

In order to calibrate the amount of P_{capt} relative to P_{out}, the gyrotron has been operated at the same parameters $(I_b, U_c, |B(z)|)$ for both directions of the magnetic field, thus generating the design co-rotating $TE_{-28,16}$ mode and the counter-rotating $TE_{+28,16}$ mode, respectively. The q.o. launcher with the double cut is only matched to one direction of rotation, namely, to the $TE_{+76,2}$ mode being generated from the co-rotating $TE_{-28,16}$ mode. The rf power generated in the counter-rotating mode is therefore not matched to the launcher system and is radiated into the vacuum chamber without any preferred direction.

With the assumption that the amount of the generated rf power is independent of the direction of the magnetic field for the given operating parameters, the value of the captured stray radiation P_{capt} can be estimated according to

$$P_{\text{capt}} = \Pi_0 * \Delta T \quad \text{with}$$
$$\Pi_0 = [\{P_{\text{out}}(-28,16) - P_{\text{out}}(+28,16)\}/\{\Delta T(+28,16) - \Delta T(-28,16)\}]$$

where $P_{\text{out}}(-28,16)$ and $P_{\text{out}}(+28,16)$ are the measured rf output power for the co- and counter-rotating mode, respectively. $\Delta T(-28,16)$ and $\Delta T(+28,16)$ are the corresponding measured values of the temperature rise in the calorimeter at the third window. When the magnetic field is reversed, the output power $P_{\text{out}}(+28,16)$ is about 30% of the corresponding output power $P_{\text{out}}(-28,16)$, indicating that about one third of the stray radiation is not captured and is radiated through the two output windows. The calibration measurements gave $\Pi_0 \cong 300$ kW/K. It should be emphasized that P_{capt} is the fraction of the stray radiation captured inside the gyrotron tube and is mainly dissipated in the walls of the tube. The amount of the captured stray radiation relative to the rf output power $P_{\text{capt}}/P_{\text{out}}$ is given in Table II for the three cases investigated. Unfortunately, the modifications performed on the rippled-wall mode converter resulted in an increase of P_{capt} by about 50%, as seen by comparison of cases 1 and 2; instead of the expected increase in converter efficiency, a decrease was observed. Efficient conversion requires extremely high mechanical accuracy, which, in practice, is very hard to achieve. The amount of W_{capt} in cases 2 and 3 is the same because no other modifications than the installation of the rf absorbing plates have been performed. Due to the enhanced rf absorption by the absorbing plates, the amplitude of the captured power P_{capt} is reduced in case 3 by about a factor of 4 relative to case 2.

C. Stability of Operation and Influence of the Stray Radiation

The gyrotron can be operated in two magnetic field configurations by adjusting the charging of the two gun coils. The velocity ratio α corresponding to the two magnetic field configurations is $\alpha \cong 1.1$ and $\alpha \cong 1.4$ at the design parameters ($U_c = 90$ kV, $I_b = 50$ A), respectively. Stable operating conditions have been found over the full parameter range only in the configuration with $\alpha \cong 1.1$ at the design parameters. The operation of the gyrotron in the configuration with $\alpha \cong 1.4$ at the design parameters was limited due to beam instabilities to values of the cathode voltage that typically occurred 5 to 10 kV below the design voltage. The beam instabilities were observed as irregular oscillations on the oscilloscope trace of the electron beam current. In general, these oscillations were accompanied by an instability of the cathode voltage. Because of these instabilities, most data have been taken with the magnetic field configuration corresponding to $\alpha \cong 1.1$ at the design parameters. For this configuration, stable operation was observed in the range indicated in Fig. 7, especially in the cases 1 and 3 with medium and low values of P_{capt}. In case 2, with high value of P_{capt}, the stability of oscillation was slightly reduced at higher voltages U_c. Strongly enhanced beam instabilities limiting the operation even in the configuration with $\alpha \cong 1.1$ at the design parameters occurred when the gyrotron oscillated in the neighboring modes ($TE_{-27,16}$ and $TE_{-29,16}$) or in the counter-rotating design mode $TE_{+28,16}$. In these cases, the amount of captured stray radiation P_{capt} is increased significantly since the modes are not matched to the rf output system. This strongly confirms the observation that captured stray radiation may enhance the occurrence of beam instabilities and, thus, may reduce the accessible parameter range. This is in agreement with previous observations with the axial version of the tube where enhanced instabilities occurred during operation in modes with

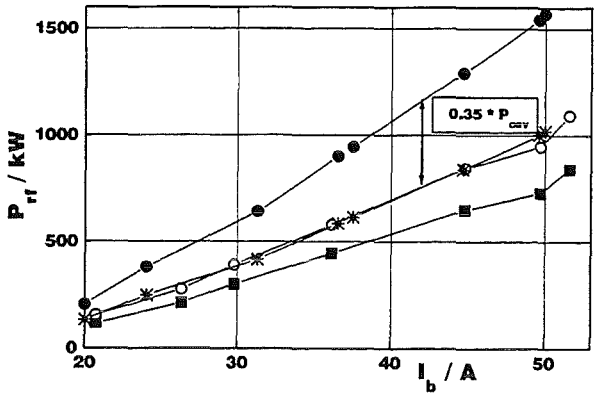

Fig. 8. Rf power versus the beam current. $B_{cav} = 5.637$ T, $U_c = 80$ to 90 kV, U_c optimized for maximum P_{out}. (—■—) P_{out}; (—○—) $P_{out} + P_{capt} + P_\Omega$; (—•—) P_{th}; (—*—) $0.65 * P_{th}$.

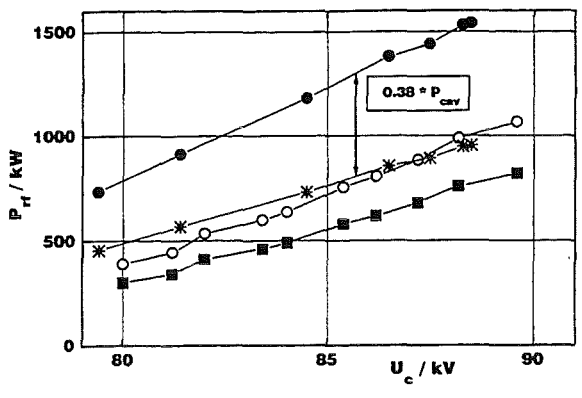

Fig. 9. Rf power versus the cathode voltage U_c. $B_{cav} = 5.623$ T, $I_b = (50 \pm 1)$ A. (—■—) P_{out}; (—○—) $P_{out} + P_{capt} + P_\Omega$; (—•—) P_{th}; (—*—) $0.65 * P_{th}$.

high window reflections [6]. It is suspected that the enhanced occurrence of the beam instabilities due to the captured stray radiation is related to the poor beam quality together with the existence of some trapped electrons.

The fact that more stable operation was possible with medium to low values of P_{capt} (cases 1 and 3) than with high values (case 2) supports the conclusion that captured stray radiation reduces the stability of operation. No significant improvement in operation was observed when the full metal beam tunnel was replaced by a tunnel with rf absorbing rings (case 2). The possible influence of the stray radiation on rf output power and efficiency is discussed in the following sections.

D. Range of Single-Mode Operation

A wide range of single-mode oscillation has been found as shown in Fig. 7. The results have been observed in both case 1 with medium and case 3 with low amount of P_{capt}. In case 2, with a high value of P_{capt}, some problems with the stability of operation occurred at higher cathode voltages U_c. Numerical calculations have been performed with a self-consistent time-dependent multimode code taking into account up to six different modes [16]. The agreement between experiment and the numerical results is good (Fig. 7). This seems to confirm the previously expressed suspicion [6] that the observed reduction of the single-mode operating range in the gyrotron with the axial rf output system was due to the influence of voltage overshooting and due to enhanced window reflections in the competing modes.

E. Dependence of RF Output Power on Operating Parameters

The measurements in the three cases with different values of P_{capt} delivered different results. Fig. 8 gives as an example the measured rf output power P_{out} versus the beam current as achieved in the case 1 with medium value of P_{capt}. The magnetic field has been kept constant during this measurement with a field distribution corresponding to $\alpha \cong 1.1$ at the design parameters. The cathode voltage U_c has been adjusted for maximum P_{out} at a given current. In order to achieve the generated rf power inside the cavity P_{exp}, the estimated

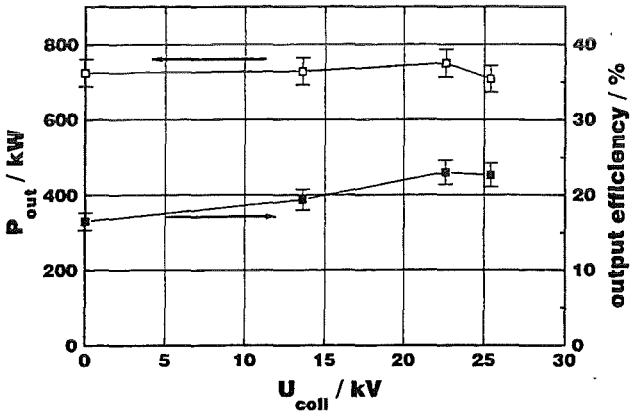

Fig. 10. Rf output power and efficiency versus retarding collector voltage U_{coll}. $I_b \approx 50$ A, $U_c \approx 88$ kV, $B_{cav} = 5.637$ T.

losses in the walls and the windows ($P_\Omega = 0.13 * P_{out}$) and the measured amount of the captured stray radiation as given in Table II ($P_{capt} = 0.14 * P_{out}$ for case 1) have been added to the output power $P_{exp} = P_{out} + P_\Omega + P_{capt}$. With a time-dependent, self-consistent multimode code, the rf power P_{th} generated in the cavity has been calculated taking the operating parameters as input. The value of α has been taken from a trajectory code and for the relative transverse velocity spread $\delta\beta_{\perp rms} = 6\%$ has been assumed in rough agreement with previous measurements of the velocity spread [12]. The results clearly demonstrate a significant discrepancy between the experimental and theoretical values. The experimentally measured rf power is only about 0.65 ± 0.05 of the calculated value. The ratio is almost constant over the whole operating parameter range. Fig. 9 shows for case 1 (medium P_{capt}) the dependence of the rf power vs. the cathode voltage U_c for a fixed magnetic field and a beam current $I_b = (50 \pm 1)$ A. As given in Fig. 8, the additional losses are added to the measured output power. The general feature of the results is similar to the last figure with $P_{exp} \cong 0.62 * P_{th}$. The observed behavior in cases 2 (high P_{capt}) and 3 (low P_{capt}) showed a very similar characteristic. Only the achieved values were slightly different as given in Table III. P_{outmax} and η_{outmax} are the maximum rf output power and the corresponding efficiency measured at the parameters U_{cmax} and I_{bmax}, which are close to the

TABLE II
CAPTURED STRAY RADIATION P_{capt} FOR THE THREE OPERATING CASES

	case 1	case 2	case 3
P_{capt} / P_{out}	≅ 0.14	≅ 0.20	≅ 0.05* (0.20)
amount of P_{capt}	medium	high	low

* the amount of the captured stray radiation is the same as in case 2, only the amplitude is reduced due to additional absorption.

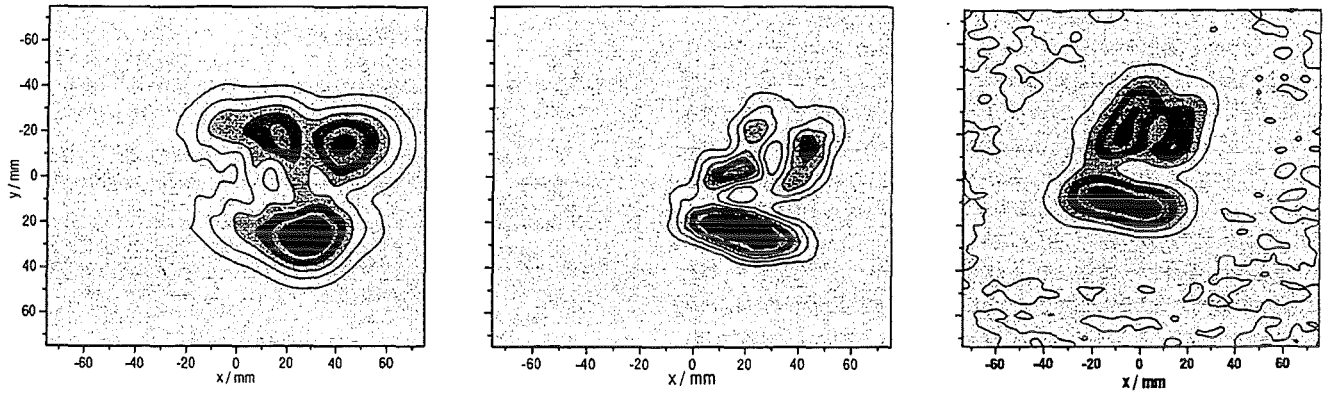

(a) (b) (c)

Fig. 11. Distribution of the rf power 37-cm outside the window. (a) Calculation. (b) Cold measurements. (c) Hot measurements.

design values. In case 2 (high P_{capt}), the value of P_{outmax} and η_{outmax}, as well as the ratio between the experimentally generated and the theoretically expected rf power P_{exp}/P_{th}, are significantly lower compared with the cases 1 (medium P_{capt}) and 3 (low P_{capt}), indicating an influence of the stray radiation on the operation. However, we do not think that the stray radiation is the only reason for the lack of efficiency that also remained significant in case 3 with its fairly low value of $P_{capt} \cong 0.05 * P_{out}$. The energy spread of the electron beam and the nonoptimal mode conversion in the rippled-wall converter are suspected to be the main reasons for the reduced efficiency. According to calculations reported in [17], we would need an energy spread of about 10% (rms-value) to explain the efficiency reduction of about 30%, as observed in case 3 (low P_{capt}). Recent measurements of the energy distribution of the electron beam performed at scaled-down parameters as reported in [18] give some indications that there may be a wide energy spread at the operating parameters presumably caused by trapped electrons as a consequence of the poor beam quality. In these measurements, the trace of the electron beam on the collecting plate showed a pronounced azimuthal nonuniformity. The degradation of the electron beam quality is thought to be mainly due to a deterioration of the emission properties of the LaB_6-emitter, which resulted from exposure to air for several times when the demountable tube was opened for modifications between experiments. In addition, mechanical deformations in the gun that accumulated during the different experimental steps could result in further degradation of beam quality.

F. Operation with a Single-Stage Depressed Collector

Results of operation with a depressed collector as achieved in case 1 are given in Fig. 10. The maximum retarding voltage

TABLE III
EXPERIMENTAL RESULTS FOR THE THREE OPERATING CASES

	P_{max} / kW	U_{cmax}/kV ; I_{bmax}/A	η_{max} / %	P_{exp} / P_{th}
case 1	875	88.2 ; 52.2	19	0.62
case 2	730	88.2 ; 51.5	16	0.5
case 3	950	90.4 ; 52.5	20	0.7

$U_{coll} = 27$ kV was limited by HV voltage breakdown at the collector. An increase would have required more high voltage conditioning of the collector. The pulse length has been extended in single pulses up to about 7 ms. The current to the body and inner rod was low (<20 mA). At longer pulses, the current to the inner rod increased up to about 60 mA with a time constant of about 2 ms being related to the neutralization time of the background gas at the operating pressure of $\approx 10^{-6}$ mbar. For longer pulse lengths, this current decreased stochastically and increased again with the mentioned time constant up to the value of about 60 mA. With the depressed collector, the rf output efficiency would rise in case 3 from 20% to 29%.

G. Distribution of the Rf Output Power

In order to optimize the power output coupling of the q.o. output system and the intensity distribution across the windows, the position of the launcher and the mirrors was adjusted in cold measurements [19], [20]. The beam image shown in Fig. 11(b) has been measured 37 cm outside the window and is in good agreement with the hot measurements as shown in Fig. 11(c). The results of calculation [Fig. 11(a)] are in qualitative agreement with the experiment.

The diffraction losses have been estimated to be about 6%. The measured losses were somewhat higher, resulting in an

overall efficiency of the q.o. output system of ≅86% in case 1. After the modification of the rippled-wall mode converter, the efficiency further decreased to ≅80%.

IV. Conclusions and Summary

A coaxial cavity gyrotron with a dual rf output has been designed, built, and operated for the first time. A two-step rf output scheme has been used. The first step converting the cavity mode into its degenerate whispering gallery mode is strictly limited to the design mode. Therefore, such a scheme is not suitable for step-wise frequency tuning. Three different cases with some small modifications resulting in different amounts of captured stray radiation have been investigated. With a magnetic field distribution resulting in a velocity ratio of $\alpha \cong 1.1$ at the design parameters, stable operation has been achieved, especially when the amount of stray radiation was not too high. A maximum output power of 950 kW has been measured with an output efficiency of 20% in case 3 with a low value of captured stray radiation P_{capt}. Compared with results of numerical calculations, there is a power and efficiency deficit of about 30%. In cases 1 and 2 with medium and high amount of P_{capt}, the power deficit is higher (about 38% and 50%, respectively). The reduction of the output power and efficiency seems to depend on the amount of P_{capt}. However, in particular in case 3 with its relatively low value of P_{capt}, other effects have to be responsible for the lack of generated rf power. One reason for the low efficiency is the unsatisfactory performance of the rippled-wall $\mathrm{TE}_{-28,16}$ to $\mathrm{TE}_{+76,2}$ mode converter. Satisfactory performance requires very high precision machining. There are some indications that an additional reason could be the energy spread of the electron beam related to trapped electrons as a consequence of poor beam quality.

A wide single-mode operating range has been found in good agreement with the theoretical expectations. Beam instabilities limited the operation at a magnetic field distribution delivering a velocity ratio $\alpha \cong 1.4$ at the design parameters. The instabilities are enhanced due to the captured rf radiation. It is suspected that the appearance of the instabilities is also related to the poor beam quality and trapped electrons.

A single-stage depressed collector was used successfully and increased the gyrotron efficiency by a factor of almost 1.5.

In order to improve the quality of the electron beam the LaB_6-emitter ring, which has been exposed to air many times, will be replaced by a new one before the next experiment. The $\mathrm{TE}_{31,17}$ mode at 165 GHz with a direct conversion of the cavity mode into the TEM_{00} mode and a single rf output window will be investigated.

Acknowledgment

This work was assigned as an ITER task to the European Home Team under the agreement among the European Atomic Energy Community, the Government of Japan, the Government of the Russian Federation, and the Government of the United States of America in cooperation with the engineering design activities of the International Thermonuclear Experimental Reactor ("ITER EDA Agreement") under the auspices of the International Atomic Energy Agency (IAEA). The authors gratefully acknowledge H. Baumgärtner, H. Budig, P. Grundel, H. Kunkel, W. Leonhardt, N. Münch, J. Szczesny, and R. Vincon of the gyrotron team technical staff for the mechanical design, the precise machining, and the careful assembly of the tube as well as for their assistance during the experiments. They also thank Prof. E. Borie for proofreading the manuscript.

References

[1] S. N. Vlasov, L. I. Zagryadskaya, and I. M. Orlova, "Open coaxial resonators for gyrotrons," *Radio Eng. Electron. Phys.*, vol. 21, pp. 96–102, 1976.

[2] C. T. Iatrou, S. Kern, and A. B. Pavelyev, "Coaxial cavities with corrugated inner conductor for gyrotrons," *IEEE Trans. Microwave Theory Tech.*, vol. 41, pp. 56–64, 1996.

[3] J. J. Barroso and R. A. Correa, "Coaxial resonator for a megawatt, 280 GHz gyrotron," *Int. J. Inf. Millim. Waves*, vol. 12, pp. 717–728, 1991.

[4] M. E. Read *et al.*, "Design of a 3-MW 140-GHz gyrotron with a coaxial cavity," *IEEE Trans. Plasma Sci.*, vol. 24, pp. 586–595, 1996.

[5] J. P. Hogge, K. E. Kreischer, and M. E. Read, "Results of testing a 3 MW, 140 GHz gyrotron with a coaxial cavity," in *Conf. Dig. 20th Int. Conf. Infrared Millimeter Waves*, Lake Buena Vista, FL, 1995, pp. 417–418.

[6] B. Piosczyk *et al.*, "A 1.5-MW, 140-GHz, $\mathrm{TE}_{28,16}$-coaxial cavity gyrotron," *IEEE Trans. Plasma Sci.*, vol. 25, pp. 460–469, 1997.

[7] C. T. Iatrou *et al.*, "Design and experimental operation of a 165 GHz, 1.5 MW coaxial-cavity gyrotron with axial RF output," *IEEE Trans. Plasma Sci.*, vol. 25, pp. 470–479, 1997.

[8] V. V. Parshin, R. Heidinger, B. A. Andreev, A. V. Gusev, and V. B. Shmagin, "Silicon as an advanced window material for high power gyrotrons," *Int. J. Infrared Millimeter Waves*, vol. 16, pp. 863–877, 1995.

[9] O. Braz *et al.*, "High power 170 GHz test of CVD diamond for ECH window," *Int. J. Inf. Millim. Waves*, vol. 18, pp. 1495–1503, 1997.

[10] B. Piosczyk *et al*, "Coaxial cavity gyrotron with dual rf beam output," in *Proc. 10th Joint Workshop ECE & ECRH*, Ameland, The Netherlands, 1997, pp. 475–482.

[11] V. A. Flyagin *et al.*, "Investigation of coaxial gyrotrons at IAP RAS," in *Conf. Dig. 22nd Int. Conf. Infrared Millimeter Waves*, Wintergreen, VA, 1997, pp. 112–113.

[12] V. K. Lygin, V. N. Manuilov, A. N. Kuftin, A. B. Pavelyev, and B. Piosczyk, "Inverse magnetron injection gun for a 1.5 MW, 140 GHz gyrotron," *Int. J. Electron.*, vol. 79, pp. 227–235, 1995.

[13] M. Thumm, C. T. Iatrou, A. Möbius, and D. Wagner, "Built-in mode converters for coaxial gyrotrons," in *Conf. Dig. 21st Int. Conf. Infrared Millimeter Waves*, Berlin, Germany, 1996.

[14] Y. Mitsumata *et al.*, "Cold test of a dual-beam mode converter for a volume-mode gyrotron," in *Conf. Dig. 20th Int. Conf. Infrared Millimeter Waves*, Lake Buena Vista, FL, 1995, pp. 279–280.

[15] M. Blank, K. Kreischer, and R. J. Temkin, "Theoretical and experimental investigation of a quasioptical mode converter for a 110 GHz gyrotron," *IEEE Trans. Plasma Sci.*, vol. 24, pp. 1058–1066, 1996.

[16] S. Kern, "Numerical codes for interaction calculations in gyrotron cavities," in *Conf. Dig. 21st Int. Conf. Infrared Millimeter Waves*, Berlin, Germany, 1996.

[17] S. Y. Cai, T. M. Antonsen Jr., G. Saraph, and B. Levush, "Multifrequency theory of high power gyrotron oscillators," *Int. J. Electron.*, vol. 72, pp. 759–777, 1992.

[18] V. L. Bratman *et al.*, "Measurements and interpretation of energy spectra in gyrotrons," in *Conf. Dig. 22nd Int. Conf. Infrared Millimeter Waves*, Wintergreen, VA, 1997, pp. 186–187.

[19] O. Braz *et al.*, "Low power excitation and mode purity measurements on gyrotron type modes of higher order," in *Conf. Dig. 21st Int. Conf. Infrared Millimeter Waves*, Berlin, Germany, 1996.

[20] O. Braz, A. Arnold, H. Kunkel, and M. Thumm, "Low power performance tests on highly oversized waveguide components of high power gyrotrons," in *Conf. Dig. 22nd Int. Conf. Infrared Millimeter Waves*, Wintergreen, VA, 1997, pp. 21–22.

B. Piosczyk, photograph and biography not available at the time of publication.

O. Braz, photograph and biography not available at the time of publication.

G. Dammertz, photograph and biography not available at the time of publication.

C. T. Iatrou, photograph and biography not available at the time of publication.

S. Illy, photograph and biography not available at the time of publication.

M. Kuntze, photograph and biography not available at the time of publication.

G. Michel, photograph and biography not available at the time of publication.

A. Möbius, photograph and biography not available at the time of publication.

M. Thumm, photograph and biography not available at the time of publication.

V. A. Flyagin, photograph and biography not available at the time of publication.

V. I. Khishnyak, photograph and biography not available at the time of publication.

A. B. Pavelyev, photograph and biography not available at the time of publication.

V. E. Zapevalov, photograph and biography not available at the time of publication.

Design of a Quasi-Optical Mode Converter for a Coaxial 165 GHz $TE_{31,17}$ Gyrotron

G. Michel*, M. Thumm*, D. Wagner†

*) Forschungszentrum Karlsruhe, ITP, Association EURATOM-FZK,
P.O.Box 3640, 76021 Karlsruhe, Germany
and Universität Karlsruhe, IHE, Kaiserstr. 12,
76128 Karlsruhe, Germany
†) Universität Stuttgart, Institut für Plasmaforschung,
Pfaffenwaldring 31, 70569 Stuttgart, Germany

Abstract

The design of a quasi optical mode converter for the extreme volume mode $TE_{31,17}$ is described. It is the operating mode of a 1.5 MW, 165 GHz coaxial cavity gyrotron to be built. The goal is to launch the operating mode directly in order to keep the converter short and the conversion losses and ohmic losses low. Due to the large azimuthal angle of this mode, the design is based on a hybrid geometrical optical and physical optical technique.

Choice of the Converter Principle

The common principle for launching a gaussian like beam from a waveguide cut is the dimple wall converter. It provokes a resonant [1] eigenmode change in the waveguide before launching the beam. For the $TE_{31,17}$ mode this can be easily achieved for a pentagram like ray structure ($\Delta m = 5$) which is well suited for a double beam launcher.

For a single beam launcher, the large spread angle ($2\Theta = 140°$) cannot be transformed into a small one with a short converter and the mode $TE_{31,17}$ as the main mode. Since a dimple wall launcher has only little advantage in this case, an ordinary Vlasov launcher is used and the transformation of the strongly divergent beam into a paraxial one is done by means of spe- mirrors. This transformation requires either a few weakly curved mirrors [2] or one strongly curved mirror.

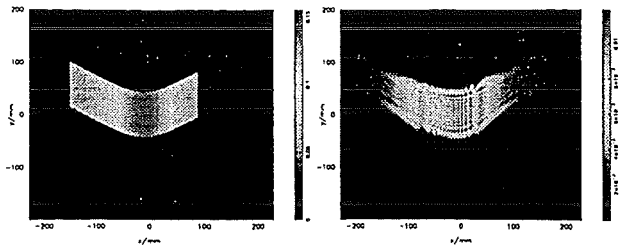

Figure 1: GO (left) and PO (right) Output of the Vlasov Launcher

In the gyrotron vacuum vessel space is limited, therefore the second solution is chosen. The strongly curved mirror, however, cannot be considered as a phase corrector in the sense of a thin lens and must be designed by means of geometrical optics. Here the Vlasov converter has the advantage that it can be easily analysed with geometrical optics. Figure 1 shows the output of the Vlasov converter calculated with the Bessel function and physical optics and with geometrical optics in the input plane of the quasi parabolic mirror.

The good argeement (except from the fine structure) comes from the high Fresnel number ($N \approx 140$). Because of the strong curvature and the large longitudinal extent of the mirror, it should not be considered as a phase corrector and it corresponds rather to a thick lens.

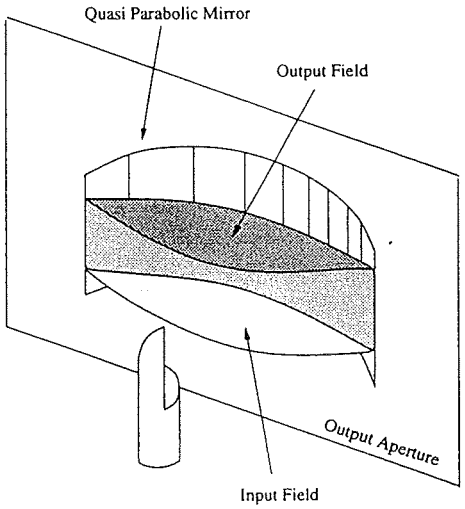

Figure 2: Output Aperture of the Quasi Parabolic Mirror

Therefore the output of the mirror is calculated with geometrical optics in the same aperture as the input (Figure 2). From here, we have a paraxial beam and can continue with physical optics. Figure 3 shows the final setup. A second ("turning") mirror directs the beam out of the gyrotron window.

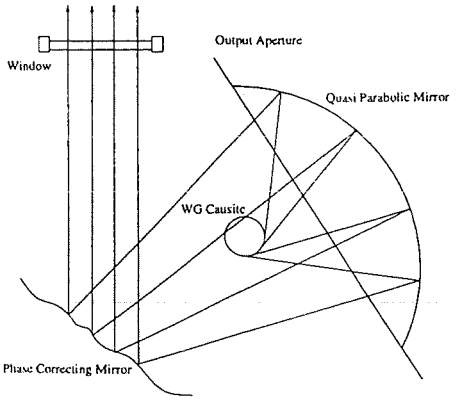

Figure 3: Setup of the Quasi Optical Mode Converter

Design of the Second Mirror

The turning mirror is designed by means of the well known error reduction algorithm [3]. For technical reasons, the gyrotron window is off axis. Therefore it must be turned around two axes. Since the beam has a large transverse extent and a large tilt angle, it is desirable to use the field in the mirror plane for the synthesis instead of the perpendicular lens approximation. This is achieved with a new propagation formula which allows the source as well as the target aperture to be rotated around all three axes. For the forward transform we get in spectral domain

$$\hat{U}(\hat{f}^1, \hat{f}^2, d) = \frac{-1}{\hat{f}^3}\check{U}(\overline{a}^1_k \underline{b}^k_j \hat{f}^j, \overline{a}^2_k \underline{b}^k_j \hat{f}^j, 0)\beta(-\overline{a}^3_k \underline{b}^k_j \hat{f}^j) e^{j2\pi d \underline{b}^3_j \hat{f}^j} \quad (1)$$

and for the backward transform

$$\check{U}(\hat{f}^1, \hat{f}^2, 0) = \frac{-1}{\hat{f}^3}\hat{U}(\overline{b}^1_k \underline{a}^k_j \hat{f}^j, \overline{b}^2_k \underline{a}^k_j \hat{f}^j, d)\beta(-\overline{b}^3_k \underline{a}^k_j \hat{f}^j) e^{-j2\pi d \underline{a}^3_j \hat{f}^j}. \quad (2)$$

Here, $\overline{\mathrm{a}}$ and $\overline{\mathrm{b}}$ are the turning dyads of the source and the target aperture, β is the ramp function, d is the distance between the apertures and $\hat{f}^3 = -\sqrt{\lambda^{-2} - (\hat{f}^1)^2 - (\hat{f}^2)^2}$. A detailed derivation of the formulae is given in [4].

In addition, (1) allows to define the target distribution on a tilted mirror. Applications in general antenna engineering or optics suggest themselves.

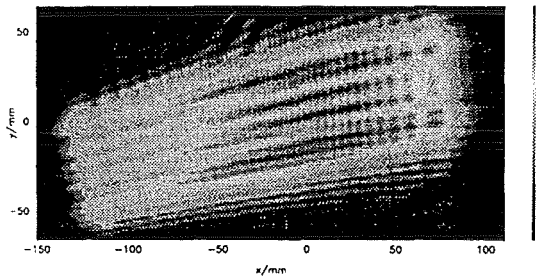

Figure 3: Input Field on the 2nd Mirror

The design goal for the second mirror is a homogeneous field distribution on the window on the one hand and a high gaussian content at some distance after the window on the other hand. Since the input field (see Figure 3) is already relatively homogeneous, both goals can be achieved with this mirror (Figure 4). At the position with the highest gaussian amplitude content, another phase correcting mirror will be placed.

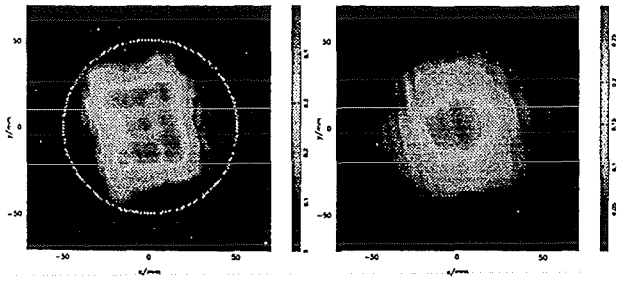

Figure 4: Field Distribution on the Window (left) and 40cm behind the Window (right)

Because of mechanical tolerances and the geometrical optical approximation on the first mirror, the real field distribution will not be as gaussian as in Figure 4. Therefore after the manufacture of the gyrotron the beam will be reconstructed by means of the error reduction algorithm [3] using (1) for oblique view angle correction. Then a pair of two phase correcting mirrors will be placed at the position with the highest gaussian content in order to match the beam to a standard transmission line with elliptical mirrors or a corrugated waveguide.

The actual problem in the design of phase correcting mirrors is the unwrapping of the phase corrector in order to get a smooth mirror surface. However, in most cases this is an ill-posed problem and an exact unwrapping without phase jumps is not possible.

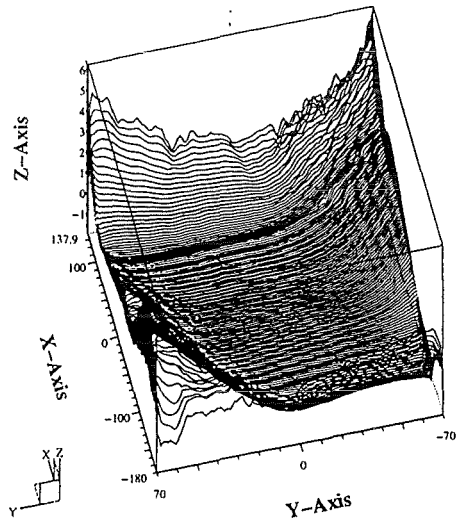

Figure 5: Contour of the Second Mirror

To overcome this problem, a new pathless algorithm was developed which always produces a smooth surface (Figure 5). For ill-posed problems it yields a least squares solution (as a side effect, this is good for compensating noise) and for well-posed problems it yields the exact unwrapped phase corrector. Hence, the algorithm is also interesting for interferometry. A detailed description is published in [4].

References

[1] G. G. Denisov, S. V. Kuzikov, *Eigenmodes Evolution Due to Changing the Shape of the Waveguide Cross-Section*, Int. J. of IR and MM-Waves, Vol. 18 (1997), No. 3

[2] Y. Hirata et. al., *Wave Beam Shaping Using Multiple Phase-Correction Mirrors*, IEEE Trans. on Microwave Theory and Techniques, Vol. 45 (1997), No. 1

[3] B. Z. Katzenelenbaum, V. V. Semenov, *Synthesis of the Phase Correctors forming a given Field,* Radiotechnika i Elektronika 12/1967, p.244

[4] G. Michel, E. Sanchez, *Investigations on Transmission Lines with Nonquadratic Mirrors*, 10th Joint Workshop on ECE and ECRH, 6-11 April 1997, Ameland, The Netherlands